KU LEUVEN

FACULTY OF SCIENCE

A role for the neuropeptide receptor NPR-6 in *C. elegans* olfactory learning?

Nathan DE FRUYT

Supervisor: Prof. L. Schoofs
Animal Physiology and Neurobiology

Mentor: Drs. M. Fadda
Animal Physiology and Neurobiology

Thesis presented in
fulfillment of the requirements
for the degree of Master of Science
in Biology

Academic year 2018-2019

HOST LAB INFORMATION PAGE

Master theses performed in the Schoofs lab comply with following house rules:

1. *Maximal education and scientific self-empowerment of students*

   Students are encouraged to learn from their mistakes through dialogue, rather than by simply being corrected by their supervisors. All writing in this document is the result of this process.

   Students get two feedback moments with respect to their writing process. One from their daily supervisor, who will advise them on format and content (*e.g.* scientific language, proper representation of results and structure of their interpretations). For this, daily supervisors interact either in person with the student, or via comments added to the manuscript. Under no circumstances do they rephrase sections of the text, which is entirely the student's wording. A second feedback session includes comments from (co)supervisors and only focuses on content. This implicates additional input with regards to the student's findings and the final discussion of results. The student's interpretation of this feedback is integrated in the final version of this manuscript, as it is presented here.

2. *Authenticity in science*

   Potential plagiarism was verified using TurnItIn. This work overall scored 3% of potential plagiarism. Sections underlying this result were manually verified by the daily supervisor, as such supporting the authenticity of this work.

AKNOWLEDGEMENTS

It was only a couple of years ago when I first heard about *C.* She was told to be a little *"primitive"* back then. Not with a bad connotation, though. She was generally known for her fluency to introduce people to the fundamental essence of our existence.

Now that I got better acquainted with *C.* while contemplating this final year of university, I got to appreciate her better and I now see that she's far less *primitive* as she and her fully known connectome might look.

In my case, Melissa taught me all I needed to know to keep *C.* happy. You see, *C.* wasn't that talkative, even though we spent hours together, sometimes all alone and separated from each other by not much more than an objective –alone with her and a couple hundreds of her sisters, that is. Not that it matters too much since they're all quite alike.

As generous as Melissa was to instruct me and others how to handle *C.* with care – especially when trying to learn *C.* new things, for example that diacetyl has nothing to do with food – she showed the same generosity towards me and I really enjoyed climbing literal and figurative walls together with her as well as to share in her history with *C.* Together with Jan, Isabel and Melissa, I learned a great deal on how to interpret *C*'s sometimes peculiar behaviour, on how to be a good scientist and on the mysterious ways in which *C.* works … or not. I wouldn't have made it this far in *C's* world without them, for which I'd like to express my gratitude.

In that regard, *C.* was very good at introducing people to each other and it was *C.* that introduced me to Sara, Rose and Martijn, resulting in an even better understanding of *C.,* through conversation, coffee and a good laugh every now and then.

Katleen and Elke knew how to guide me in the sometimes less structured environment in which *C.* is to be found and together with Marijke, they helped me in getting specific parts of *C.* shine brighter than before, especially at a wavelength of 395 nm, for which I am them grateful as well. Similarly, without the glamorous strain ZX2038 that was kindly provided by Prof. Alexander Gottschalk at Frankfurt university, it would have been impossible to conduct my experiments. Sebastien Santini was of help too, as he manages a convenient tool to construct phylogenetic trees.

The contemplation of this master's dissertation has been an ultimately instructive, but even more so surprisingly joyful experience. Therefore, I would also like to thank to Prof. Schoofs who granted me the opportunity to perform my experiments in her lab and who taught me more on the scientific world and the bigger picture in which *C.* resides.

Finally, I'd like to thank Elisa to take it so well that I showed so much interest in *C.* and for her not bothering too much when I started explaining theories I invented about *C.* until she couldn't follow anymore. Usually the moment when she put my feet back on the earth which I probably also needed from time to time.

TABLE OF CONTENTS

LIST OF ABBREVIATIONS

5-HT – serotonin (5-hydroxytryptamine)
AD – autoclaved distilled water
bp – base pairs
BSA – bovine serum albumin
cDNA – complementary DNA
C. elegans – *Caenorhabditis elegans*
CHO K1 cells – Chinese hamster ovary K1 cells
CI(s) – chemotactic index (/indices)
CTX buffer – chemotaxis buffer
DA – diacetyl
DAF – abnormal dauer formation
DMEM/F12 – Dulbecco's Modified Eagles Medium nutrient mixture F12-Ham
DiI – 1,1'-Dioctadecyl-3,3,3',3'-Tetramethylindocarbocyanine Perchlorate
D. melanogaster – *Drosophila melanogaster*
DNA – deoxyribonucleic acid
EDTA – ethylenediaminetetraacetic acid
FLP – FRMFamide like peptides
gDNA – genomic DNA
GFP – green fluorescent protein
GPCR – G-protein coupled receptor protein
ILP – insulin-like peptides
KCs – Kenyon cells
LB – lysogeny broth
MB – mushroom body
mQ – autoclaved Ultra-pure milliQ water (Millipore)
MOD-1 – modulation of locomotion defective 1
MOD-5 – modulation of locomotion defective 5
NGM – nematode growth medium
NLP – neuropeptide like peptide
(s)NPF – (short) neuropeptide F
(s)NPFR(s) – (short) neuropeptide F receptor(s)
NPR(s) – neuropeptide receptor(s)
NPR-6 – neuropeptide receptor 6
NPY – neuropeptide Y
NPY2R(s) – neuropeptide Y receptor Y2
ODR-10 – odorant response abnormal 10
PCR – polymerase chain reaction
PrRP – prolactin releasing peptide
PrRP-R – PrRP receptor
PYY – peptide YY
RCO – relative cell occupancy
SER – serotonin/octopamine receptor
$\overline{v}$ – average speed over all behaviours
wt – wild-type Bristol strain *C. elegans*

SAMENVATTING

Voor Eumetazoa is het vermogen om te leren uit voorgaande ervaringen essentieel om zich aan te passen aan een continu veranderlijke omgeving. Daarnaast is de mensheid sinds lang gefascineerd door de moleculaire en cellulaire mechanismen die bijdragen tot het leerproces. *Caenorhabditis elegans* is als modelorganisme bijzonder geschikt om dergelijke fundamentele en vaak geconserveerde processen te bestuderen.

Neuropeptide receptor 6 (NPR-6) werd geïdentificeerd als een *C. elegans* homoloog van de *short neuropeptide F* (sNPF) *receptor* (sNPFR) in arthropoden. sNPF beïnvloedt verschillende gedragingen, waaronder leergedrag. Preliminaire data suggereerde bovendien leerdefecten in mutanten zonder deze receptor, wat ons dreef om een mogelijke rol voor NPR-6 in olfactorisch associatief leergedrag te karakteriseren.

Onze gegevens bevestigen de voornoemde structurele homologie met de sNPFR en sturen bovendien ook aan op gelijkaardige functies. Zo lijkt NPR-6 een anorexigeen signaal over te brengen, net zoals de sNPFR in insecten verzadigingssignalen doorgeeft. Hoewel de voorgestelde rol in associatief leergedrag deels onopgehelderd blijft, suggereren onze gegevens dat NPR-6 olfactorische perceptie kan moduleren in reactie op de voedselbeschikbaarheid. Daarnaast beïnvloedt NPR-6 voedsel-georiënteerde veranderingen in bewegingspatronen, komt *npr-6* tot expressie in neurale netwerken die voedsel-georiënteerd gedrag moduleren en zijn alle neuropeptiden die wij identificeerden als veelbelovende bindingspartners voor NPR-6 reeds gekend als regulatoren van dergelijk gedraging.

Verzadigingssignalen en geur-georiënteerde chemotaxis drijven agrarische pestsoorten, parasitaire nematoden en ziekte-overdragende insecten ertoe om hun gastheer te infecteren. Daarom dragen verbeterde inzichten in de moleculaire mechanismen van deze processen bij aan de zoektocht om toekomstige economische verliezen tegen te gaan en de wereldwijde gezondheid te verbeteren.

SUMMARY

Incorporating past experiences in future behaviour is essential for animals to adapt to a continuously changing environment. Moreover, understanding the molecular and cellular mechanisms of learning have intrigued many generations. As a model, *Caenorhabditis elegans* is particularly amenable to assess the fundamental and often conserved mechanisms of learning.

Neuropeptide receptor 6 (NPR-6) has been indicated as a *C. elegans* homologue to the insect short neuropeptide F receptor (sNPFR), which affects many behaviours, including learning and memory. Led by preliminary data suggesting learning deficits in mutants that lack this protein, we set out to characterise a potential analogous role for NPR-6 in olfactory learning.

Our data confirm structural similarity, and also suggest comparable functions for both receptors: in line with a widely reported role of the insect sNPFR in satiety signalling, our results indicate that NPR-6 may transmit an anorexigenic signal. Although its role in olfactory learning remains partially inconclusive, our data suggest that NPR-6 might instead modulate olfaction in a food-dependent way. Moreover, NPR-6 appears to modulate food-dependent locomotion, is expressed in neural networks that modulate several other food-dependent behaviours and all of the *C. elegans* neuropeptides that we identified as novel promising ligands of NPR-6 are known to modulate similar food-dependent behaviours.

Satiety signalling together with olfactory chemotaxis and memory drive agricultural pest species, parasitic nematodes and insect disease vectors to infect their respective host species. Therefore, elucidating the molecular mechanisms of these processes in *C. elegans* might contribute to mitigate huge economic losses and improve worldwide human health.

I. INTRODUCTION

1. Learning and Memory: state of the art

Learning and memory are one of the most vital properties of animals, allowing them to adapt to a continuously changing environment (Kandel 2001; Sasakura and Mori 2013). It was historically often assumed that these features were exclusively limited to humans (Ardiel and Rankin 2010; Kandel 2001; McDiarmid *et al.* 2015). However, it is now clear that learning and the ability to retain memories evolved early in metazoan evolution and that these traits are common in all metazoans (Beets *et al.* 2012; Sasakura and Mori 2013; Schoofs *et al.* 2017).

1.1 Types of learning

From a behavioural perspective, learning comprises a variety of behaviours (McDiarmid *et al.* 2018). These can be categorised as either non-associative or associative learning and memory (Ardiel and Rankin 2010). Moreover, this distinction translates into distinct molecular pathways and neuronal circuits and it is therefore not purely semantic (Alcock 2012; Ardiel and Rankin 2010; Stein and Murphy 2014).

Non-associative learning includes sensitization as well as habituation. Sensitization denotes a state of enhanced sensitivity to formerly neutral stimuli in response to a signal that is considered to be inflicting harm (Bear *et al.* 2016; Kandel 2001). To illustrate, electrical stimulation of the tail in the sea slug *Aplysia californica* also increases the duration of gill withdrawal upon touching the siphon, two responses that are usually not displayed simultaneously (Kandel 2001, 2012). In contrast, habituation, also referred to as stimulus adaptation, points to the actively decreased response to a recurring or continuous stimulus (Ardiel and Rankin 2010; Morrison *et al.* 1999). The first discovered example of habituation in *Caenorhabditis elegans* came by repeatedly eliciting the tap-withdrawal response (Rankin *et al.* 1990). Naively, *C. elegans* will reverse in response to a tap to the side of the cultivation plate. When this is done several times with short intervals of time, the likelihood and magnitude of the reversal behaviour diminishes. This should not be misinterpreted as sensory adaptation or motor fatigue (Rankin *et al.* 1990). While habituation involves active plasticity in the circuit, sensory adaptation indicates a diminished response solely due to receptor saturation: the receptor is chemically unable to transfer the signal (Morrison *et al.* 1999; Zhang *et al.* 2005). Motor fatigue refers to the disability of initiating a behaviour because of motor defects, while the neuronal signalling might be unaffected (McDiarmid *et al.* 2018). The distinction between habituation and sensory adaptation or motor fatigue becomes clear after applying a dishabituating stimulus. This is a stimulus that resets the learned behaviour to the naive behaviour, which would not happen in case of receptor saturation or motor fatigue (Ardiel and Rankin 2010).

Associative learning includes classical conditioning (Alcock 2012). In classical conditioning, two independent stimuli are associated with each other, of which one, the unconditioned stimulus, naively evokes a specific behavioural response, while the other, the conditioned stimulus, does not. If a test subject is exposed to both stimuli together for a repeated number of times or for a prolonged duration, an association can be formed in which the conditioned stimulus will now evoke the same response as the unconditioned stimulus (Alcock 2012; Ardiel and Rankin 2010).

Finally, both associatively and non-associatively learned responses can be maintained on a different temporal scale after learning and also here, the molecular and cellular mechanisms that result in short, intermediate and long-term memory formation differ (Kandel 2001; Kauffman *et al.* 2010; Stein and Murphy 2014).

1.2 Cellular mode of action

Plasticity in the neuronal network originates from changes in the electrophysiological signalling properties between two cells (Bargmann 2012; Bentley *et al.* 2016). Increasing the electrophysiological signalling properties leads to an enhanced excitability of the post-synaptic neuron, while decreasing them will result in decreased excitability of the post-synaptic neuron (Kandel 2012). The electrophysiological properties are determined by the connectivity of the interacting cells and the excitability of perisynaptic neurons. Connectivity here denotes all ways in which two cells interact, including electrical and chemical synapses, as well as extrasynaptical signalling (Bargmann 2012). Therefore, plasticity can be obtained in two ways. On the one hand, anatomically observable remodelling of the neural network increases the connectivity between neurons (Bear *et al.* 2016; Carulli *et al.* 2011; Kandel 2012). On the other hand, neuromodulation can result in increased or decreased pre-synaptic neurotransmitter release or in altered responsiveness or numbers of the neurotransmitter receptors in the post-synaptic neuron, thereby altering synaptic signalling properties (Bargmann 2012; Bentley *et al.* 2016; Kandel 2012; Taghert and Nitabach 2012).

Remodelling the wiring diagram comprises neurogenesis and neurodegeneration, as well as synaptogenesis and synaptic elimination, (Bear *et al.* 2016; Carulli *et al.* 2011; Kandel 2012; Kandel 2001). The potential outcomes of a neuronal circuit are eventually determined by the connectome, whereas the actual functionality and outcome of the hard-wired neuronal circuit is determined by neuromodulation (Bargmann 2012; Yan *et al.* 2017).

Importantly, neuromodulation can occur both directly within a neuronal network via synaptic signalling, as well as extrasynaptically in a paracrine or endocrine, ‘wireless’ fashion (Bentley *et al.* 2016; Chen *et al.* 2013; Cohen *et al.* 2009).

Neuromodulation appears to be conserved over animal evolution from organisms with a limited nervous systems up to the very complexely wired brains of primates (Bargmann 2012; Jekely 2013; Mirabeau and Joly 2013). Accordingly, a great number of homologous neuromodulators and their receptors can be found across the animal kingdom (Jekely 2013; Marder 2012; Mirabeau and Joly 2013; Nässel and Wegener 2011; Taghert and Nitabach 2012).

Monoamines and neuropeptides constitute the major part of the known neuromodulators and both groups are actively involved in learning and memory formation, retention and loss (Bargmann 2012; Beets *et al.* 2012; Bentley *et al.* 2016; Peymen *et al.* 2014; Van Sinay *et al.* 2017). For example, the functionally homologous monoamine signalling system of norepinephrine in vertebrates, octopamine and tyramine in insects and tyramine in *C. elegans*, have been identified as modulators of learning and memory (Kandel 2012; Kandel 2001; Zhang *et al.* 2005). In addition, several neuropeptidergic neuromodulatory systems were also proven to be conserved. These include insulin and insulin-like peptide signalling, the oxytocin/vasopressin system, gastrin signalling and many more (Nässel and Wegener 2011; Peymen *et al.* 2014; Schoofs *et al.* 2017).

These examples illustrate how insights in neuromodulatory systems of invertebrates, such as *C. elegans*, can not only help us understand conserved principles on the function of neuromodulation, but might also expand our current knowledge on specific molecular interacting partners in neuromodulator systems.

A first pathway of learning, concerns long and short term memory formation at the glutamatergic synapse (de Bono and Maricq 2005). Kandel (2012, 2001) used his experience with the early experiments on *A. californica* to summarise a mode of action that was later proven to be conserved among species. In this model, serotonergic stimulation of a synapse induces short-term associative memory. Intracellularly, this is established via cyclic adenosine monophosphate (cAMP) and calcium signalling which directly modulate the excitability specifically at the stimulated synapses (Kandel 2001; Stein and Murphy 2014). These changes include the mentioned synthesis and storage of neurotransmitters in the presynaptic neuron as well as functional changes to postsynaptic receptor proteins and ion channels, together increasing their responsiveness (Kandel 2001).

Intermediate- and long-term memory, however, need additional protein transcription and translation (Kandel 2012, 2001). Transcription is activated by the cAMP-responsive element binding protein 1 (CREB1) basic leucine zipper domain (bZIP) transcription factor (Shen *et al.* 2014). As studies in *A. californica* showed, a cAMP mediated protein kinase A (PKA) first recruits p42 mitogen activated protein kinase (MAPK) and this complex translocates to the nucleus to phosphorylate CREB1 (Kandel 2012). After phosphorylation, CREB1 is active and binds to the cAMP-responsive element, thereby promoting gene transcription. Eventually, this results in the expression and translation of CREB-associated genes (Kandel 2001; Shen

et al. 2014; Stein and Murphy 2014). Next to this, many other positive and negative regulators of long-term memory exist. Examples of negative regulators are protein phosphatase 1 (PP1) and calcineurin (Kandel 2012). These two phosphatases inactivate transcription factors (Kandel 2012). Known targets of these phosphatases include CREB2 in *A. californica*, activating transcription factor 4 (ATF4) in mice and resistant to dieldrin (Rdl) in Drosophila (Shen *et al.* 2014). Eventually, gene transcription and protein synthesis can result in long-term facilitation by an increase in the number of receptors at the synapse and neuro- and synaptogenesis as mentioned before (Kandel 2012). Conversely, long-term depression (i.e. a decrease in post-synaptic excitability) is caused by a decrease in the number of receptors at the synapse and neurodegeneration and synaptic elimination (Kandel 2012).

2. C. elegans *as model organism in neuroscience*

2.1 Introduction to *C. elegans*

Historically, investigation of the cellular, physiological and molecular mechanisms that mediate learning and memory, has been carried out in organisms that were closely related to humans (Ardiel and Rankin 2010; Kandel 2001). Later however, with the discovery of the cellular mechanisms of memory in *A. californica*, the gate to invertebrates as a model organism for learning and memory was opened (Kandel 2001; Stein and Murphy 2014). The nematode *C. elegans* was already known as a model organism in other research fields for its convenient size (~1 mm for adult hermaphrodites), which made it suitable to be cultivated on a Petri dish covered in a bacterial film as nourishment and its easy breeding. Conveniently, *C. elegans* hermaphrodites allow the creation of genetically traceable lines as a self-fertilizing parent generation will produce genetically identical offspring (Brenner 1974). Furthermore, it completes its development through four larval stadia to adulthood in about 3 days at 20°C, making it easy to rapidly produce a large number of new offspring (Brenner 1974). Because its entire life cycle ends within a matter of weeks, it's been proven to be a good model for ageing studies as well. Because of these characteristics, interest in *C. elegans* as a model organism grew and led to the development of many genetic tools, leading to highly advanced genetic technologies such as calcium imaging, optogenetics and lately also CRISPR-Cas9 induced site-specific mutations (McDiarmid *et al.* 2018; Sasakura and Mori 2013; Van Sinay *et al.* 2017). In addition, more classical methods such as forward and reverse genetics are often performed, as deviating phenotypes can be relatively easily screened for in large libraries of *C. elegans* mutant strains, the *C. elegans* genome was sequenced early in the history of the *C. elegans* field and RNAi knockdown generally works well (Ardiel and Rankin 2010; Sasakura and Mori 2013). Moreover, it is an organism particularly suited for tracking development as it is transparent and the cell lines are invariant, making each cell traceable (Gilbert and Barresi 2018).

This enabled researchers to relatively easily map the entire nervous system anatomically together with their synaptic connections. With 302 neurons and about 5,000 synapses in an adult hermaphrodite worm, this was the first connectome ever to be described (Figure 1; White *et al.* 1986).

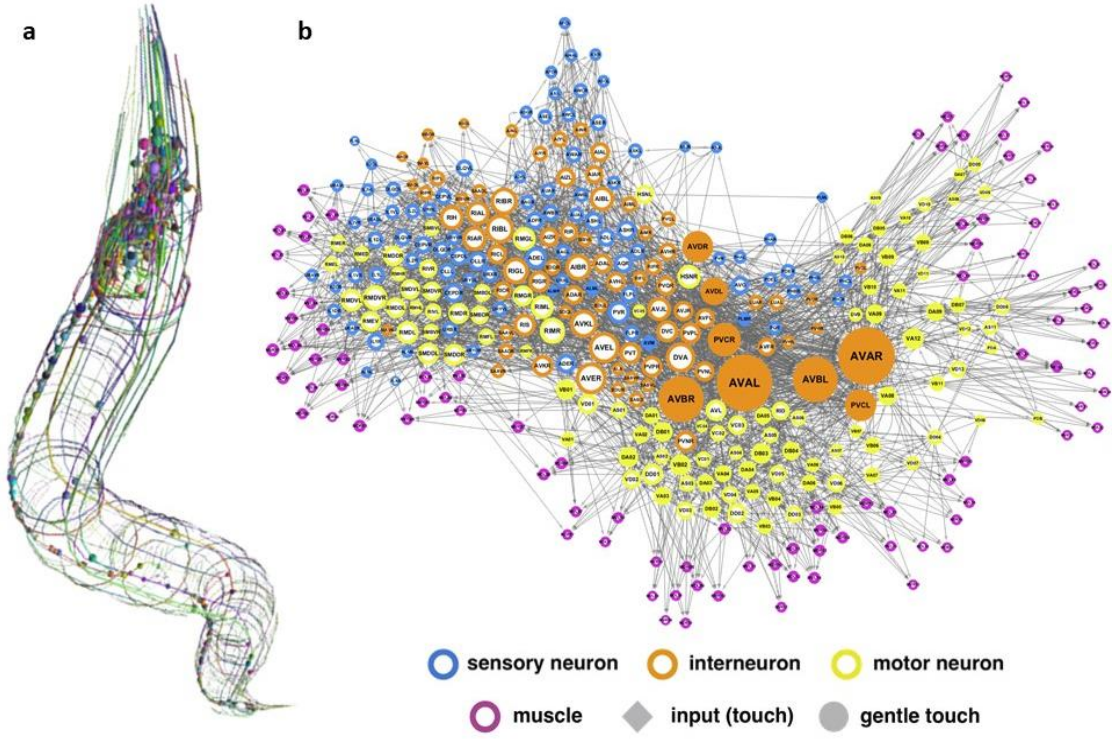

Figure 1:The* C. elegans *connectome a) *visual representation of the connectome (The OpenWorm Project)* ***b)*** *neuronal network of all neurons based on the connectome (Yan et al. 2017; Reproduced with permission of Nature Publishing Group)*

Although the *C. elegans* nervous system is in theory identical in each individual, these organisms still have proven to show a wide variety of plasticity in their behaviour towards olfactory, gustatory, thermal and mechanosensory cues based on previous experiences and environmental conditions (Ardiel and Rankin 2010; McDiarmid *et al.* 2015). Given the limited number of sensory neurons, the initiation of these behaviours can be related to specific neurons and therefore, the perception of the signal is a good starting point to investigate the downstream wiring and physiological effects of these stimuli. In this way, the AWA, AWB and AWC neurons appeared invaluable for olfactory perception (Sengupta *et al.* 1996). Similarly, many other sensory neurons were assigned to the perception of their respective affecting stimuli (Bargmann and Horvitz 1991; Mori and Ohshima 1995).

Combined efforts have shown that the same memory formation mechanisms that are present in other organisms are also conserved in *C. elegans* (Kauffman *et al.* 2010; Peymen *et al.* 2019b; Stein and Murphy 2014). Using mutants, several research groups showed the requirement of adenylate cyclase for short-term memory formation, and the requirement of PKA and CaMKII, phosphatases and CREB for long-term memory formation, much as in other organisms (Kauffman *et al.* 2010; Stein and Murphy 2014).

Taken together, the manageable size of the connectome, the available genetic tools, the invariability of the nervous system, the conserved mechanisms for memory formation and the plasticity in synaptic excitability, create a convenient well-controlled and reproducible framework for neurophysiological research (McDiarmid *et al.* 2015; Piggott *et al.* 2011). Importantly, many genes seem to be conserved between *C. elegans* and other organisms, including mammals (Ikeda *et al.* 2008; Stein and Murphy 2014). Therefore, conclusions regarding fundamental processes may be extrapolated across species. Finally, the *C. elegans* community provides convenient platforms to study complex phenotypes as both data and wet and dry lab methods are generally freely shared (McDiarmid *et al.* 2018). This creates transparency and reproducibility and allows faster progression in the field.

2.2 Chemotaxis in a learning context

Next to reproduction, feeding is the main occupancy of *C. elegans* and therefore, cues indicative of food guide *C. elegans* during locomotion (Sasakura and Mori 2013; Sengupta *et al.* 1996). Accordingly, *C. elegans* shows an innate chemotaxis towards several gustatory and olfactory stimuli that provide basic information on its environment (McDiarmid *et al.* 2015; Morrison *et al.* 1999; Sasakura and Mori 2013).

Two behaviours enable *C. elegans* to orient its movement towards attractants during chemotaxis: biased random walk and klinotaxis, together constituting a strategy that is highly similar to bacterial chemotaxis (Iino and Yoshida 2009; Pierce-shimomura *et al.* 1999). Biased random walk denotes an interplay between short runs and random reorientation events. Moving through its environment, *C. elegans* senses changes in concentrations of attractants (Pierce-shimomura *et al.* 1999). Increases in concentrations cause a proportional decrease in the probability of random reorientations to occur, thereby biasing *C. elegans'* orientation towards the stimulus (Klein *et al.* 2017). In contrary, klinotaxis indicates the active, directed orientation towards the stimulus source (Iino and Yoshida 2009).

The innate response of *C. elegans* towards stimuli, be it attraction or repulsion, can be modified by associative learning. Often, gustatory, thermosensory, olfactory or mechanosensory cues are coupled to attractive cues, e.g. the presence of food, or to repulsive cues such as the absence of food, pathogenic bacteria or harmful substances, e.g. Cu^{+} or acetic acid (Ha *et al.* 2010; McDiarmid *et al.* 2015; Sasakura and Mori 2013; Zhang *et al.* 2005). When the learning routine is sufficiently repeated with defined intervals, memory is formed and the learned response can persist over long time intervals (Kauffman *et al.* 2010; McDiarmid *et al.* 2015; Sasakura and Mori 2013). Mutant strains that are deficient in learning, short-term or long-term memory formation, will act divergently from wild-type strains upon presentation of the stimuli after conditioning (Morrison *et al.* 1999).

Several learning assays have been developed to test learning and memory in *C. elegans*. Depending on the research question, the read-out of the experiment can be adjusted. Different stimuli can be chosen to apply the conditioning paradigm. Odours that are often used in olfactory memory assays include the diacetyl, butanone, octanol and benzaldehyde, each of which has a distinct attractive appeal to *C. elegans*.

To investigate whether learning and memory has been formed and to what degree, a chemotaxis index (CI) is usually calculated (Bargmann *et al.* 1993). This is a score to measure attraction towards a chemical stimulus, while penalizing for attraction to the control odorant before and after conditioning (§4.2).

2.3 Diacetyl sensing and downstream signalling

To evaluate mutant associative learning abilities, we made use of an olfactory learning assay based on the innate attraction to diacetyl (DA) as olfactory cue (Bargmann *et al.* 1993). DA binds to the odorant response abnormal 10 receptor (ODR-10), the first olfactory receptor protein defined in *C. elegans* (Sengupta *et al.* 1996). Fusion to a green fluorescent protein (GFP) tag further proved its expression in the AWA neurons, which were already known to be necessary and sufficient for *C. elegans* to perceive low DA concentrations (Figure 2; Bargmann *et al.* 1993; Sengupta *et al.* 1996).

Next to AWB, AWC, ASH and ADL, the AWA neurons are one of five main olfactory chemosensory neuron pairs that can be found in the specialised symmetrical amphid organs, localised rostrally in *C. elegans* (Bargmann *et al.* 1993). The amphids are ciliated extensions that protrude in the cuticula, thereby being separated from the external environment by a secreted matrix only (Figure 2a and c; Bargmann *et al.* 1993). Together, AWA and AWC sense the attractive olfactory cues, whereas stimulation of the AWB, ASH and ADL neurons evokes an aversive response (Li and Liberles 2015; Li *et al.* 2012). Activation of the ODR-10 leads to stimulation of two transient receptor potential vanilloid (TRPV) related channels, encoded by osmotic avoidance abnormal 9 (*osm-9*) and capsaicin receptor-related 2 (*ocr-2* ;Tobin *et al.* 2002). Signal transduction from ODR-10 to the TRPV-related channel happens via ODR-3, a G_{α}-protein, a signalling pathway that is specific to AWA and ASH (Roayaie *et al.* 1998). This eventually results in depolarization of the AWA neurons to an uncommon all-or-none calcium action potential (Larsch *et al.* 2015). Instead, ODR-3 in AWB, AWC and ADL activates a guanosine triphosphate (GTP) cyclase which converts GTP to cyclic guanosine monophosphate (cGMP), that in turn activates a cGMP-gated ion channel (de Bono and Maricq 2005).

One of the major targets of the AWA neurons are the AIA interneurons that are connected via bidirectionally signalling gap junctions (Larsch *et al.* 2015). This connection is shown to play a role in reversal of locomotion, thus assisting in gradient-guided chemotaxis

(Larsch *et al.* 2015). Moreover, the AWA neurons form several other connections to the AIY and AIZ first-layer interneurons, much as the AWC and the salt-sensing ASE neurons do (Bargmann *et al.* 1993). The AIY and AIZ neurons transfer chemosensory as well as thermal information to the RIA premotor interneurons (Kobayashi *et al.* 2016).

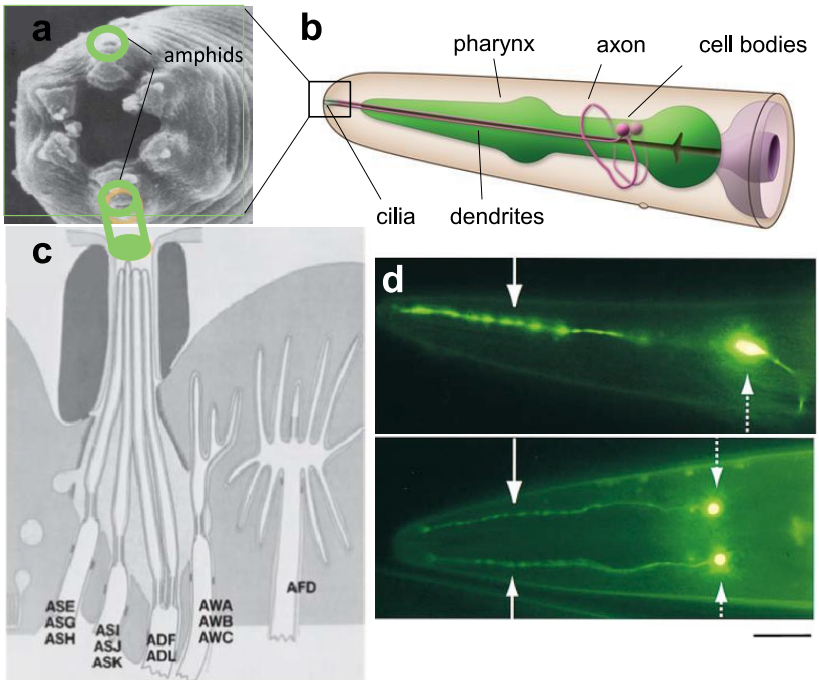

Figure 2: Anatomy of the amphid sensory organs and the position of the AWA chemosensory neuron. a) *scanning electron micrograph of the head with amphids (encircled in green);* ***b)*** *position of the AWA neurons (note the rostral nerve ending);* ***c)*** *schematic representation of an amphid with its main sensory neurons;* ***d)*** *fluorescence micrograph of the AWA neurons (de Bono and Maricq 2005; WormAtlas; Reproduced with permission from Annual Reviews)*

2.4 Learning and memory mutants in *C. elegans*

In 1997, *learn 1 (lrn-1)* and *learn-2 (lrn-2)* were the only genes described for which corresponding deletion mutants have an associative learning defect in a gustatory conditioning assay (Wen *et al.* 1997). Two years later, Morrison *et al.* (1999) confirmed that the same two mutants were generally defective in associative learning. All tested strains (wild type, *lrn-1* and *lrn-2*) naively avoid the odour of acetic acid (AA), whereas they are attracted to low concentrations of DA. After exposure to AA in the presence of DA, only wild-type worms had a decreased chemotaxis towards DA, indicating successful associative learning in wild-type, but not in mutant worms. Non-associative learning was not affected in the *lrn-1* and *lrn-2* mutant strains (Morrison *et al.* 1999). Surprisingly, the identity of neither of these genes has been shown (WormBase; de Bono and Maricq 2005). Since then, however, several more learning and/or memory mutants have been discovered in both forward and reverse genetic screens.

Several mutants were used to show the conservation of the canonical CREB-mediated pathway of memory formation in *C. elegans* and loss-of-function mutants of these genes are defective in learning and memory formation (Stein and Murphy 2014). In addition, glutamate receptor family (AMPA) 1 (*glr-1*) and eating 4 (*eat-4*) mutants, involved in glutamatergic synaptic signalling, don't show functional long-term potentiation (Lee *et al.* 1999; Morrison and Van Der Kooy 2001; Rose *et al.* 2003).

Mutants with defective calsyntenin/alcadein homologue 1 (*casy-1*), show diminished learning in both gustatory, thermal and olfactory associative learning tests (Ikeda *et al.* 2008). Furthermore, insulin related 1 (*ins-1*) mutants show similar, but independent defects in gustatory tests (Ikeda *et al.* 2008).

From distinct learning assays in which olfactory and noxious Cu^{2+} stimuli, starvation and cultivation temperature or starvation and salt sensing were combined, also the hesitation behaviour 1 (*hen-1*) gene appears indispensable for various types of plasticity based on integration of two stimuli (Ishihara *et al.* 2002). The HEN-1 protein was localised to the cell body and axon endings of the ASE salt sensory neurons and AIY interneurons (Ishihara *et al.* 2002). Since axonal vesicular transport was required for proper functioning, HEN-1 is predicted to be a neuromodulator (Ishihara *et al.* 2002).

Furthermore, *C. elegans* enhanced olfactory learning 1 (*eol-1*), a gene involved in mRNA 5'-capping, has an opposite role compared to the memory-deficient mutant genes previously described. Mutation of *eol-1* enhances olfactory memory formation (Shen *et al.* 2014). Wild-type learning could be rescued by *eol-1* re-expression in the URX oxygen sensory neurons as well as by transgenic expression of mouse downstream of Maternal Effect Sterile (Mes) homologue Z (*Dom3z*), its mammalian homologue. Accordingly, ablation of the URX neuron severely impaired learning (Shen *et al.* 2014).

Together, these results indicate the involvement of many components at different levels in the general process of learning and memory. Moreover, they prove similarity between this process in *C. elegans* and other organisms. Hence, they provide a base to extrapolate the results obtained in *C. elegans* into a context of learning and memory formation in other phyla.

3. *Neuronal circuits and neuromodulation of olfactory memory*

This chapter will give a general overview on the current knowledge of neurons that are part of neural circuits involved in learning and memory, as well as signals that are involved in the modulation of these neuronal circuits. Different types of signals – e.g. gustatory, olfactory or thermal stimuli – will activate at least partially different neuronal circuits. In the perspective of this masters dissertation, this chapter will therefore have its focus on reported cases of olfactory learning and olfactory memory. In order not to lose track in the names and connectivity of all mentioned neurons, figure 3 provides a graphical representation of most of the individual neurons and their connections that will be discussed in this next section.

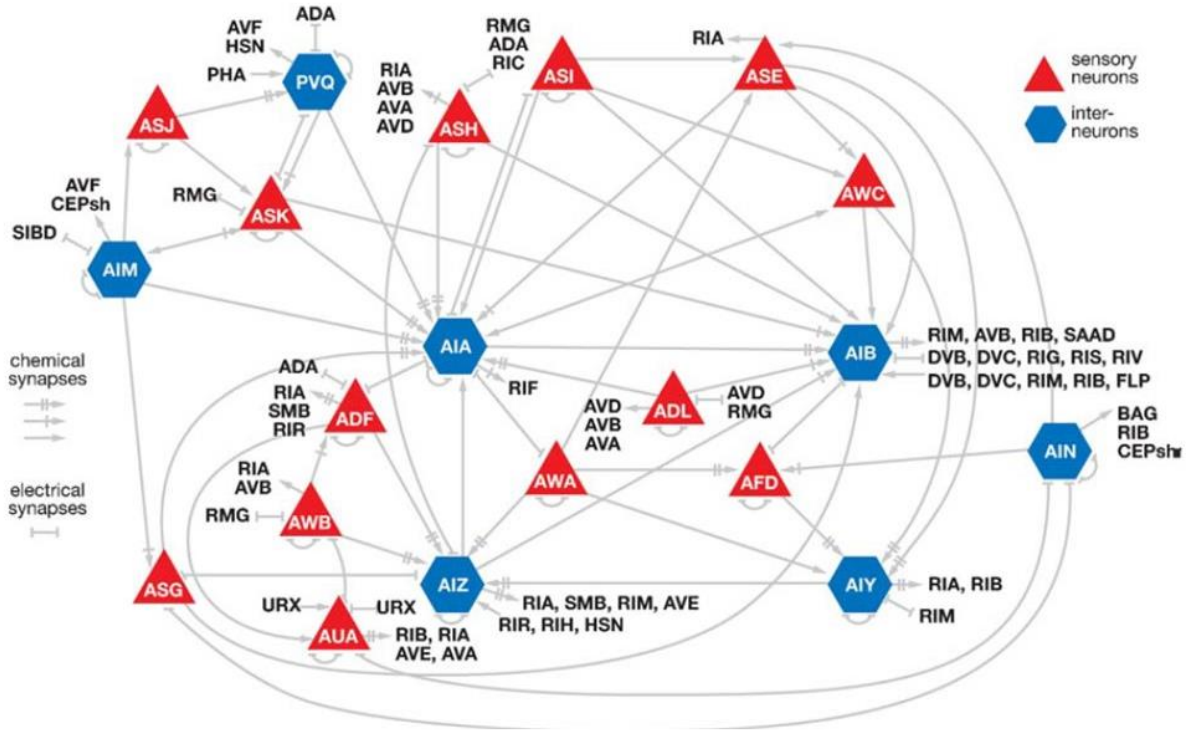

Figure 3: Schematic overview of the anatomical and partially functionally confirmed interactions of a selection of sensory neurons and primary layer interneurons*. Other interacting neurons are textually denoted in the figure (de Bono and Maricq 2005, adopted from White et al. 1986; Reproduced with permission of Annual Reviews).*

3.1 Aminergic neuromodulation of olfactory memory

In *C. elegans*, serotonin (5-HT) and dopamine have been related to plasticity in responsiveness to odorants in the presence or absence of food (Chao *et al.* 2004; Zhang *et al.* 2005). Chao *et al.* (2004) showed that an increased aversive response to the repellent odorant octanol in the presence of food can be mimicked by addition of exogenous 5-HT in the absence of food. Loss-of-function tryptophan hydroxylase 1 (*tph-1*) mutants, deficient in serotonin production, show a similar response as wild-type animals in the absence of food.

Conversely, Ardiel *et al.* (2016) found that dopamine signals the absence of food through dopamine receptor 4 (DOP-4), as dopamine deficient *C. elegans* mutants do not show the same increase in habituation towards 1-octanol upon food deprivation as observed in wild-type *C. elegans*. Amongst many other processes, dopamine is also involved in the habituation to noxious stimuli sensed by the ASH neurons (Ardiel *et al.* 2016).

5-HT is also involved in food preferences and learned aversion from pathogenic bacterial strains and 5-HT production by the ADF serotonergic neurons is induced by activation of a MAPK cascade (Meisel and Kim 2014; Zhang *et al.* 2005). Analogous to 5-HT-gated ion channels in vertebrates, binding of ADF-produced 5-HT onto the modulation of locomotion defective 1 (MOD-1) serotonin gated chloride channel modulates the existing learning circuit (Ha *et al.* 2010; Zhang *et al.* 2005). MOD-1 is expressed on the AIY, AIB and AIZ interneurons that lie postsynaptically of ADF (Ha *et al.* 2010). Furthermore, Ha *et al.* (2010) showed that ablation of the RIA interneurons, SMD motorneurons or ADF neurons separately attenuated the conditioned response. This indicates that RIA and SMD are also necessary in this experience-dependent plasticity and that they might well be the target of ADF produced serotonin in this learned aversive response (Ha *et al.* 2010).

These examples illustrate how 5-HT is required in several learning processes, including aversion from pathogenic bacteria and starvation-induced decrease of odorant selectivity (Li and Liberles 2015).

In addition, tyramine appeared to be essential in olfactory learning of an aversive response from pathogenic bacteria (Jin *et al.* 2016). Tyramine is required for adult olfactory learning as well as olfactory imprinting, a form of memory that is established in the first larval (L1) stage and is persistent till adulthood (Jin *et al.* 2016). Using histamine-gated chloride channels to silence neurons, Jin *et al.* (2016) showed that the RIM and AIB neurons are involved in imprinting during the L1 stage. Conversely, the RIA and AIY neurons are necessary for memory retrieval at the adult stage (Jin *et al.* 2016). Next to electrical signalling via a gap junction between the RIM and AIY neurons, extrasynaptic tyramine signalling between the RIM and AIY neurons takes place. The RIM neurons produce tyramine that binds to the serotonine/octopamine receptor family tyramine receptor (SER) 2, which is expressed on AIY (Jin *et al.* 2016). Importantly, this functional system mediated by tyramine signalling is only necessary for imprinting and not for associative learning. Tyramine administration in the L1 stage restored the imprinted response in both tyrosine decarboxylase 1 (*tdc-1*) mutants or RIM-ablated worms, which are otherwise deficient in this response (Jin *et al.* 2016). Cell-specific rescue of *tdc-1* in *tdc-1* mutants also restored this response (Jin *et al.* 2016). Both serotonin and tyramine are necessary, but not sufficient to evoke the response, indicating the requirement of a modulatory network that still relies on other components to be fully functional (Jin *et al.* 2016).

Considering the neural networks in both previous paragraphs, the RIA neurons appear as a general hub for many learning paradigms and many sensory neurons wire onto RIA. These include AWC, AWB, ASE and ADF. Therefore, it is clear that RIA has a major role in memory formation and retrieval (Ha *et al.* 2010; Jin *et al.* 2016).

3.2 Neuropeptidergic neuromodulation of olfactory memory

The over 250 neuropeptides for which the *C. elegans* genome codes are a second major source of neuromodulators (Bargmann 2012; Bentley *et al.* 2016; De Haes *et al.* 2015; Husson *et al.* 2005, 2007, 2014; Li and Kim 2008; Van Bael *et al.* 2018). Neuropeptides are generally translated to a prepropeptide that is first cleaved into a propeptide and a signal peptide (Figure 4; Husson *et al.* 2007; Li and Kim 2014; Schoofs *et al.* 2017; Van Bael *et al.* 2018). Subsequently, several neuropeptides are cleaved off by proprotein convertases after which they get additional modifications (Li and Kim 2014; Van Bael *et al.* 2018). These posttranslational events occur within the vesicular transport system of the Golgi complex through which they eventually undergo exocytosis in dense core vesicles (Schoofs *et al.* 2017).

In *C. elegans*, three classes of neuropeptides were assigned: the FMRFamide like peptides (FLPs), the insulin-like peptides (ILPs) and a third category comprising any other neuropeptide that does not belong to either of the other categories, which are called the neuropeptide-like peptides (NLPs) (Husson *et al.* 2007, 2014; C. Li and Kim 2014; Troy A. McDiarmid *et al.* 2015). The FLP-family in *C. elegans* comprises by far the largest part with over 70 family members defined and a cumulative expression in about 50% of the neurons (Peymen *et al.* 2014). With a few notable exceptions (e.g. insulin-like signalling), neuromodulators usually signal through highly specific G-protein coupled receptors (GPCR), which pose the advantage of a dose-dependent cellular effect. This stands in contrast to the rather limited versatility of aminergic neurotransmitters (Bargmann 2012; Frooninckx *et al.* 2012; Mirabeau and Joly 2013; Schoofs *et al.* 2017).

Insulin and insulin-like signalling were shown to be involved in olfactory learning and memory. Several insulin-like peptides were already shown to differentially modulate olfactory learning in response to pathogenic bacteria (Chen *et al.* 2013). Chen *et al.* (2013) suggest a model in which insulin-related 6 (INS-6), expressed in the ASI chemo- and thermosensory neurons, inhibits insulin-related 7 (INS-7) expression in the thermo- and oxygen-sensory URX neurons. INS-7, in turn, inhibits olfactory learning in the RIA interneurons. INS-7 presumably induces nuclear localization of the forkhead box O (FOXO) transcription factor abnormal dauer formation (DAF) 16. Thereby, INS-6 relieves DAF-2 insulin receptor expression from DAF-16 inhibition and activates the circuit by which the RIA neurons integrate olfactory cues with the

ingestion of pathogenic bacteria to avoid this smell in the future. Thus, environmental conditions determine the activity of the learning circuit (Chen *et al.* 2013).

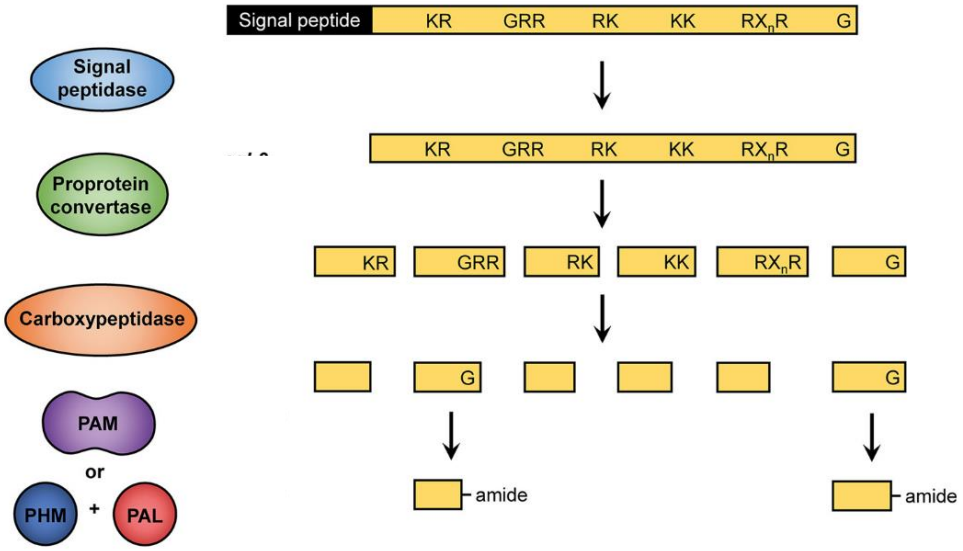

Figure 4: Neuropeptide post-translational processing: *neuropeptides are translated as a prepropeptide containing several isoforms of the neuropeptide. First, a signal peptide is recognised and cleaved off by signal peptidases. Next, proprotein convertases cleave after specific amino acid residues that are later removed by carboxypeptidases. Finally, amidation by a peptidylglycine α-amidating monooxygenase (**PAM**) or a combination of a peptidylglycine α-hydroxylating monooxygenase (**PHM**) and a peptidyl-α-hydroxyglycine α-amidating lyase (**PAL**) takes place if a glycine residue is found at the carboxyl terminus. This research was originally published in the Journal of Biological Chemistry. (Van Bael et al. 2018) © the American Society for Biochemistry and Molecular Biology or © Van Bael et al.*

Furthermore, although insulin signalling and starvation clearly had opposite effects on long-term memory formation, *daf-2* mutants were not affected in butanone olfactory learning assays (Kauffman *et al.* 2010). The insulin receptor defective mutant *daf-2* has a prolonged long-term associative memory (Kauffman *et al.* 2010). Conversely, dietary restriction resulted in decreased long-term associative olfactory memory (Kauffman *et al.* 2010). This was shown using *eat-2* (Eating: abnormal pharyngeal pumping 2) mutants that have defects in pharyngeal pumping that result in impaired bacterial ingestion (Kauffman *et al.* 2010).

Moreover, using cell-specific rescue constructs, mutant lines and photo-activated phosphatidylinositol-3-phosphate kinase (PI3K), Ohno *et al.* (2014) suggest a mechanism for insulin signalling in salt avoidance upon starvation. Thereby these results corroborate the hypothesis of a general role for insulin-like signalling in learning and memory. In this model, food signals induce MAPK, in turn activating kinesin light chain 2 (KLC-2; a kinesin-1 motor component), which is used by CASY-1 (§2.4) to transport the insulin receptor orthologue abnormal dauer formation isoform C (DAF-2C) to the synapse. DAF-2C activates phosphoinositide 3 kinase (PI3K), thereby recruiting newly phosphorylated DAF-16 to the cytosol. This eventually leads to salt avoidance.

3.3 The short neuropeptide F receptor NPR-6: a role in olfactory learning?

Short neuropeptide F (sNPF) is an 8 to 12 amino acid neuropeptide that is characterised by the C-terminal consensus sequence M/T/L/FRF of which the first residue depends on the species (Fadda *et al.* 2019). sNPF in insects has been associated with a variety of behaviours, including learning and memory (Fadda *et al.* 2019; Johard *et al.* 2008; Knapek *et al.* 2013).

Recently, a class A rhodopsin-like neuropeptide receptor in *C. elegans* has been indicated as a candidate receptor for sNPF: Although previously reported as a member of the 11 neuropeptide Y (NPY)-like receptors, more recent analyses of sequence homology cluster NPR-6 together with the insect sNPF receptors (sNPFR; Cardoso *et al.* 2012; Cohen *et al.* 2009; Hu *et al.* 2011; Mirabeau and Joly 2013). In addition, the *Caenorhabditis briggsae* NPR-6, an orthologue of the *C. elegans* NPR-6, also clustered together with insect sNPFRs (Altschul *et al.* 1990; G. Jekely 2013; States and Gish 1991). Other *C. elegans* NPRs, including NPR-1 through NPR-5, NPR-10 and NPR-13 were also revised and assigned to this cluster (Cardoso *et al.* 2012; Mi *et al.* 2019a, 2019b; Mirabeau and Joly 2013).

An important remark to avoid any confusion is that although implications of homology can be made on the invertebrate neuropeptide F (NPF) class of neuropeptides and the vertebrate neuropeptide Y (NPY), sNPF and NPF only share a distant ancestor and sNPF has no significant structural relation to the NPY system (Fadda *et al.* 2019; Nässel and Wegener 2011). Whereas the NPY/NPF system appears to be conserved across the animal kingdoms, the sNPF system seems to be limited to the invertebrate lineage (Fadda *et al.* 2019; Nässel and Wegener 2011). Alternatively, the prolactin releasing peptide (PrRP) system has also been proposed as the vertebrate homologue of protostomian sNPF (Fadda *et al.* 2019; Jekely 2013).

In line with a role for sNPF in learning and memory, an *npr-6* mutant containing a deletion in the coding region of *npr-6*, showed a deviating response in a pilot study for these mutants in the DA associative learning assay (host lab, personal communication).

3.3.1 Reported functions of NPR-6 in C. elegans

Oranth *et al.* (2018) reported on a role for NPR-6 in food-dependent regulation of body bending angles. Dependent on the amount of time since it last encountered food, *C. elegans* shows a continuous change in its locomotion patterns (Calhoun *et al*. 2014). On food, *C. elegans* displays dwelling behaviour, in which it moves minimally at low speed and turns frequently (Gray *et al.* 2005). Shortly after removal of food, local search behaviour is promoted, characterised by vigorous turning and increased speed (Calhoun *et al.* 2014; Roberts *et al.* 2016). Finally, in the prolonged absence of food, roaming behaviour allows for further dispersal

since this behaviour comprises high overall speed and low fractions of turning (Calhoun *et al*. 2014; Flavell *et al.* 2013; Klein *et al.* 2017).

These behaviours are reflected in body bending angles as well, since turning during local search behaviour results in maximal body bending and propulsion during roaming correlates with intermediate bending angles (Oranth *et al.* 2018). Therefore, both behaviours are distinguishable from minimal body bending angles during dwelling on food (Oranth *et al*. 2018).

When the mechanosensory AVK neurons are dysfunctional due to ablation or photoinhibition, bending angles during the early roaming phase increased to values reminiscent of local food search (Oranth *et al.* 2018). Moreover, Oranth *et al.* (2018) show that FMRF-like peptide 1 (*flp-1*) and *npr-6;frpr-7* double mutants display an identical increase in bending angle (*frpr-7*: FMRFamide peptide receptor 7). Although *npr-6* and *frpr-7* single mutants do not display spontaneous increase in bending angle, *npr-6* mutants show no increase in bending angle upon photoinhibition of the AVK neurons (Oranth *et al.* 2018). This is in contrast with *frpr-7* mutants where photoinhibition of the AVK neurons does evoke this phenotype.

Based on these and other results, Oranth *et al*. (2018) propose a mechanism in which AVK secretes FLP-1 upon mechanosensation of the absence of food. According to these researchers, FLP-1 subsequently activates NPR-6 that is expressed amongst others on the head SMB motorneurons and the cholinergic VC motorneurons (Oranth *et al.* 2018). Cell-specific expression of NPR-6 in these neurons could remediate aberrant bending angle defects in a *npr-6* mutant background (Oranth *et al.* 2018).

To our knowledge, this is the only case in which a functional role for NPR-6 has been appointed. However, FLP-1 only has a low potency to activate NPR-6 *in vitro* as compared to high potency binding of FLP-1 to FRPR-7 (Oranth *et al.* 2018). Therefore, we a high-affinity ligand of NPR-6 remains to be identified.

3.3.2 Predicted sNPF-type neuropeptides in C. elegans

In comparison to other taxa, there is a much higher diversity in predicted nematode sNPF peptides and receptors, possibly indicative of vibrant diversification in functions (Fadda *et al.* 2019; Mirabeau and Joly 2013). *flp-15*, *flp-18* and *flp-21* display the canonical motive for sNPF in other protostomes (Fadda *et al.* 2019). As for sNPF in insects, mainly a role in feeding-related behaviours is described for these predicted nematodes sNPF neuropeptides (Fadda *et al.* 2019).

The *flp-15* gene encodes three putative peptides (FLP15-1, FLP15-2A and FLP15-2B) that bind the NPR-3 receptor, but information on any biological roles is missing (Kubiak *et al.* 2003;

Li and Kim 2014). This stands in contrast with the six putative *flp-18* gene products, of which expression is known to be important in several processes (Li and Kim 2014). A first role is in the AIY and RIG interneurons, which require *flp-18* for food-search behaviours (Cohen *et al.* 2009). FLP-18 production by AIY evokes a switch from local food search to exploration of larger areas through a reduced number of turns and reversals, that otherwise keep the animal from dispersing over larger distances (Cohen *et al.* 2009). Moreover, Cohen *et al.* (2009) found that distinct isoforms of FLP-18 are sensed by NPR-4 and NPR-5 in physiological concentrations and mutations in either of the receptors elicits different defects. Both receptor mutants show the same increase in fat storage as *flp-18* mutants (Cohen et al. 2009). However, *npr-4* mutants lack the switch to exploration of larger areas for food search and exhibit a decreased fat storage, whereas *npr-5* mutants behaved as wild-type animals in food search area switch behaviour. *npr-5;daf-7* double mutants exhibited enhanced constitutive dauer-formation relative to *daf-7* single mutant phenotypes a phenotype that was also displayed by *flp-18* mutants (Cohen *et al.* 2009). *npr-4* and *npr-5* show partially overlapping expression patterns in a variety of neurons, including in several amphid neurons, such as AWA, the serotonergic ADF, the nociceptive ASH and ASE neurons, the gustatory sensory ASK neurons, DAF-7 producing ASI, ILP expressing ASJ neurons, and many more, as well as some interneurons, such as AIA and AUA (Cohen *et al.* 2009). This allows for a wide variety of neuromodulatory signalling downstream of FLP-18.

Earlier, the same research group also proved relevant binding of FLP-18 and FLP-21 to the NPR-1 receptor (Rogers *et al.* 2003). These peptides inhibit social feeding, a trait that occurs variably in nature, due to a polymorphism in NPR-1 at the 215th amino acid position. The 215 phenylalanine (F) allele in social strains is assumed to be ancestral and is substituted with valine (V) in some solitary isolates (Rogers *et al.* 2003). Introducing a *flp-21* deletion disrupts bordering behaviour in the solitary *npr-1* 215V strains, but not in either the social *npr-1* 215F strain or *npr-1* (null) mutants, while it enhances social feeding in both *npr-1* isolates (Rogers *et al.* 2003). Because *flp-18* mutants were also affected in their movements, the role of *flp-18* in social behaviour was not further assessed (Rogers *et al.* 2003).

Furthermore, *flp-18* expression levels were shown to increase upon starvation, whereas it decreases upon CREB1/CRH1 increments (Bhardwaj *et al.* 2018). Bhardwaj *et al.* (2018) further showed that FLP-18 activates NPR-1 and NPR-4, but not NPR-5, in the AVA and ASE inter- and gustatory sensory neurons respectively. In response, these neurons are inactivated, which leads to a decreased number of reversed body bends and reversal lengths, conversely increasing the distance covered during each run. In their conclusion, Bhardwaj *et al.* (2018) hypothesise that the earlier reported regulation of ASE and AVA on AWC and AIB might play a role in this process.

NPR-1, as well as NPR-2, also has a function in food-avoidance behaviour (Ezcurra *et al.* 2016). After repeated exposure to a repellent, such as cupper, *C. elegans* adapts its behaviour to this stimulus, by decreasing the naive reversal response upon exposure. In the absence of food, wild-type *C. elegans* adapts faster than in the presence of food (Ezcurra *et al.* 2011). However, similar to mutants with defective dopamine signalling, *npr-1* and *npr-2* mutants as well as *npr-1*;*npr-2* double mutants, show adaptation speeds that resemble wild-type fed-state responses in both presence and absence of food (Ezcurra *et al.* 2016). This deficient adaptation phenotype in the starved state could be rescued by *npr-1* or *npr-2* expression in the ASH neurons of the respective mutants (Ezcurra *et al.* 2016). Moreover, NPR-1 and NPR-2 appeared to act in parallel pathways as the double mutant displayed an enhanced difference from wild type adaptation, relative to either of the single mutants (Ezcurra *et al.* 2016).

Unexpectedly, *flp-18* and *flp-21* mutants resembled wild-type *C. elegans* rather than *npr-1* or *npr-2* responses. This suggests that there must be either another unknown signal or a more complicated neuropeptide signalling network to activate these receptors (Ezcurra *et al.* 2016). Based on previous results (Ezcurra *et al.* 2011), these researchers suggested a model in which dopamine inactivates unknown NPR-1 activating neuropeptide release in dopamine receptor DOP-1 expressing AUA neurons.

Acuity towards other noxious or repellent signals is also affected by other stressors than starvation. Upon hypoxia, 5-HT produced by ASG and ADF is perceived by the pharyngeal M4 motoneurons which in turn produce FLP-21 that acts on NPR-1 in the AQP, PQR and URX neurons. Thereby salt gustatory learning is enhanced unde hypoxic conditions (Pocock and Hobert 2010). Similarly, the thermal threshold for heat avoidance is increased in *flp-21* mutants (Glauser *et al.* 2011).

Finally, *C. elegans* has a sleep-like state in between larval stages, which was named lethargus (Choi *et al.* 2013). This state is decreased in *npr-1*, *flp-18* and *flp-21* mutants (Choi *et al.* 2013).

3.3.3 sNPF signalling in insects

sNPF was discovered in *D. melanogaster* and several sNPF peptides have been found in other arthropods as well (Nässel and Wegener 2011). In arthropods, sNPF signalling has roles in moulting, reproduction, regulation of locomotion, regulation of osmotic and metabolic stress and hormonal release at the corpora cardiaca (Bao *et al.* 2018; Dillen *et al.* 2014; Kahsai *et al.* 2010a, 2010b; Nässel and Wegener 2011) . Furthermore sNPF and isoforms are expressed in the sLNvs and LNd clock neurons, indicating a potential function in the circadian clock (Johard *et al.* 2008). To date, the most extensively studied role of sNPF remains the modulation of feeding-related behaviour (Dillen *et al.* 2014; Fadda *et al.* 2019; Nässel and Wegener 2011).

As Fadda *et al.* (2018) point out, the combined results of several studies using either transcriptomics, peptidomics, *in vitro* data or sNPF injections, have stated opposite effects of sNPF-sNPFR signalling in feeding-related behaviour of different insect species.

In one group, including *D. melanogaster*, *Bactrocera dorsalis, Apis mellifera, Bombyx mori, Leptinotarsa decemlineata* and *Periplaneta Americana*, sNPF is an orexigenic signal, as it is upregulated by starvation and induces food search, food intake behaviours or diapause (Ament *et al.* 2011; Christ *et al.* 2017; Huybrechts *et al.* 2004; Jiang *et al.* 2017; Ko *et al.* 2015; Mikani *et al.* 2012; Root *et al.* 2011).

This stands in contrast to the other group, which comprises amongst others *Aedes aegypti, Culex quinquefasciatus, Schistocerca gregaria* and *Solenopsis invicta*, in which sNPF signalling performs the role of an anorexigenic signal with increased expression upon satiety and accordingly, a decrease in these same behaviours (Chen and Patricia 2006; Dillen *et al.* 2014; Fadda *et al.* 2019; Liesch *et al.* 2013; Nagata *et al.* 2011; Onken *et al.* 2004).

The sNPF signalling pathway in insect feeding and feeding related behaviours is best studied in *D. melanogaster* (Fadda *et al.* 2019; Nässel and Wegener 2011). Lee *et al.* (2008) characterised a signalling pathway in which sNPF, originating from sNPFergic cells, activates sNPFR1 in adjacent insulin producing cells (Figure 5). Similar to mouse pancreatic β-cells, downstream of sNPFR1 ligand binding, ERK is activated, causing expression of ILPs, *Dilp1* and *Dilp2*. Dilp1 and Dilp2 signal through the *D. melanogaster* insulin receptor (dInR) expressed on target cells such as the fat body. In turn dInR activates Akt, resulting in a cytoplasmic localisation of the dFOXO transcription factor (TF). The latter event initiates and modulates many physiological processes that eventually yield observable differences in body size between the smaller *sNPF* hypomorphic mutants, medium sized wild-type flies and larger *sNPF* overexpressing mutants (Lee *et al.* 2008). Moreover, *sNPF* and *sNPFR* knockdown mutants exhibited increased expression of *Dilp2, 3* and *6*, whereas they exhibited decreased expression of *Dilp5*, and other genes downstream of dFOXO (Lushchak *et al.* 2015).

Finally, Root *et al.* (2011) published a study that focused on the dynamic function of the receptor. They showed that starvation promotes *sNPFR1* expression in olfactory receptor neurons in *D. melanogaster*, whereas *sNPF* expression remains constant throughout the feeding process. Starvation in this case is sensed through insulin signalling. They proved this with the observation that flies with a constitutively active insulin receptor (InR) did not display upregulated starvation-induced food-searching behaviour. Conversely, inhibition of PI3K that acts downstream of InR sensitised fed flies as if they were starved, while RNAi knock-down of *sNPFR*1 abolished this effect and showed the same phenotype as untreated *sNPFR1* knock-down flies. *sNPFR1* signalling also increases attraction towards appetitive odours, by inducing olfactory receptor expression in the antennal lobes (Ko *et al.* 2015).

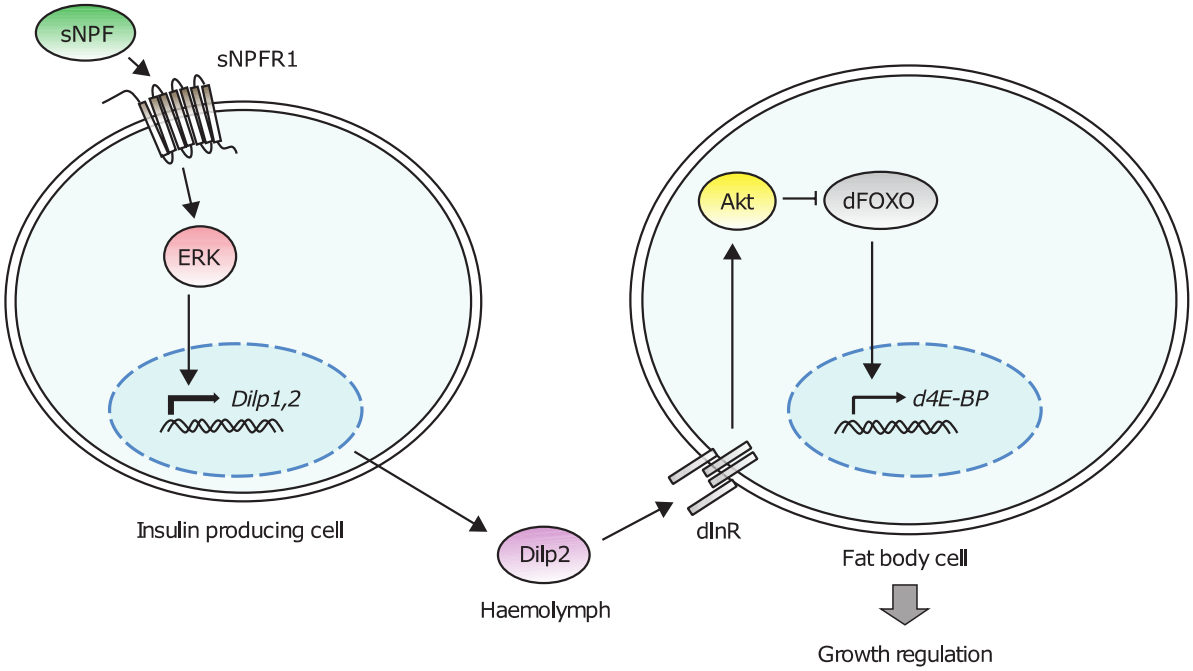

Figure 5: Example of sNPF signalling in D. melanogaster *with downstream insulin-like peptide signalling.* ***sNPF:*** *short neuropeptide F;* ***Dilp:*** *Drosophila insulin-like peptide;* ***dInR:*** *Drosophila insulin receptor,* ***dFOXO:*** *Drosophila FOXO transcription factor. (Lee et al. 2008; Reproduced with permission of Nature Publishing Group in the format of Thesis/Dissertation)*

3.3.4 sNPF in olfactory memory

Despite a role for the sNPFR-like proteins NPR-1 and NPR-2 in adaptation towards noxious stimuli, there have been no reported cases on a potential role of any of the predicted *C.elegans* sNPF neuropeptides nor their receptors in olfactory memory, to the extent of our knowledge (Ezcurra 2011, 2016). However, *D. melanogaster sNPF* knockdown mutants display defects in olfactory memory (Knapek *et al.* 2013). In *D. melanogaster*, olfactory sensory neurons are located primarily at the antennae and palps. The antennal lobe contains glomeruli, a type of specialised structures, which are connected via projection neurons to both the lateral horn and the mushroom body (MB; Li and Liberles 2015). The lateral horn is involved in innate odour-evoked response, while the MB is thought to be of major importance for learning and memory formation (Li and Liberles 2015). The intrinsic cells of the MB, i.e. the Kenyon cells (KCs), have been predicted to direct olfactory memory by integrating sensory information, after which this signal is relayed to other neuropils (Nässel and Wegener 2011).

Amongst expression in other (nervous) tissues, *sNPF* is expressed abundantly in the KCs of both adult and larval *D. melanogaster* (Johard *et al.* 2008; Nässel *et al.* 2008). As was shown using immunohistochemistry and fluorescent in situ hybridization, *sNPF* transcription and translation is highest at the end portions of the α/β- and γ-lobe of the MB (Crocker *et al.* 2016; Johard *et al.* 2008; Nässel *et al.* 2008). *sNPF* transcript and sNPF neuropeptide levels

are lower in the inner portion of these lobes and sNPF or its transcript is absent in the α'/β'-lobes (Johard *et al.* 2008; Nässel *et al.* 2008). Knapek *et al.* (2013) expressed the thermal activated cation channel dTRPA1 in the KCs of the α/β-lobe of the MB in *D. melanogaster*. Upon activation, they measured decreasing levels sNPF using immunofluorescent staining. This indicates that the KCs of the α/β- and γ-lobes secrete sNPF upon stimulation (Knapek *et al.* 2013). For both pan-neuronal and MB-specific *sNPF* knockdown mutants, olfactory memory was severely impaired in an odorant preference assay (Knapek *et al.* 2013). Conversely, pan-neuronal, but not MB-specific knockdown of the *sNPFR* transcript evoked a similar aberrant phenotype and MB-specific inhibition of *sNPFR* knockdown did not change this phenotype (Knapek *et al.* 2013). These results support a role of sNPF in signalling from the MB to other *D. melanogaster* brain regions (Knapek *et al.* 2013).

Next to sNPF, acetylcholine and the vesicular acetylcholine transporter are also needed in the KCs for wild-type olfactory memory to form in a odorant preference assay (Barnstedt *et al.* 2016). Moreover, M4/6 MB output neurons express the nicotinoid acetylcholine receptor and display transient calcium peaks upon proximal application of acetylcholine (Barnstedt *et al.* 2016). These transient calcium responses increased when acetylcholine was applied in combination with sNPF, whereas they were absent when sNPF was applied alone (Barnstedt *et al.* 2016). According to Barnstedt *et al.* (2016), this might indicate a modulatory role for sNPF that possibly facilitates cholinergic signalling at the KC-M4/6 neuron synapse.

Finally, Crocker *et al.* (2016) showed upregulation of *sNPF* expression after olfactory memory formation. Similarly, Jones *et al.* (2018) confirmed that transcripts involved in cholinergic and sNPF signalling are upregulated in the KCs after courtship memory formation. Courtship learning is a form of associative learning that involves several cues, including olfactory stimuli (Jones *et al.* 2018).

As mentioned, *npr-6* was reported to be a *C. elegans* sNPFR homologue and preliminary data suggested a learning deficit in *npr-6* deletion mutants. Therefore, we hypothesise that NPR-6 might perform a similar function in regulation of *C. elegans* olfactory memory as in *D. melanogaster* olfactory associative learning.

4. Objectives

Led by preliminary data and homology to the insect sNPFR, which is required for olfactory memory, we aimed to characterise a role for NPR-6 in olfactory associative learning (Cardoso *et al.* 2012; Knapek *et al.* 2011).

However, NPR-6 still is often mentioned as an NPFR homologue, in contrast to more recent findings (Cardoso *et al.* 2012; G. Jekely 2013; Mirabeau and Joly 2013). Therefore, we set out to first asses how NPR-6 relates phylogenetically to the sNPFR and NPFR clades with respect to another reported homologue, the vertebrate neuropeptide Y Y2 (NPY2R; Altschul *et al.* 1990; Cardoso *et al.* 2012; G. Jekely 2013; Mirabeau and Joly 2013; States and Gish 1991).

In line with the aforementioned findings in *D. melanogaster* we next investigated the suggested role for NPR-6 in associative learning (Knapek *et al.* 2011). To this purpose, we used the same DA associative learning assay in which a deficient learning phenotype was earlier identified for *npr-6* mutants. In this regard, it is important to distinguish potentially affected associative learning of mutant animals from (1) impaired wild-type phenotypes in response to either of the coupled stimuli starvation and diacetyl, from (2) potential locomotory defects and from (3) off-target genomic defects. Therefore, we also tested wild-type and *npr-6* mutant responses towards the uncoupled stimuli starvation or diacetyl. Moreover, we assessed proper locomotor abilities in a commonly used locomotion assay. To distinguish potential off-target genomic mutations that might cause the observed phenotypes in the DA assay, we included a rescue line that re-expresses *npr-6* in an *npr-6* deletion mutant background.

The *sNPFR* is widely expressed in the mushroom body in insects, which is indicative of a function in olfactory memory (Johard *et al.* 2008). To identify a potential role for NPR-6 in neural circuits associated with learning, we set a third goal to identify neurons that express *npr-6,* by the use of an extrachromosomal reporter construct from which *gfp* is transcribed together with the *npr-6* gene under regulation of the *npr-6* promotor region.

Finally, to fully understand NPR-6 mediated signalling, it is crucial to identify the conditions and cells from which its ligand is released. However, no high affinity ligand for NPR-6 has been reported. Up until now, only the low affinity ligand FLP-1 has been proven to act on NPR-6. Therefore, we aimed to identify other potential ligands by in an aequorin-mediated bioluminescence receptor screen.

II. MATERIALS & METHODS

1. Sequence Homology

To confirm homology of NPR-6 with insect sNPFR, we assessed phylogeny of NPR-6 with regard to three reported homologous receptor protein clades: arthropod sNPFR, arthropod NPFR and vertebrate NPY2R (Altschul *et al.* 1990; Cardoso *et al.* 2012; Jekely 2013; Mirabeau and Joly 2013; States and Gish 1991).

1.1 Phylogenetic tree construction

PROTEIN SEQUENCE ACQUISITION – The predicted translation of the *C. elegans npr-6* gene sequence was obtained from WormBase. All other protein sequences for phylogenetic analysis were obtained from the National Center for Biotechnology Information (NCBI; Table 1 and accession numbers therein; Kapustin *et al.* 2008; Lowe and Eddy 1997; Nawrocki *et al.* 2015; Pruitt *et al.* 2014; Thibaud-nissen *et al.* 2013).

PHYLOGENETIC TREE CONSTRUCTION - Tree construction was performed using an online tool, curated by Sebastien Santini (Dereeper *et al.* 2008). This tool conveniently combines several algorithms for phylogenetic analysis (Dereeper *et al.* 2008). In the standard protocol that was sufficient for our search, the Multiple Sequence Comparison by Log-Expectation (MUSCLE) iterative algorithm was applied for multiple sequence alignment (MSA; Madeira *et al.* 2019), after which the Gblocks program eliminated poorly aligned sequences (Talavera and Castresana 2007). Subsequently, PhyLM 3.0 software performed a maximum-likelihood estimation of phylogeny and a phylogram was rendered using TreeDyn (Chevenet *et al.* 2006; Guindon *et al.* 2010). The maximum number of bootstrapping permutations (100) within the PhyLM 3.0 software was opted to calculate branch support values. Finally, we visualised the percentage identity matrix (PIM) created by the MUSCLE algorithm using a custom script in RStudio v3.5.3.

1.2 Protein Alignment and Domain Prediction

The MUSCLE-generated protein alignment that was used for phylogenetic tree construction was visualised and annotated in JalView v2 and a snake plot was adapted from a snake plot made using TOPO2 (Johns 1996; Waterhouse *et al.* 2009). Transmembrane regions were predicted using InterPro and the location of residues predicted to be important for ligand binding and protein kinase C phosphorylation were highlighted as well (Christ *et al.* 2018; Mitchell *et al.* 2019). Simple metrics considering sequence coverage and identity were calculated using custom Python3.6 and R scripts in Spyder v3 and RStudio v3.5.3.

Table 1: WormBase ID and NCBI accession numbers for protein sequences used in phylogenetic analysis*. Protein names:* ***NPR-6,*** *neuropeptide receptor 6,* ***NPY2R****, neuropeptide Y receptor Y2,* ***(s)NPFR****, (short) neuropeptide F receptor. Method indicates how the protein sequence was obtained:* ***cDNA,*** *conceptual translation from a published cDNA sequence,* ***gDNA****, predicted translation from published genomic sequence; Status indicates whether the sequence has been predicted (P) or cloned and functionally confirmed (C).*

Organism	Protein	Accession Number	Method	Status
Caenorhabditis elegans	NPR-6	F41E7.3.1	cDNA	C
Mus musculus	Npy2r	AAI04734.1	cDNA	C
Takifugu rubripes	Npy2r	ABU87345.1	cDNA	C
Homo sapiens	NPY2R	NP_001357109.1	cDNA	C
Macaca mulatta	NPY2R	NP_001028004.1	cDNA	C
Gallus gallus	NPY2R	NP_001026299.1	cDNA	C
Nothobranchius furzeri	Npy2r	SBP53518.1	cDNA	P
Danio rerio	Npy2r	XP_021331562.1	gDNA	P
Drosophila melanogaster	NPFR	NP_524245.3	gDNA	C
Bombyx mandarina	NPFR	XP_028043671.1	gDNA	P
Armadillidium vulgare	NPFR	RXG67131.1	gDNA	P
Drosophila erecta	NPFR	XP_015009571.1	gDNA	P
Blattella germanica	NPFR	PSN42328.1	gDNA	P
Bicyclus anynana	NPFR	XP_023948220.1	gDNA	P
Drosophila serrata	NPFR	XP_020798669.1	gDNA	P
Anopheles gambiae	NPFR	AAT81602.1	cDNA	C
Aedes aegypti	NPFR	XP_001660966.3	cDNA	C
Helicoverpa armigera	NPFR	XP_021189904.1	gDNA	P
Rhodnius prolixus	NPFR	AKO62910.1	cDNA	C
Schistocerca gregaria	sNPFR	AGC54822.1	cDNA	C
Solenopsis invicta	sNPFR	AAY88918.1	cDNA	C
Anopheles gambiae	sNPFR	ABD96049.1	cDNA	C
Drosophila melanogaster	sNPFR	NP_524176.1	cDNA	C
Scylla paramamosain	sNPFR	AXK69167.1	cDNA	C
Culex quinquefasciatus	sNPFR	AVR59280.1	cDNA	C
Aedes aegypti	sNPFR	AVR59278.1	cDNA	C

2. C. elegans *strains and culture*

Wild-type *C. elegans* (Bristol strain; N2) was originally obtained from the *C. elegans* genetics centre (CGC). The deletion mutants for *npr-6* (LSC1493; from here onwards referred to as *npr-6* mutants) and *flp-26* (LSC1585; from here onwards referred to as *flp-26* mutants) were obtained from the National Bioresource Project (NBRP) and CGC respectively and outcrossed in the host lab. The strain ZX2038 was kindly provided by Alexander Göttschalk at Frankfurt University (all strains can be found in supplementary table D).

Unless stated otherwise, all strains were cultured in an incubator at 20°C on nematode growth medium (NGM: 1.7% agar, 0.75% bactopeptone, 25 mM KH_2PO_4/K_2HPO_4 pH 6.6, 50

mM NaCl, 13 mM cholesterol, 1 mM $CaCl_2$, 1mM $MgSO_4$ in autoclaved distilled water [AD]) with 250 µl *Escherichia coli* OP50 as a food source. In preparation of the diacetyl learning assay, the locomotion assay and before injection, *C. elegans* were cultured in a climate regulated room at 20°C and 40% relative humidity.

3. Molecular biology

To visualise *npr-6* expression and to create a rescue construct to inject in *npr-6* mutants, we attempted to insert 2,000 bp of the *npr-6* promotor promotor region (*npr-6p*), followed by the wild-type *npr-6* genomic DNA (gDNA) or complementary DNA (cDNA) sequence, into a pSM vector. pSM-*npr-6p::npr-6::sl2::gfp* was the envisioned construct.

3.1 Transgenesis

VECTOR CONSTRUCTION (supplementary section b) – We first amplified the regions of interest (*npr-6p* and *npr-6*) using Q5® High-Fidelity DNA polymerase (NEB) with the appropriate primer pairs in a polymerase chain reaction (PCR; supplementary table B). In our attempts to insert these regions into the plasmid vector, we followed two distinct workflows that use a different means to open the circular vector: (1) restriction-digestion of the vector and PCR amplified fragment with the restriction enzyme BamHI and (2) PCR amplification of the vector with Q5® high fidelity Taq DNA polymerase (NEB; Supplementary table B), followed by ligation using the Gibson Assembly® kit (NEB) of the PCR amplified region of interest in the pSM vector. In addition, we attempted to create an *npr-6* rescue line with a linear fragment comprising 2,000 bp in the *npr-6* promotor region (*npr-6*p), followed by *npr-6*.

C. ELEGANS CULTURE – The day before injection, approx. 50 *C. elegans* in the fourth larval stage (L4) were picked on an NGM plate and incubated at 15°C to make sure to have young adult *C. elegans* at the right time on the day of injection.

INJECTION MIX PREPARATION – Both the plasmid for localization (pSM-*npr-6p::npr-6::sl2::gfp*) and the linear construct for functional rescue (*npr-6p::npr-6*) were purified using the Wizard® SV Gel and PCR Clean-Up System (Promega). Before injection, all constructs were verified by sequencing. Sample preparation and sequencing was done according LGC genomics instructions. Initially, 25 ng/µl of plasmid/PCR fragment was combined with 50 ng/µl coinjection marker. For the localisation plasmid, the coinjection marker *uncp-122*::*DsRed* was used, whereas for the linear rescue fragment, we used *uncp-122::gfp*. Before injection, this injection mix was centrifuged at maximum speed (16,000 rpm) for ten minutes to remove any aggregates.

C. ELEGANS *PREPARATION* – At the time of injection, two to three young adult hermaphrodite worms were handpicked in a droplet of halocarbon oil on a 2% agarose pad. Subsequently, individual worms were gently pushed into the agarose pad using an eyelash picker to immobilise the worms. The agarose pads were made in advance by squeezing a droplet of 2% agarose in between two cover slits after which one of the cover slits was removed and the pads were dried overnight at 37°C.

INJECTION – Injections were performed by trained personnel (Elke Vandewyer, Katleen Peymen and Marijke Christiaens) as described before (Peymen 2019a): 2µl of supernatant was loaded into a borosilicate needle (Harvard Apparatus Ref.30-0067 1.5 OD x 1.17 x 150 L mm) that were pulled *ad hoc* from a heated capillary. The needle was inserted into birefringent particles at the widest part of the distal core cytoplasm of one gonadal arm, in a sharp angle to the body surface. Next, solution was injected until the gonads swell, after which the needle was removed. Each time, the needle was cleaned before to move on to the next worm injection.

C. ELEGANS *RESCUE* – After injection, injected worms were released from the agarose pad and halocarbon oil in a drop of physiological M9 buffer (1M H_2PO_4/Na_2HPO_4 pH 7.5, 85 mM NaCl, 1 mM $MgSO_4$, in autoclaved Ultra-pure milliQ water [mQ; Millipore]) and all worms on each agarose pad were picked with an eyelash picker onto one 25 mm NGM plate seeded with 50 µl of *E. coli* OP50. The plates were maintained in an incubator at 20°C and were checked regularly for the appearance of fluorescent worms. Maximally five fluorescent offspring individuals were singled out from each parental plate on a separate 90 mm NGM plate.

3.2 Expression pattern analysis

VISUALISATION – Prior to visualisation, approximately twenty worms were picked to a drop of M9 buffer solution on a fresh 2% agarose pad. The drop of M9 buffer solution allows to easily mount the worms on the pad and 3 µl of 1M sodiumazide (NaN_3; Sigma-Aldrich) was added to paralyse the worms. Expression patterns were visualised using an Olympus Fluoview FV1000 (IX81) confocal microscope.

NEURON IDENTIFICATION – Confocal Z-stack projections were combined to a three-dimensional reconstruction from which representative pictures were obtained using Imaris 7.2 (Bitplane) software. Some neurons can be identified based on a particular position and morphology (Albertson and Thomson 1975; Altun and Hall 2005).

In addition, 1,1'-Dioctadecyl-3,3,3',3'-Tetramethylindocarbocyanine Perchlorate (DiI; Invitrogen) was used to specifically stain ADL, ASH, ASI, ASJ, ASK and AWB, as well as PHA, PHB, IL1, IL2, ILsh and ILso cells. Two densely populated NGM plates were washed off using physiological M9 buffer and transferred with a plastic Pasteur pipette into a 15 ml Falcon™

tube. Worms were spun down at 1,200 rpm for two minutes. The pellet was washed at least two times with M9 buffer until it was clear. Next, the pellet was transferred to a 1.5 ml Eppendorf tube® and spun down at 1200 rpm for 1 minute. Supernatans was removed, and 1 ml of M9 was added, together with 5 µl of DiI. The tube was incubated at 20°C for 1.5 hours in a rotor to provide sufficient oxygen. After 1.5 hours, *C. elegans* were spun down again at 1,200 rpm and washed several times with M9 to remove the excess of dye. 20-50 *C. elegans* were pipetted on the agarose pads and immobilised as described before and co-localisation was assessed.

4. Olfactory plasticity – Olfactory associative learning assay

To test for olfactory learning, we made use of the diacetyl learning assay as described before (Stetak *et al.* 2009; Vukojevic *et al.* 2012). This assay makes use of the innate attraction of *C. elegans* towards diacetyl. After three hours of exposure to DA, combined with the absence of food, wild-type animals display decreased attraction towards DA.

4.1 Synchronization of a population

One week prior to the assay, worms were picked to fresh NGM plates and maintained in a temperature-controlled room at 20°C in the absence of any traces of diacetyl. 72 hours before the assay, the *C. elegans* population was synchronised by bleaching:

Young adult animals were washed off three densely populated NGM culture plates with physiological M9 buffer and collected in a 15 ml Falcon™ tube using a plastic Pasteur pipet. Adult worms were pelleted by centrifuging for two minutes at 1,200 rounds per minute (rpm). The supernatans, containing bacteria was discarded and the pellet of adult worms was washed with M9 and centrifuged until the supernatans was clear.

When supernatans was clear, the pellet of adult worms was transferred carefully to a 1.5 ml Eppendorf tube®. M9 was added again up to the 1.5 ml mark and adult worms were pelleted again by centrifugation at 1,200 rpm for one minute.

Next, 500 µl bleaching solution (40% 1M NaOH, 60% 1M NaClO) was added to each tube to lyse adults without affecting the mature eggs residing within the ovaries. After approximately four minutes of gently inverting the tubes, M9 was added and the solution was shaken well to neutralise the pH. The eggs were pelleted by centrifugation at 2200 rpm for one minute. The pellet of eggs was washed with M9 for several times, until the pellet loses its initial yellowish colour and the smell of the bleach solution disappears. Supernatans was discarded after each washing step. After the final wash, the pellet was not resuspended and with a P10 micropipette tip with a cut tip, 2.5 µl of eggs was plated on at least three NGM plates.

4.2 Naive Chemotaxis

POURING CHEMOTAXIS PLATES – On the day of the assay, fresh chemotaxis plates (2% agar, 5 mM KH_2PO_4/K_2HPO_4 pH 6.6, 1 mM $CaCl_2$, 1mM $MgSO_4$ in AD) were poured and let to dry to the air on benchtop in the room where the assay will take place and the bleached *C. elegans* culture plates were brought in the room to acclimate.

NAIVE CHEMOTAXIS – After ca. 30 minutes of acclimation, worms were washed off the NGM plates with chemotaxis buffer (CTX buffer; 5 mM KH_2PO_4/K_2HPO_4 pH 6.6, 1 mM $CaCl_2$, 1mM $MgSO_4$, in AD) and collected in a 15 ml Falcon™ tube. *C. elegans* were allowed to precipitate by gravitation. After they precipitated, supernatans was discarded and the pellet was washed with CTX buffer twice until the supernatans was clear. While letting *C. elegans* precipitate by gravitation, the chemotaxis plates were prepared to assess the naive chemotaxis to diacetyl: on the bottom half of the chemotaxis plates, a template was drawn, consisting of three circles equidistantly positioned towards each other (Figure 6). 1 µl 1M NaN_3 (Sigma-Aldrich; an acetylcholine receptor inhibitor that paralyses *C. elegans*) was spotted centrally in two of the three circles. In addition, 100% ethanol was added to one NaN_3 spot and 0.1% DA (in ethanol; Sigma-Aldrich) was added to the other NaN_3 spot.

3 µl containing approximately 100 worms was transferred from the Falcon™ tube to a marked region on the chemotaxis plate as illustrated in figure 6 and excess buffer was briefly dried using a piece of paper towel. The lid was kept closed as much as possible in order to avoid DA to dilute from the plate or to influence chemotaxis on nearby plates. At least three replicate plates were run per chemotaxis assay.

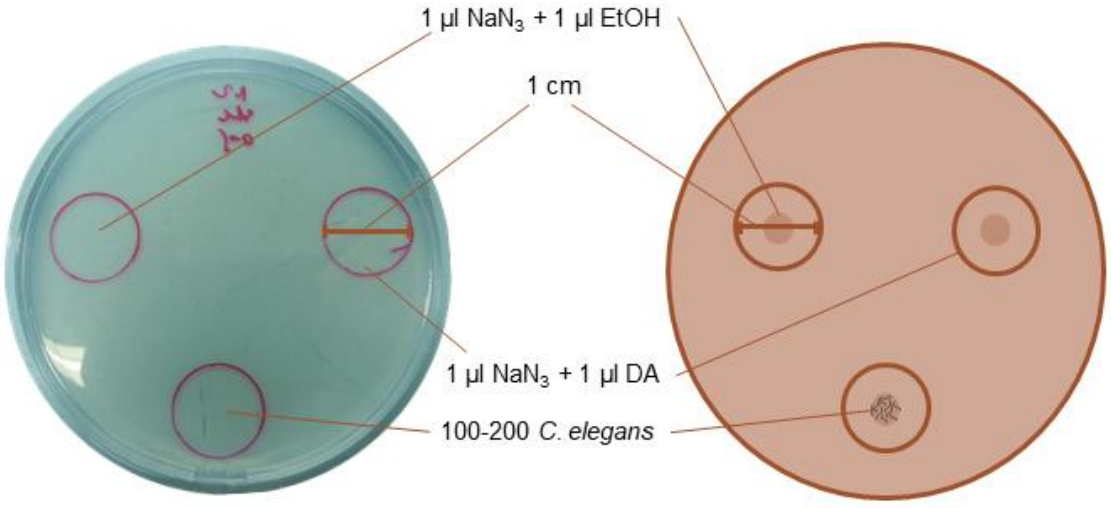

Figure 6: chemotaxis plates organisation. *3 µl of pelleted worms (ca. 100-200 worms) was placed as indicated. To calculate the chemotaxis index (CI), the amount of worms within a radius of 0.5 cm from the centre of the ethanol* ***(EtOH)*** *or diacetyl* ***(DA)*** *spot is counted after one hour of chemotaxis. 1 µl of sodiumazide* ***(NaN_3)*** *is used to paralyse the worms.*

CI CALCULATION – After one hour of chemotaxis, the number of individual *C. elegans* was counted in the DA circle and in the ethanol circle as well as the number of *C. elegans* that can be found in neither of the circles or the origin. These values were used to calculate a chemotaxis index (CI; equation 1), which gives a measurement of the proportion of worms that was attracted towards the DA spot, while penalizing attraction towards ethanol (Stetak *et al.* 2009; Vukojevic *et al.* 2012). In this way, the CI takes into account both the potential attraction towards ethanol as well as the probability of *C. elegans* being paralysed on a non-directed path.

$$CI = \frac{N_{DA} - N_{EtOH}}{N_{total}} \qquad \textbf{Equation 1}$$

In the equation, N_{DA} denotes the number of worms in the diacetyl spot, N_{EtOH} the number of animals in the ethanol spot and N_{total} the total number of worms on the chemotaxis plate (excluding the origin spot). In conclusion, the CI indicates the population-wide attraction towards DA. Since the rescue strain ZX2038 expresses *npr-6* from an extrachromosomal array, only those worms that expressed the reporter gene *gfp* were counted.

4.3 Diacetyl conditioning

To check whether a strain has a normal phenotype for learning, its chemotaxis after conditioning was compared with wild type.

CONDITIONING – For conditioning, three times 10 µl of adult *C. elegans* from the same initial population that was collected for naive chemotaxis was spotted on a chemotaxis plate for conditioning. Excess buffer was briefly dried with a piece of paper towel. At least two plates were used for conditioning. Finally, a line of 2 µl of 0.1% DA was spread on the lid of the chemotaxis plates. In this way, there was no physical contact possible with the drop of DA and the DA cue can only be perceived by olfactory sensory neurons.

The animals were left without food for at least three hours, making sure that they starve to enable short term associative memory formation. After three hours of conditioning, chemotaxis was assessed again (§4.2).

UNCOUPLED RESPONSES – To validate whether observed differences in CI were due to a conditioned response and not due to an altered CI upon exposure to only DA or starvation, the response to either of the conditioning cues was assessed as well. In this case, two additional conditions were used: (1) starvation-only plates, i.e. chemotaxis plates without DA on the lid and (2) DA-only plates, i.e. NGM plates seeded with *E. coli* OP50 in which a line of 2 µl of 0.1% DA was spread on the lid. As DA is highly volatile, starvation-only plates were sealed with Parafilm® to avoid any contact with the odorant. To avoid the spreading of bacterially produced odours, DA only plates were kept in a closed box on the other end of the room.

4.4 Statistical analysis

All analyses were carried out using a custom script in RStudio v3.5.3. We only used the data of an experiment when the assay worked for the wild-type strain, i.e. a mean naive CI > 0.65 and a mean conditioned CI < 0.65. We ran a linear mixed model using the lme4 package on the CI as dependent variable with condition and strain as fixed factors. The day and time of the experiment was considered a random factor to account for daily differences in the environment for which we could not accommodate. Residuals showed a normal distribution (Shapiro-Wilk W=0.919). Significance of pairwise comparisons across conditions and strains were assessed with a Tukey post-hoc analysis and we adjusted p-values for unequal variance across groups. Adjusted p-values < 0.05 were considered statistically significant.

5. NPR-6 deorphanization assay

5.1 Aequorin bioluminescence Assay

The host lab for this thesis is known for an extensive library of synthetic *C. elegans* (neuro)peptides that are challenged to orphan GPCRs in a reverse-pharmacological approach to identify potential ligands for these orphan receptors (Figure 7; Beets *et al.* 2011; De Haes *et al.* 2015; Peymen *et al.* 2019b; Van Sinay *et al.* 2017). This library is composed of 428 synthetic *C. elegans* (neuro)peptide gene derived peptides and isoforms that were synthesised on request of the host lab by Thermo Scientific and GL Biochem Ltd (Van Sinay *et al.* 2017).

CELL CULTURE – Chinese hamster ovary (CHO) K1 cells that were used in this assay were cultured in a monolayer at 37°C and 5% CO_2 in Dulbecco's Modified Eagles Medium nutrient mixture F12-Ham (DMEM/F12; Sigma-Aldrich) with addition of 10% fetal bovine serum (Invitrogen), 100 units/ml penicillin/streptomycin (Invitrogen), 250 µg/ml zeocin (Invitrogen) and 2.5 µg/ml fungizone (Amphotericin B; Invitrogen) in a humified incubator. Every three days, cell cultures were passaged (1:10) by detaching the cells with 2.5 ml trypsin-EDTA solution (0.25%, 2.5 g/l porcine trypsin, 0.2 g/l tetrasodium ethylenediaminetetraacetic acid [EDTA] in Hanks' Balanced Salt solution with phenol red; Sigma-Aldrich) from the culture flask .

TRANSFECTION – Prior to the receptor screen and at 60-80% confluency, Chinese hamster ovary (CHO) K1 cells cultured at 37°C were transfected with 13.8 µg *npr-6*/pcDNA3.1 plasmid, using 60µl Lipofectamine LTX and 24 µl Plus Reagent (Invitrogen) in a 30 minute time interval (Van Sinay *et al.* 2017). This cell line stably expresses a promiscuous human $G_{\alpha 16}$-subunit, mitochrondrially targeted apo-aequorin, which is a Ca^{2+} indicator, and a zeocin resistance gene. After 16-18 hours and 24 hours before the Ca^{2+}-mobilisation assay, cultures were provided with DMEM/F12 and put at 28°C.

CELL PREPARATION – At the day of the assays, cell cultures were washed with approximately 6 ml of phosphate buffered saline (PBS) after which they were resuspended in 30ml complete DMEM/F12 to which EDTA was added to detach cells from the surface. Cells were counted with a NucleoCounter (Chemotec) and if confluency was around 90%, they were resuspended in bovine serum albumin (BSA) medium (DMEM/F12 without phenol red with addition of L-glutamine, 15 mM 4-(2-hydroxyethyl)-1-piperazineethanesulfonic acid [HEPES; Gibco] and 0.1% BSA [Sigma-Aldrich]). Prior to the assay, the cells were incubated together with 5µM coelenterazine h (Invitrogen) at room temperature for four hours. Coelenterazine complements aequorin to a photoactive Ca^{2+}-sensitive protein (Van Sinay *et al.* 2017).

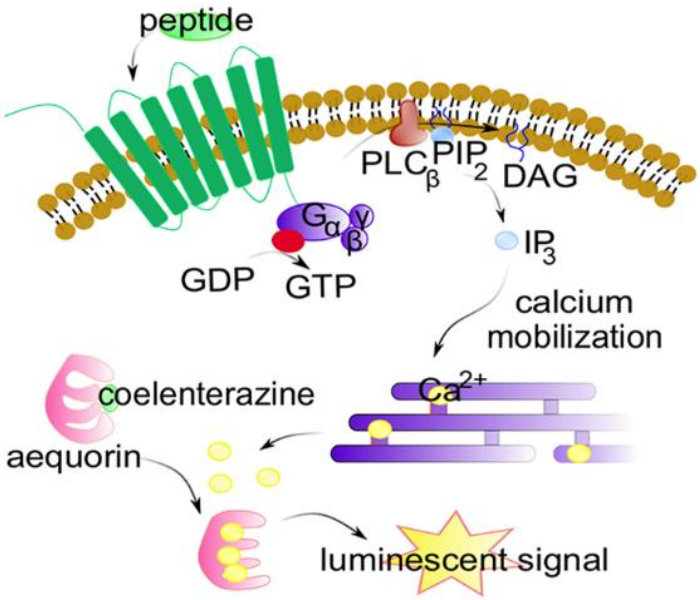

Figure 7: Schematic representation of aequorin bioluminiscence receptor deorphanisation*: ligand binding to a GPCR of interest, expressed on CHO K1 cells , activates signalling thorugh a promiscuous G_{α}-subunit, which in turn evokes Ca^{2+} mobilisation from the endoplasmatic reticulum. Upon binding of Ca^{2+} to the coelenterazine-aequorin complex, a luminescent signal appears.* ***GDP****, guanosine diphosphate,* ***GTP*** *guanosine triphosphate,* ***PLC$_{\beta}$*** *phospholipase C isotype β,* ***PIP$_2$,*** *phosphatidylinositol 4,5-biphosphate,* ***DAG,*** *diacylglycerol,* ***IP$_3$,*** *inosityol 1,4,5-triphosphate (Adapted from Peymen et al. 2019b, under license of the creative commons).*

PEPTIDE PREPARATION – Peptides from the library were solubilised in DMEM/F12 to a final concentration of 10µM after all acetonitrile, i.e. stock solvent, was evaporated in a SpeedVac device (ThermoFisher). Biogenic amines –octopamine hydrochloride (Sigma-Aldrich), tyramine hydrochloride (Sigma-Aldrich), dopamine hydrochloride (Sigma-Aldrich), melatonin (Sigma-Aldrich) and serotonin (Sigma-Aldrich) – were dissolved in BSA medium to a final concentration of 1 mM. Adenosine triphosphate (ATP) and BSA medium were included as positive and negative controls respectively.

Ca^{2+} MOBILISATION ASSAY – All five plates were mounted into a MicroBeta^2 Lumijet® reader the library was screened at 469 nm. 50 µl of cells were injected at a density of 250,000 cells/well and Ca^{2+}-mobilisation was measured for 30 seconds, after which Triton X-100 was added. Triton X-100 lyses the cells and releases all available Ca^{2+} from the mitochondria. Thereby, cell lysis leads to a maximal bioluminescence, allowing to estimate the total amount of cells in each well. Triton X-100 induced Ca^{2+} mobilisation was measured for another 30 seconds.

5.2 Data analysis

The calcium mobilisation response over a 30 minutes interval was summed as an approximation of the area under each curve. These values were first normalised over the Triton X-100 response to relative light units of which z-scores were calculated for every ligand. This was done separately for every plate, since ATP responses increased markedly across plates. A peptide response was considered a hit when the z-score exceeded a threshold value of two, which coincides with a value of two standard deviations from the median z-score per plate. The distribution of z-scores was used to confirm hit values visually. Peptides that were marginally not significant, i.e. between one and two standard deviations from the median z-score, were also visually evaluated and mentioned. All analyses were performed using a custom script in RStudio v3.5.3.

6. Locomotion assays

6.1 Video acquisition

To assess the innate locomotion behaviour of *C. elegans* strains either on or off food, we make use of a tracker platform created in-house by Drs. Jan Watteyne.

C. ELEGANS PREPARATION – In a climate-controlled room at 20°C, 25 to 30 worms were picked on an NGM plate that was either freshly seeded with *E. coli* OP50 or on an NGM plate that was left unseeded. For the fed condition, worms were directly transferred from their culture plate to the assay plate, whereas for the starved condition, worms were first picked into a watch glass filled with M9. After gently shaking the watch glass to remove most of the *E. coli* OP50, M9 was replaced once. Subsequently, worms were pipetted onto an unseeded NGM plate. Fed and starved animals were left to acclimate to the assay plate for 30 and 60 minutes respectively of which in both conditions at least 10 minutes on the light source.

VIDEO ACQUISITION – The tracker platforms included four 10 megapixel cameras (GigE PRO GP11004M NET ½,3” CMOS 3840 x 2748) each with a 10 megapixel lens (LM16JC10M Mp KOWA 2/3” F1.8) that were directly connected to a computer. In order to obtain easily trackable footage, the locomotion plates were placed on top of a glass stage that was placed over a

12”x12” inch diffuse LED light source (Rosco LitePad) and diffusion screen. Two consumer privacy filters in between the light source and the plates enhanced the contrast. Videos were acquired at 2 frames per second using StreamPix 6 Multicamera recording software which allowed to record several plates a time. This decreased the impact of temporal environmental differences amongst replicates that might appear when videos would be acquired sequentially. Plates were recorded for 10 minutes. For each condition, at least four different plates were recorded across two different days on a random time point between 9 am and 1 pm.

WORM TRACKING – The StreamPix software renders the data as a .seq file. To process data per frame, this was converted to individual pictures (.bmp) using a custom Python script. Worm tracking and behavioural segmentation was done for each worm using a custom MatLab script (developed by Drs. Jan Watteyne). Several parameters considering the position, body posture orientation and derived behaviours of the worm in each frame were collected in an excel file for analysis.

6.2 Statistical analysis

All analyses were carried out in RStudio v3.5.3. We ran a separate linear mixed model for each of the dependent variables speed in all behaviours, fraction of runs, fraction of turns, and fraction of pauses. Condition and strain were considered as fixed factors, whereas the experiment was considered a random factor to account for circadian and daily differences in the environment for which we could not accommodate. Significance of pairwise comparisons across conditions and strains was assessed with a Tukey posthoc analysis. P-values < 0.05 were considered statistically significant.

III. Results

1. *NPR-6 is a homologue of the arthropod sNPFR*

Two groups independently showed that *npr-6* is a close homologue of the arthropod sNPFR sequence, which was also automatically confirmed via the DIOPT v7.1 tool on FlyBase (Cardoso *et al.* 2012; Hu *et al.* 2011; Mirabeau and Joly 2013). In addition, *C. briggsae* NPR-6 also clusters near the insect sNPFRs (Jekely 2013). Accordingly, in the PANTER (Protein Analysis Through Evolutionary Relationships) classification system, NPR-6 clusters in the GH23382P subfamily, together with insect sNPFR receptor (Mi *et al.* 2019a, 2019b)

To confirm this finding and to investigate the position of NPR-6 with regard to two other homologues receptors, the arthropod NPFR and the vertebrate NPY2R, we constructed a phylogenetic tree for the predicted translation of the *C. elegans npr-6* gene (Figure 8).

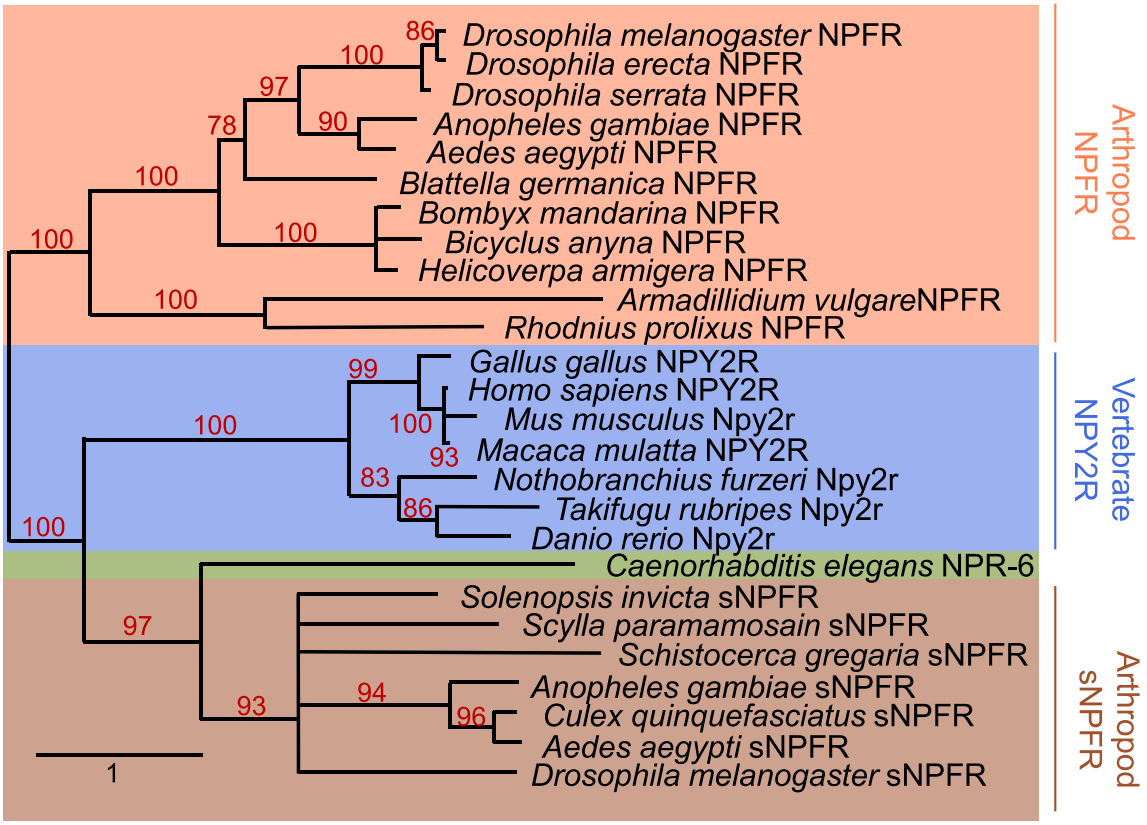

Figure 8: Phylogram for* C. elegans *npr-6 predicted translation, arthropod sNPFR protein sequences, arthropod NPFR protein sequences and vertebrate NPY2R protein sequences. *The arthropod sNPFR clade is highlighted in red. The position of npr-6 is highlighted in green. Vertebrate NPY2Rs are highlighted in blue, whereas arthropod NPFR sequences are highlighted in yellow. The tree was constructed using the maximum-likelihood estimation method build in the PhyML v3.0 software. Branch support values are shown as percentages based on 100 bootstrap permutations. Scale bar indicates evolutionary distance.* ***npr-6,*** *neuropeptide receptor family 6,* ***sNPFR*** *short neuropeptide F receptor,* ***NPY2R*** *neuropeptide Y receptor Y2,* ***NPFR,*** *neuropeptide F receptor. Accession numbers can be found in* ***table 1****.*

Our results confirm earlier findings that NPR-6 is a *C. elegans* homologue of the arthropod sNPFR, rather than a homologue of the arthropod NPFR as was previously assumed (Cardoso *et al.* 2012; Cohen *et al.* 2009b; Fadda *et al.* 2019; Mirabeau and Joly 2013). Furthermore, branch support values for our phylogenetic analysis are high and all sNPFR, NPFR and NPY2R protein sequences cluster together in separate monophyletic groups, in line with earlier findings (Cardoso *et al.* 2012; Mirabeau and Joly 2013).

The multiple protein sequence alignment used to construct the tree indicates that 20% of the 402 predicted NPR-6 amino acid residues was strictly conserved in all eight sNPFR protein sequences, including *C. elegans* NPR-6 (Figure 9; supplementary figure C). Moreover, 51.5% of the *npr-6* conceptual translation was aligned to an identical amino acid in at least one arthropod sNPFR. Within predicted transmembrane regions, this percentage was even higher (63.4%) and the highest percentages of strictly conserved residues lie within the predicted ligand binding regions (66.6%; Figure 9, supplementary figure C; Christ *et al.* 2017; Käll *et al.* 2004).

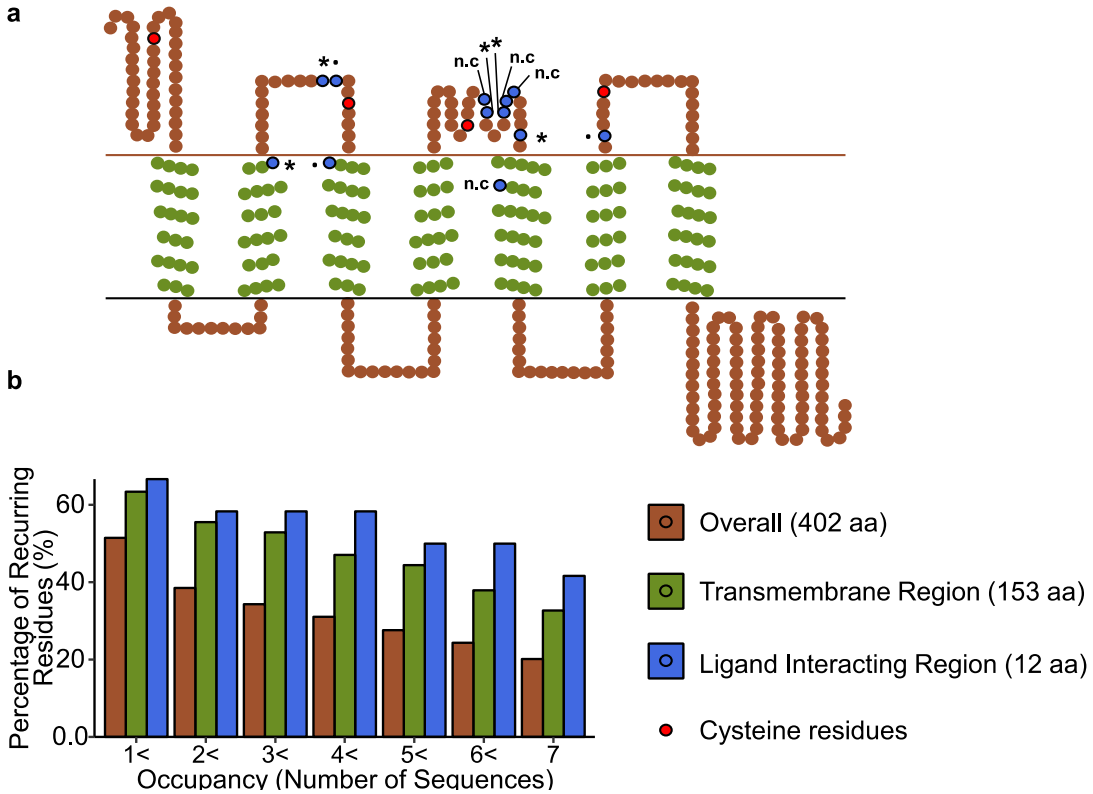

Figure 9: Predictions based on multiple sequence alignment: a) *snakeplot showing predicted transmembrane regions (green), residues predicted to be important for ligand binding (blue; Käll et al. 2004) and cysteine residues indicating potential cysteine-bridges. Conservation of the predicted ligand binding residues is represented as* ******* *when occupancy = 7; ·, when occupancy >1;* ***n.c*** *when occupancy = 0. (For full alignment, see supplementary Figure C)****; b)*** *Percentage of identical recurring residues over sequences is higher in transmembrane regions and predicted ligand interacting regions. Based on the MUSCLE-generated multiple sequence alignment, conservation appears to be highest in predicted regions for ligand interaction (69%, blue). Predicted transmembrane regions (green) were similarly enriched in identical recurring residues in aligned sequences (63.6%) as compared to overall percentage (red; 51.5%).*

2. NPR-6 might have a modulatory role in DA olfactory learning

In insects, *sNPF* is highly expressed in the mushroom body, a structure that is associated with olfactory learning and memory (Johard *et al.* 2008). Moreover, knockdown of *sNPF* or *sNPFR* impaired olfactory associative learning (Knapek *et al.* 2013). Since *C. elegans* NPR-6 has been reported as a sNPFR homologue, we assessed how NPR-6 interferes with olfactory learning. Unless stated otherwise, numerical values for the CI in the following chapters are the average CI for the indicated population of worms across experiments.

PRELIMINARY RESULTS – In line with a role for the *D. melanogaster* sNPFR in olfactory learning, host lab pilot experiments suggested a deficiency for *npr-6* mutants in the DA learning assay (data included in figure 10a): Upon three hours of conditioning on plates without food and in the presence DA, *npr-6* deletion mutants displayed only an insignificant decrease in CI relative to naive worms. This diminished decrease differs significantly from a marked decrease in CI for wild-type conditioned worms ($CI_{\text{conditioned } wt}$= 0.26, n = 5; $CI_{\text{conditioned } npr\text{-}6}$ = 0.60, n = 6; p-value = $3.23 \cdot 10^{-3}$). Naive animals of both strains displayed similar chemotaxis towards DA ($CI_{\text{naive } wt}$= 0.93, n = 4; $CI_{\text{naive } npr\text{-}6}$= 0.87, n = 4; p-value = $9.78 \cdot 10^{-1}$), suggesting that there are no defects in sensing DA or in the naive attraction towards it.

Led by these data, we attempted to further characterise the presumed aberrant learning phenotype of *npr-6* mutants. Moreover, the first learning assays performed in the context of this master's thesis corroborated earlier findings from the host lab (Figure 10a; $CI_{\text{naive } wt}$= 0.86; $CI_{\text{naive } npr\text{-}6}$= 0.75; $CI_{\text{conditioned } wt}$= 0.26; $CI_{\text{conditioned } npr\text{-}6}$= 0.60; p-value= $1.75 \cdot 10^{-4}$). However, additional repetition of the assay including uncoupled controls and a *npr-6* rescue line could not replicate the defect initially observed for *npr-6* mutants (cf. infra).

UNCOUPLED RESPONSES – The observed difference in CI across conditions per strain could be caused by a true learning defect, or as a response to three hours of exposure to either of the stimuli used for conditioning. Therefore, we assessed the chemotactic response after exposing both strains for three hours to either DA in the presence of food (DA-only control) or to starvation in the absence of DA (starvation-only control). For wild type, coupled conditioning caused the largest decrease in CI (figure 10b; $CI_{\text{naive } wt}$= 0.91; $CI_{\text{conditioned } wt}$= 0.48; p-value= $8.94 \cdot 10^{-7}$), exposure to DA alone caused an intermediate decrease in CI ($CI_{\text{DA only } wt}$= 0.61; p-value= $4.98 \cdot 10^{-2}$) and starvation-only caused a smaller decrease in CI ($CI_{\text{starved } wt}$= 0.67; p-value= $8.82 \cdot 10^{-4}$).

Surprisingly, the learning defect of *npr-6* mutants was only marginally observable in these assays since the CIs of the conditioned *npr-6* mutants were not significantly different from those of wild-type animals ($CI_{\text{conditioned } wt}$= 0.48; $CI_{\text{conditioned } npr\text{-}6}$= 0.53; p-value= 0.999). DA-only exposed *npr-6* mutants behaved in a similar way as DA-only wild type ($CI_{\text{DA only } wt}$= 0.61; $CI_{\text{DA only npr-6}}$= 0.62). However, starved only *npr-6* mutants exhibited a visually larger

decrease in CI as compared to wild type ($CI_{\text{starved } wt}$ = 0.67; $CI_{\text{starved } npr\text{-}6}$ = 0.42; p-value= $1.87 \cdot 10^{-3}$). This difference in CI upon starvation varied significantly across strains (p-value$_{\text{condition*strain interaction}}$ = $2.79 \cdot 10^{-2}$).

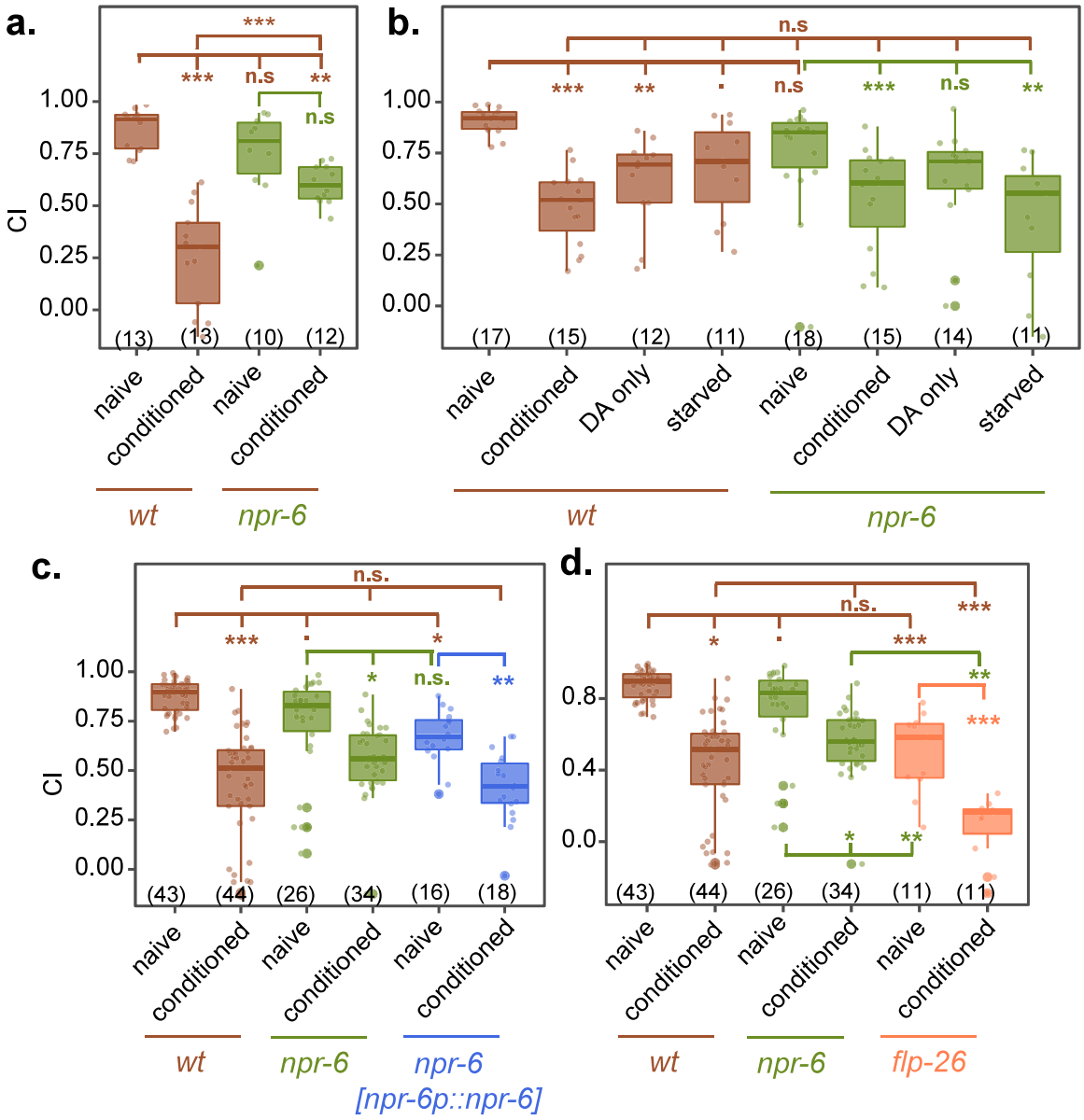

Figure 10: Results of the DA olfactory associative learning assay**. **a)** Preliminary results pooled with our results from initial assays we performed: npr-6 mutants have a higher CI after three hours of coupled conditioning than wild type; **b)** Uncoupled responses: DA-only and starvation-only conditioning also decreases CI. Starvation-only conditioned npr-6 mutants show lower CIs than starvation-only conditioned wild type; **c)** After performing more replicates, wild-type conditioned CI was higher than in preliminary data and there was no longer a difference between conditioned wild-type and npr-6 mutants. Rescued worms had decreased naive CIs. Conditioned rescue worms show no difference in CI. **d)** flp-26 has a diverging CI both in naive state as after three hours of conditioning**; *CI = chemotaxis index (equation 1); **DA** = diacetyl, **wt** = wild type; **npr-6:** LSC1493; **npr-6 (npr-6p::npr-6)** = ZX2038, the rescue strain; **flp-26** = LSC1585; ***, p-value < 0.001; **, p-value < 0.01; *, p-value < 0.05; ·, p-value < 0.1; **n.s.,** non-significant; individual dots represent replicate assay plates (numbers in brackets)*

NPR-6 RESCUE PHENOTYPE – Next, we asked whether the preliminarily observed differences might be rescued by expressing *npr-6* from the *npr-6* promoter in the same original background as the *npr-6* deletion mutants, i.e. LSC1493 (NBRP *mutant mt1497*). Despite several trials, we were unable to construct this line ourselves, but were kindly provided the strain ZX2038 by Prof. Alexander Gottschalk at Frankfurt University. This *npr-6* rescue strain expresses *npr-6* from an injected plasmid (pAO07-*npr-6p::npr-6::sl2::gfp*). ZX2038 animals showed a significantly decreased naive CI relative to wild type and a slightly lower naive CI than *npr-6* mutants ($CI_{\text{naive } wt}$=0.88; $CI_{\text{naive } npr\text{-}6}$=0.74; $CI_{\text{naive ZX2038}}$= 0.67; p-value= $1.36 \cdot 10^{-2}$). These results therefore suggest a decreased naive attraction to DA. Although the conditioned response of the rescue strain was more similar to wild-type conditioned responses than *npr-6* mutant conditioned CI, we could not identify significant differences between the CI of either of the strains ($CI_{\text{conditioned } wt}$= 0.43; $CI_{\text{conditioned } npr\text{-}6}$= 0.56; $CI_{\text{conditioned ZX2038}}$=0.42).

After having repeated the DA learning assay several times, *npr-6* mutant CIs after conditioning resembled the values which we initially observed. However, even though *npr-6* mutant CI was on average still smaller than that of wild type, the wild-type CI upon conditioning was markedly higher than the values observed in the preliminary data. Moreover, *npr-6* conditioned mutants behaved not significantly different from conditioned wild type (Figure 10c; p-value= 0.113).

FLP-26 PHENOTYPE – Finally, FLP-26 was earlier identified as a promising ligand of NPR-6 (host lab, unpublished data). Therefore, we also included *flp-26* deletion mutants in the DA assay. Naive *flp-26* mutants showed a decreased CI as compared to both wild type and *npr-6* mutants in naive condition (Figure 10d; $CI_{\text{naive } flp\text{-}26}$ = 0.49; p-values= $1.93 \cdot 10^{-6}$ and $2.41 \cdot 10^{-2}$ respectively). In addition, the CI of conditioned *flp-26* mutants differed significantly from that of all other strains after conditioning (Figure 10d; $CI_{\text{conditioned } flp\text{-}26}$ =0.08; p-values = $1.93 \cdot 10^{-6}$, $9.07 \cdot 10^{-9}$ and $1.03 \cdot 10^{-3}$ respectively for wild type, *npr-6* mutants and rescue strain).

These data suggest that *flp-26* mutants do not behave in the same way as *npr-6* mutants in the DA assay and that *flp-26* have altered sensation of or attraction to DA already in the naive condition.

3. NPR-6 is expressed in neural circuits related to food-dependent behaviour

Since our results from the olfactory learning assay are partially ambiguous, we explored whether *npr-6* is expressed in neural circuits that might explain the observed chemotactic behaivours.

To visualise *npr-6* expression and translation, we tried to construct a pSM vector (pSM-*npr-6p::npr-6::sl2::gfp*) in which *gfp* is transcribed from the *npr-6* promotor together with *npr-6.* Despite several trials, we did not succeed in this attempt. Therefore, we injected wild-type *C.*

elegans with a highly similar vector (pSM-*npr-6p::npr-6::sl2::gfp*) that accidently contained a 99 bp deletion spanning exon 9 and 10 in the *npr-6* cDNA sequence (Supplementary figure D). This vector was made by Jeroen Tuttens, who completed his master's thesis in the host lab (2018). Two stable lines from independent founding animals were obtained (LSC1821 and LSC1823) and the observed expression patterns were consistent across both lines.

CELL IDENTIFICATION – Because of their particular shape (WormAtlas) and by comparing our images with the expression pattern reported by Oranth *et al.* (2018), we could identify the pharyngeal neurons I6, I4, MC, MI, NSM, and ALA with high confidence among the *npr-6* expressing neurons (Figure 11; Albertson and Thomson 1975). We also suspect expression in AIM, based on its projections to the nerve ring and position ventrally and posterior to the terminal bulb of the pharynx (Figure 11; supplementary figure E). Expression in AIM, however, needs to be confirmed by co-localisation with AIM-specific reporter gene expression. For example, *mbr-1p* is known to be expressed in AIM and some non-serotonergic head neurons (Kage *et al.* 2005). Alternatively co-expression of a reporter gene from *dop-5p* or *lgc-53p* with *cat-1p* also previously enabled identification of AIM (Bentley *et al.* 2016).

In addition, based on its shape and location, we also recognised the amphid sheath glial cell (AMsh; supplementary figure F). Furthermore, co-localisation with DiI staining allowed the identification of the sensory neurons ASK and ASI as *npr-6* expressing cells as well. Due to time limits, we could not cross our *npr-6* reporter strain with neuron-specific reporter strains, leaving some neurons unidentified.

NEURONAL FUNCTIONS – Most of the neurons we identified can roughly be assigned to one of three partially overlapping categories: First, MC, MI, NSM, I6, and I4 are all part of the pharyngeal nervous system that consists of 20 neurons of 14 subtypes and these neurons function to regulate pharyngeal pumping and food intake (Albertson and Thomson 1975; Avery and Horvitz 1989). Second, ALA has also been reported to initiate lethargus, a sleep-like state in between larval moults (Van Buskirk and Sternberg 2007; Raizen *et al.* 2008). Lethargus comprises a decrease in pharyngeal pumping and locomotory quiescence (Raizen *et al.* 2008). Thirdly, ASI and ASK are both sensory neurons that have repeatedly been reported together with NSM and AIM for their modulatory role in food-dependent locomotion (Bargmann and Horvitz 1991; Cohen *et al.* 2009b; Flavell *et al.* 2013; Hilliard *et al.* 2002; Jafari *et al.* 2011; Rhoades *et al.* 2019). Finally, relative to the identified neurons, the amphid sheath glial cell (AMsh) governs a wide range of functions, including regulation of neuronal development, modulation of synaptic transmission and guiding neuronal remodelling (as reviewed by Shaham 2015).

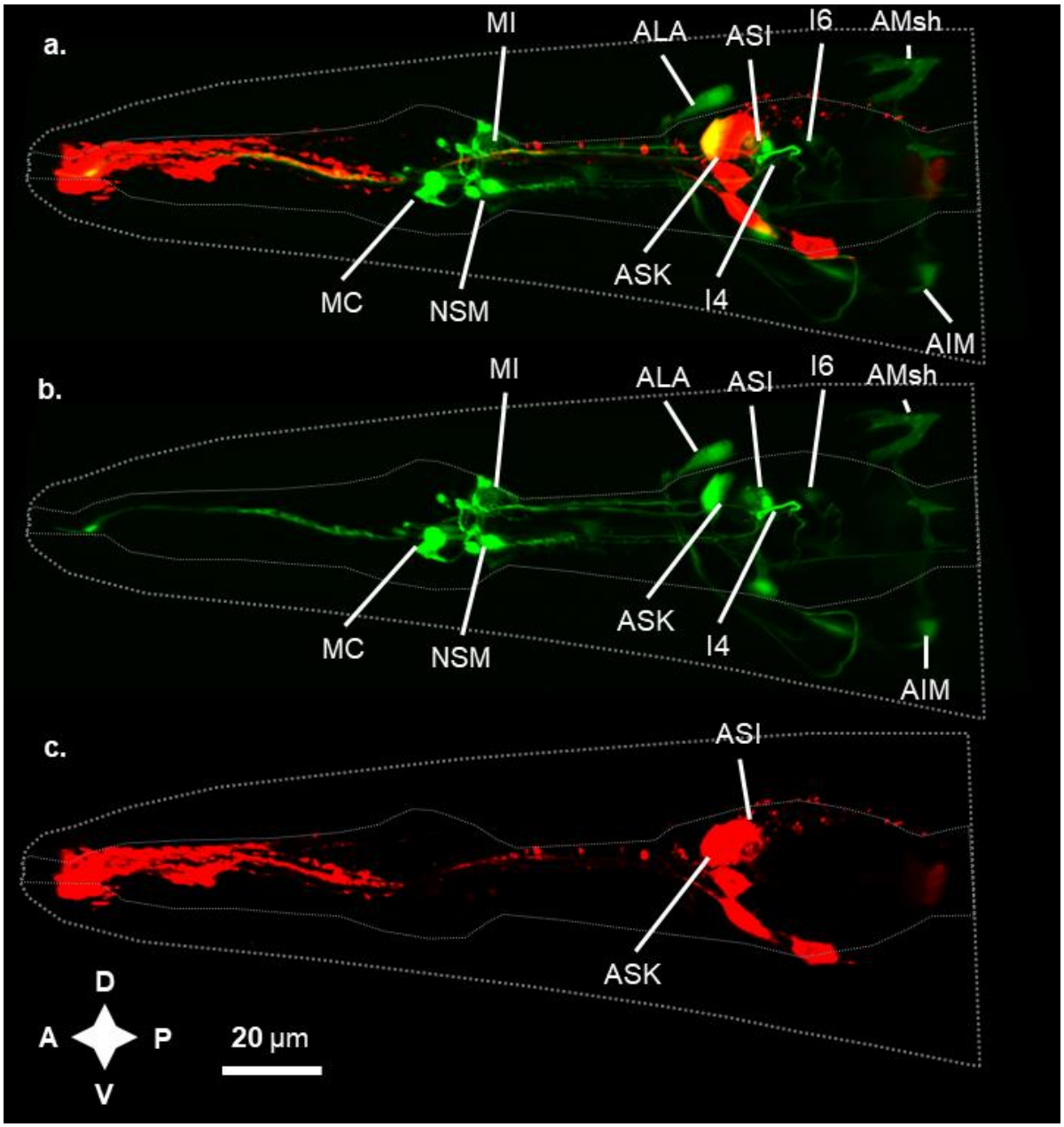

Figure 11: Lateral view on a representative example of the expression pattern of npr-6 using a) *gfp as an expression marker together with a red fluorescent DiI staining. gfp xpression was identified in MC left and right (MCL and MCR, resp.), MI, NSM, ALA, I6 and AMsh together with co-expression of gfp and DiI in ASK and ASI;* ***b)*** *gfp channel only;* ***c)*** *DiI staining only*

4. Promising ligands for NPR-6

flp-26 mutants showed a marked difference in naive chemotaxis towards DA as compared to *npr-6* mutants and had *in vitro* binding affinity in micromolar concentrations only (host lab, unpublished data). Therefore, we hypothesise that NPR-6 is not the main receptor through which FLP-26 acts. In literature, NPR-6 has been proven to be a low-potency receptor for FLP-1 (Oranth *et al.* 2018). *npr-6* mutants did not fully account for the altered locomotion phenotype of *flp-1* mutants and FLP-1 binds NPR-6 *in vitro* only in a concentration range of 10 to 100 µM, suggesting additional ligands for NPR-6.

To identify other potential ligands alongside FLP-26 and FLP-1, we challenged transfected CHO K1 cells expressing NPR-6, with the entire in-house *C. elegans* peptide library, as well as with five biogenic amines (octopamine, thyramine, melatonin, serotonin and dopamine). Four peptides with a z-score larger than two standard deviations from the mean z-score over

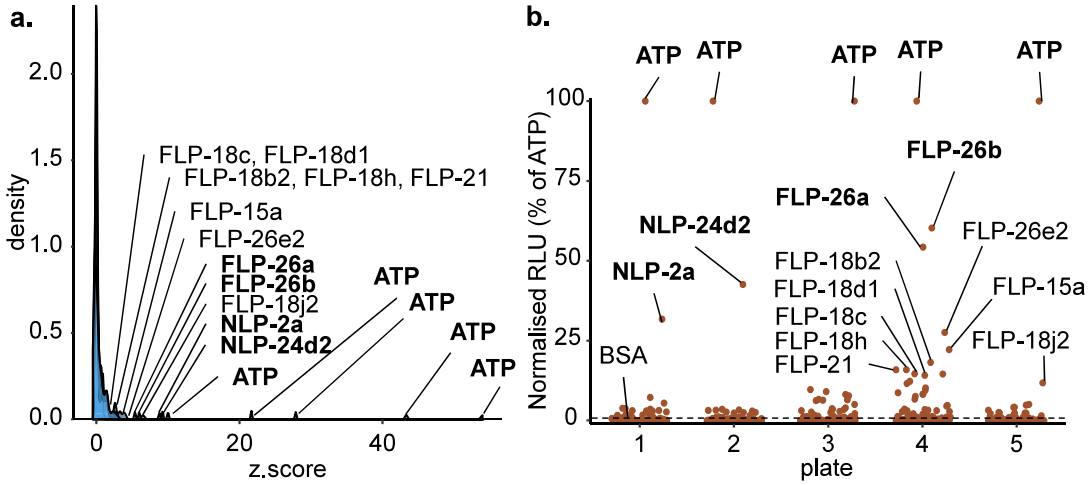

Figure 12: Promising potential ligands identified in the Ca^{2+}-mobilisation assay. a) *Density distribution of the z-scores for all peptides. Hits identified by an arbitrary threshold of two standard deviations from the mean z-score for all peptides per plate are visually recognisable.* ***b)*** *Proportional Relative light units (RLU) normalised per plate given as percentage of RLU of the positive control ATP. Both high confidence and low confidence hits can be visually distinguished from non-hit peptides;* ***bold*** *peptides indicate high confidence (2< standard deviations from the mean z-score for each plate), annotated non-bold peptides indicate lesser confidence (1< standard deviations from the mean z-score for each plate).* ***BSA*** *(negative control) shows where baseline levels lie.*

all peptides are expected to have high affinity for NPR-6 (Figure 12; Supplementary figure G): as expected, *flp-26* derived peptides a and b (FLP-26a and FLP-26b) were amongst these (host lab, personal communication), together with *nlp-2* derived peptide a (NLP-2a) and *nlp-24* derived peptide d2 (NLP-24d2). Peptides that had a lower z-score – between one and two standard deviations from the mean z-score – included *flp-18* derived peptides b2, c, d1, h and j2 (FLP-18b2, FLP-18c, FLP-18d1, FLP-18h and FLP-18j2), *flp-15* derived peptide a (FLP-15a), FLP-21, and *flp-26* derived peptide e2 (FLP-26e2).

5. NPR-6 affects locomotion behaviour

To interpret results from the DA learning assay as learning defects, proper locomotory function is required. Moreover, several neurons in which *npr-6* is expressed are reported to be involved in food-related locomotion. Therefore, we wondered whether the suggested *npr-6* mutant defects in the DA olfactory learning assay were not caused by a defect in locomotion. To investigate locomotory behaviour, we performed a commonly used assay in which wild type and *npr-6* mutants were tracked both on a plate with food in well-fed conditions as well as on

a plate without food after one hour of starvation (Figure 13). Afterwards, we extracted the average speed during all behaviours, a dispersal parameter (relative cell occupancy) and the fraction of runs, turns and pauses for each tracked animal.

AVERAGE SPEED – As described before (Calhoun *et al.* 2014), average speed ($\bar{v}$) of both strains increased in starved worms relative to well-fed worms (Figure 13a; $\bar{v}_{\text{fed } wt}$= 0.073 mm/s; $\bar{v}_{\text{fed } npr\text{-}6}$= 0.076 mm/s; $\bar{v}_{\text{starved } wt}$= 0.11 mm/s; $\bar{v}_{\text{starved } npr\text{-}6}$= 0.11 mm/s; p-value$_{\text{condition, } wt}$ = $1.34 \cdot 10^{-8}$; p-value$_{\text{condition } npr\text{-}6}$ = $7.08 \cdot 10^{-3}$). There were no observable differences across strains, although *npr-6* mutants had a slightly higher on-food median speed (median v_{wt} = 0.063 mm/s; median $v_{npr\text{-}6}$= 0.073 mm/s).

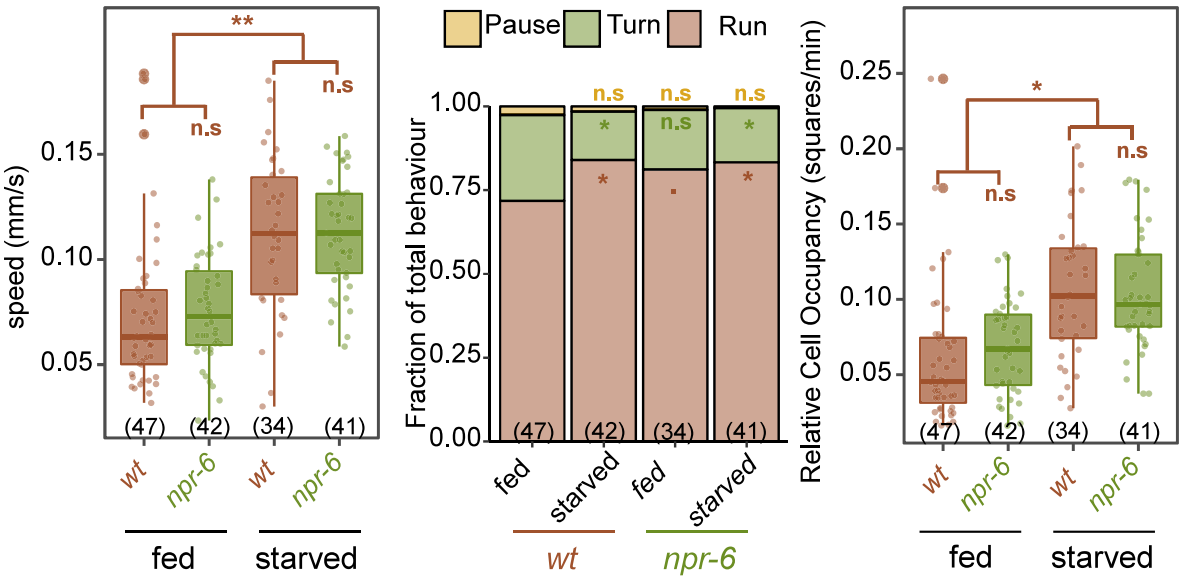

Figure 13: Locomotion behaviour of wild type and npr-6 mutants on food and after one hour of starvation off food a) *average speed across all behaviours (mm/s) was higher in both strains after one hour of starvation. Although not significant, on food speed is slightly higher in npr-6 mutants* ***b)*** *Wild-type relative fraction of runs, turns or pauses is higher off food, npr-6 mutant fraction of runs, turns or pauses did not differ across conditions; significances are compared to wild type fed condition, other comparisons were not significant.* ***c)*** *Relative cell occupancy, i.e. the number of squares in a hypothetical grid that were entered, normalised over the duration for each track is higher off food for both strains. On food, npr-6 mutants have slightly higher relative cell occupancy values; each dot represents individual worm tracks (numbers in brackets);* *****,*** *p-value < 0.01;* *******, *p-value < 0.05, ·, p-value < 0.1;* ***n.s.,*** *non-significant.* ***wt,*** *wild type* C. elegans*,* ***npr-6****, LSC1493: npr-6 mutant* C. elegans.

FRACTION OF RUNS, TURNS AND PAUSES – As expected (Calhoun *et al.* 2014; Roberts *et al.* 2016), the fraction of all behaviours that wild type spent running increased from 71.8% in well-fed condition to 84.1% in starved state (Figure 13b; p-value = $1.70 \cdot 10^{-2}$). Even though the *npr-6* mutant turning fraction was still slightly smaller in fed condition (81.2%), the difference with the fraction of turning in starved condition (83.3%) is insignificant.

Conversely, the wild-type fraction of turning decreased markedly from 25.6% in fed condition to 14.4% in starved condition (p-value = $2.66 \cdot 10^{-2}$), whereas *npr-6* mutant turning fractions did not differ significantly between well-fed (17.8%) and starved condition (16.2%). The fraction of pauses did not differ across strains or conditions.

RELATIVE CELL OCCUPANCY – Relative cell occupancy (RCO) is a measure to describe spatial exploration behaviour and indicates the amount of 1 mm² squares entered by individual worms relative to the duration of each track. Concomitant with increased speed and an increased fraction of runs, the mean RCO increased from fed to starved condition in both *npr-6* mutants and wild type (Figure 13c; mean $RCO_{\text{fed } wt}$ = 0.11 squares/min; mean $RCO_{\text{fed } npr\text{-}6}$ = 0.10 squares/min; mean $RCO_{\text{starved } wt}$ = 0.059 squares/min; $RCO_{\text{starved } npr\text{-}6}$= 0.068 squares/min; p-$value_{\text{condition effect}}$ = $9.05 \cdot 10^{-7}$). Although the median RCO for well-fed *npr-6* mutants (0.067 squares/min) was slightly larger than that of well-fed wild type (0.045 squares/min), this difference appeared not significant. There is no observable difference between both strains in starved condition either.

IV. DISCUSSION

1. NPR-6 is a sNPFR homologue

According to two reports and automatic homology searches on the FlyBase platform, NPR-6 is a *C. elegans* homologue of the arthropod sNPFR sequences (Cardoso *et al.* 2012; Hu *et al.* 2011; Mirabeau and Joly 2013). Moreover, *C. briggsae* NPR-6 was also clustered together with insect sNPFRs (Jekely 2013). This stands in contrast with earlier assumptions that NPR-6 is a homologue of the arthropod 'long' NPFR (Cohen *et al.* 2009).

To address the phylogeny of NPR-6 in regard of the arthropod sNPF and NPF receptor, we included several more confirmed protein sequences of insect sNPFRs and NPFRs and based on predicted homology, we also added vertebrate NPY2Rs to the multiple sequence alignment (Altschul *et al.* 1990; Cardoso *et al.* 2012; Mi *et al.* 2019a, 2019b; Mirabeau and Joly 2013; States and Gish 1991). Our phylogenetic analysis confirms with high confidence earlier findings that NPR-6 is a *C. elegans* homologue of the arthropod sNPFR and not of the arthropod NPFR (Figure 8, supplementary figure B; Cardoso *et al.* 2012; Mirabeau and Joly 2013). Moreover, NPR-6 shows an increased percentage of conserved residues within predicted transmembrane regions and regions that are predicted to be important for ligand binding (Figure 9; supplementary figure C). Therefore, we suspect that NPR-6 might also share ligand-binding properties with insect sNPFRs.

In earlier reports, the position of the vertebrate NPY receptor Y2 is ambiguous and clustered either together with the arthropod NPFR or together with the sNPFR (Cardoso *et al.* 2012; G. Jekely 2013; Mirabeau and Joly 2013). In our analysis, the sNPF receptors cluster more closely to vertebrate NPY2Rs, in line with finding of Cardoso *et al.* (2012). The phylogenetic tree by Cardoso *et al.* (2012), however, was constructed using the neighbour joining method, which is less accurate in clustering several sequences based on overall similarity of a sequence to a group of sequences, whereas the maximum likelihood and Bayesian clustering algorithms used by Mirabeau *et al.* (2013) are less dependent on these paired comparisons. The results of Mirabeau *et al.* (2013) are in line with subfamily GH23382P in the PANTHER classification database (Mi *et al.* 2019a, 2019b) . Although our tree was constructed using a maximum likelihood estimation method too, we only included three receptor clades in our analysis. We suspect that this might not be representative for the larger clustering.

In conclusion, based on gene and protein sequence homology, as well as conserved residues on predicted functionally important positions, our data confirm that NPR-6 is a *C. elegans* homologue of the insect sNPFR.

2. NPR-6 signalling may affect Chemotaxis Towards DA

2.1 *npr-6* mutants display increased chemotaxis upon conditioning

Both preliminary results from the host lab and our preliminary results suggested a learning defect in *npr-6* deletion mutants when compared to wild-type *C. elegans* in the DA olfactory learning assay (Figure 10). After repeating the assay with the same mutants several more times, this preliminary trend was no longer significant. Based on these results we could not confirm direct involvement of NPR-6 in DA olfactory learning. However, whereas observed CIs for *npr-6* mutants did not differ relative to preliminary data, wild-type CIs were markedly higher after repeating the assay.

The DA olfactory learning assay is very prone to environmental changes. Chemotaxis can be affected by many cues, including odours, temperatures, and light conditions. Since preliminary wild-type conditioned CIs were close to wild-type conditioned CIs reported before (Melissa Fadda, personal communication; Stetak *et al.* 2009; Vukojevic *et al.* 2012), we suspect that wild-type conditioning was not as successful in the major part of the diacetyl olfactory learning assays. Therefore, we consider these assays not sufficiently reliable to interpret with high confidence, whereas based on the combination of the host lab's and our preliminary results, we still suspect at least a minor defect in the altered chemotaxis response after three hours of conditioning with DA and starvation.

The high CI observed for *npr-6* mutants after three hours of conditioning can emerge due to (1) reduced associative learning capabilities, due to (2) locomotory defects or due to (3) altered responses to the cues to which worms are exposed during conditioning (starvation and DA).

To explore whether the high CI of *npr-6* mutants after three hours of conditioning was really an associative learning defect, i.e. solely evoked by presenting both cues together, we observed wild-type and mutant chemotaxis upon exposure to the uncoupled cues (figure 10b).

As expected, both wild type and *npr-6* mutants showed decreased attraction to DA upon prolonged exposure to DA, a phenomenon described in literature as stimulus adaptation (§I.1.1; Colbert and Bargmann 1995). Although not significant, DA-only conditioned worms were still slightly more attracted to DA than after coupled conditioning, which indicates that adaptation probably does not entirely explain the decrease in CI upon coupled conditioning.

Prolonged starvation caused a significant decrease in the *npr-6* mutant chemotactic response towards DA – a trend that was less expressed and insignificant, but still distinguishable for wild-type worms (Figure 10b). This observation was not as expected, since starved worms usually show near-naive chemotaxis towards DA (Melissa Fadda, personal communication). In this regard, it is important to notice that starved plates were kept in the same room as the coupled conditioning plates on which DA was applied every 30 minutes. A single layer of Parafilm® was the only barrier to separate worms on starvation plates from the

very penetrant odour DA. Therefore, there is a possibility that a low concentration of DA still reached worms on starvation-only plates. Even though the observed difference between strains might be caused by biological variation due to low numbers of replicates, our earlier observation that *npr-6* mutants might display impaired olfactory learning conflicts with this current explanation that links the diminished chemotaxis to a possible learned response, especially since the decrease in CI upon starvation is more expressed in *npr-6* mutants.

Alternatively, differences in CI after starvation could also be explained by an alteration in the attraction towards DA in response to starvation. Starved *C. elegans* respond differently to odours, such as benzaldehyde and isoamyl alcohol relative to well-fed worms (Colbert and Bargmann 1997). Moreover, whereas hermaphrodite *odr-10* expression is not as clearly dependent on feeding-state, male chemotaxis towards DA is increased by starvation-induced upregulation of the DA receptor gene *odr-10* (Ryan *et al.* 2014). Similarly, sNPF signalling in the fly species *D. melanogaster* and *B. dorsalis* increases sensitivity towards attractive olfactory signals, whereas it decreases aversive responses towards repellent odours (Jiang *et al.* 2017; Lushchak *et al.* 2015; Root *et al.* 2011; Tsao *et al.* 2018). Starvation-evoked upregulation of the *sNPFR* has been proposed to promote this behaviour and *sNPFR* knockdown animals displayed decreased attraction reminiscent to that of fed flies (Jiang *et al.* 2017; Ko *et al.* 2015).

According to these examples, we would expect that attraction to a cue that is naively attractive and indicative of food would increase upon starvation. Therefore, it is rather surprising that both wild type and *npr-6* mutants show decreased and not fed-state or increased chemotaxis towards DA in response to starvation. In the host lab, wild-type chemotactic behaviour upon exposure to the uncoupled responses is usually more similar to naive chemotaxis (Melissa Fadda, personal communication). With this in mind, our earlier hypothesis that traces of DA still reached the worms, resulting in a coupled conditioned response instead of a response towards starvation only is more likely to explain decreased attraction towards DA. However, the concentration of DA to which starved-only worms were exposed must have been much lower than DA concentrations on coupled conditioning plates.

As illustrated earlier in this paragraph, sensory acuity increases upon starvation. Next to sensory acuity, starvation was also shown to also enhance associative as well as forms of non-associative learning such as stimulus adaptation (Ardiel *et al.* 2016; Ezcurra *et al.* 2016; Ezcurra *et al.* 2011; Pocock and Hobert 2010). Since wild-type chemotaxis after coupled-conditioning is much higher than usually reported, the observed coupled-conditioned responses might not have been caused by associative learning: rather, starvation may have enhanced DA sensation. In turn, enhanced DA sensation could have enlarged the adapted response after exposure to DA only. In this perspective, differences in CI across strains might not be caused by a difference in associative learning capabilities, but by a difference in

alteration of DA sensation upon starvation. A generally lesser satiation of *npr-6* mutants due to disrupted anorexigenic signalling might turn *npr-6* mutant animals more responsive to DA at the start of the DA treatment, whereas wild-type animals might still have been more satiated shortly after transfer to the conditioning plates. This could be one mechanism that may explain our results. However, the potentially observed increased responsiveness to DA in *npr-6* mutants needs to be verified in a separate room when no DA was present during conditioning.

Nevertheless, our other observations contribute to the proposed hypothesis of NPR-6 involvement in anorexigenic signalling (cf. infra).

2.2 Overexpression of *npr-6* decreases naive chemotaxis towards DA

ZX2038 transgenic animals express *npr-6* from an extrachromosomal array in an *npr-6* mutant background. The exact number of injected copies of the vector is unknown and therefore this rescue strain might also overexpress *npr-6*. The rescue strain displayed a significantly decreased CI in the naive condition relative to wild type, but only a slightly smaller compared to *npr-6* mutants (Figure 10c). This decrease compared to wild type can originate from the way how we filtered the our data or by a true decrease in naive chemotaxis towards DA.

We opted to only include data from an experiment when wild type showed the expected decreased chemotaxis upon three hours of conditioning. Only those experiments for which naive wild type had an average CI above 0.65 and conditioned wild type had an average CI below 0.65 were retained. Seven out of 27 experiments failed these criteria and were not included in our analysis. This could partially explain the relatively small variation in the wild-type strain and also results in a higher probability to find a difference between the naive groups. In this regard, *npr-6* mutants show a marginally insignificant difference in naive chemotaxis relative to wild type too, which we ignored supported by this argument. However, the smaller sample size for the rescue strain withholds us from drawing the same conclusion.

Alternatively, in line with our other results and a hypothesised difference in sensory acuity of wild-type and *npr-6* mutant animals strains, NPR-6 might transmit a similar anorexigenic signal as the sNPFR in several insect species (Fadda *et al.* 2019; Nässel and Wegener 2011): since wild-type *C. elegans* is less responsive to attractive olfactory cues in fed than in starved state, increased anorexigenic signalling could increase fed-state modulatory pathways (Colbert and Bargmann 1997). Thus, increased anorexigenic NPR-6 signalling due to overexpression could decrease naive attraction towards DA.

Here too, it is important to note a potential conflict in our hypotheses since the putative *npr-6* overexpressing rescue strain shows a similar decrease in CI upon coupled-conditioning whereas we could expect this strain to be less responsive to double conditioning. However, if NPR-6 transmits an anorexigenic signal, such satiety signalling might be restricted to on-food conditions, without interfering with starvation signalling.

3. NPR-6 modulates food-dependent locomotion behaviours

3.1 NPR-6 signalling affects runs, pauses and turns in well-fed conditions

Because locomotion defects can also alter CIs, we evaluated whether *npr-6* mutants are unaffected in their locomotion abilities in order to correctly interpret results we obtained in the DA learning assay.

C. elegans displays a spectrum of locomotion behaviours depending on the presence of food (Flavell *et al.* 2013; Fujiwara *et al.* 2002; Gray *et al.* 2005; Wakabayashi *et al.* 2004). On food, *C. elegans* exhibits dwelling behaviour, which is characterised on average by low velocity, low rates of runs, small body bending angles and high rates of turning, pausing, and reversals as compared to off food conditions (Flavell *et al.* 2013; Gray *et al.* 2005). Shortly after removal from food, local search behaviour is initiated, a behaviour that is characterised by intermediate speed, low running rates, and maximal turning rates which are reflected in high body bending angles (Calhoun *et al.* 2014; Gray *et al.* 2005; Oranth *et al.* 2018). Finally, prolonged fasting induces a gradual transition from local search to roaming behaviour, which is in turn characterised by high velocity, high running rates, and low rates of turns and pauses (Calhoun *et al.* 2014; Flavell *et al.* 2013; Klein *et al.* 2017; Oranth *et al.* 2018). During dispersal sigmoidal propulsion increases body bending angles in comparison to dwelling, but they are slightly smaller than maximal bending angles during turns (Oranth *et al.* 2018)

While we observed wild-type locomotion behaviour in starved *npr-6* mutants on plates without food, well-fed *npr-6* mutants in the presence of food had a tendency towards starved-state behaviour with higher fractions of running, lower turning rates, slightly increased average speed and a similar minor increase in RCO (Figure 13). Despite these differences in average speed and RCO being not significant, both observations are indicative of slightly increased traveling distances on food – a trait that characterises roaming behaviour.

In addition to our results, Oranth and coworkers (2018) found that NPR-6 is required for proper mechanosensation of food. As such, they found a difference in local food search behaviour in *npr-6* mutants ten minutes after removal from food when compared to wild type: *npr-6* mutants had on average more than a twofold lower velocity than wild type (Oranth *et al.* 2018). Relative to wild type, *npr-6* mutants also dispersed less far from the origin and had slight, but non-significant decreases in body bending angles shortly after removal of food (Oranth *et al.* 2018). Since addition of food did not affect mean bending angles, they suggested that *npr-6* mutants lack a switch in locomotory behaviour shortly after the removal of food.

From our observations of *npr-6* mutant chemotactic behaviour we inferred a potential defect in anorexigenic signalling that might affect sensory acuity. Moreover, locomotion activity has also been extensively correlated with metabolic state (Bendesky *et al.* 2011; Calhoun *et al.* 2014;

Flavell *et al.* 2013; Gray *et al.* 2005). These findings are therefore in harmony with our earlier hypothesis on the role of NPR-6 in anorexigenic signalling.

A common observation between earlier observations and our findings is that *npr-6* mutants partially lack a switch in locomotory behaviour when food is removed. Whereas Oranth *et al.* (2018) found partial dwelling-like behaviour instead of local food search shortly after the removal of food, we interpreted our observations on food as partial roaming behaviour instead of dwelling. How these observations relate to each other remains to be investigated in detail.

3.2 *npr-6* is expressed in neural circuits that modulate locomotion

NPR-6 expression was previously reported by Oranth *et al.* (2018), who used an *npr-6p::gfp* transcriptional reporter strain to visualise *npr-6* expression. We created two independent transgenic lines by injecting the vector pSM-*npr-6p::npr-6::sl2::gfp*, containing a 99 bp deletion in exons 9 and 10. We obtained a more restricted expression pattern that was consistent across individuals of both independently founded strains.

We confidently identified expression of *npr-6* in a restricted number of neurons (figure : ASI, ASK, NSM, AIM, MC, MI, I6, I4 and ALA; and in one glial cell: AMsh. The more extensive expression pattern reported by Oranth *et al.* (2018) compared to the restricted pattern we observed might be explained by a different type of constructs used for the localization. Oranth *et al.* (2018) used a transcriptional vector in which *gfp* expression is regulated only by the *npr-6* promotor region, whereas in our construct *gfp* is preceded by *npr-6,* both genes being separated by a spliced leader recognition site (*sl2*). Therefore, potential additional sites for expression regulation contained within the *npr-6* gene sequence were lost in the construct of Oranth *et al.* (2018). In this respect, it should be noted that our vector contained the cDNA sequence and not the gDNA sequence. Therefore, our reporter could still miss additional regulatory elements in the introns.

In regard of the observed partial defect in dwelling to roaming behaviour on food, we wondered what neurons could explain these observations. Several neurons in which *npr-6* is expressed (ASI, ASK and NSM) are reported to regulate locomotion in *C. elegans* (Flavell *et al.* 2013; Gray *et al.* 2005; Rhoades *et al.* 2019; Wakabayashi *et al.* 2004).

ASI and ASK have repeatedly been related to the regulation of runs and turns. During local search, ASI and ASK promote opposite behaviours: whereas ASI increases the fraction of runs by which dispersal is promoted, ASK decreases the fraction of runs, which maintains local search behaviour shortly after removal from food (Gray *et al.* 2005; Wakabayashi *et al.* 2004). The downstream effects of ASI and ASK are integrated with the input of many other sensory neurons by a subset of interneurons: AIA, AIB, AIY and AIZ (Figure 3; Wakabayashi *et al.* 2004). Each of these interneurons has been reported to modulate a switch in locomotory

behaviour in response to food availability (Wakabayashi *et al.* 2004). Expression of *npr-6* upstream of these neurons suggests possible modulation of these behaviours upon NPR-6 activation.

In addition, ASI and ASK integrate information on external food availability with internal nutritional status. On the one hand, sensation of food availability is required to successfully exhibit the appropriate behaviour; be it dwelling when food is present, local search when food was recently present and roaming when food has been absent for a prolonged period of time. Upon ingestion of food, 5-HT is released form the food sensory NSM neurons and binds to the inhibitory MOD-1 5-HT receptor to inactivate ASI neurons (Flavell *et al.* 2013; Gray *et al.* 2005; Rhoades *et al.* 2019). Since ASI activity increases the fraction of runs, inactivation of ASI leads to a decrease in the fraction of runs and a concomitant increase in the fraction of turns (Gray *et al.* 2005). Hence, NSM released 5-HT induces dwelling in the presence of food. Moreover, *npr-6* is also expressed in AIM, a neuron that reabsorbs 5-HT by the MOD-5 serotonin transporter. In this way, AIM has been hypothesised to create a gradient of 5-HT that modulates local neurons to affect food-dependent locomotory behaviour and *mod-5* mutants show an increased locomotive response upon starvation (Jafari *et al.* 2011).

On the other hand, internal nutritional cues allow to adjust locomotion maximally to meet metabolic needs. In that regard, ASI activity is modulated upon exposure to nutrient signals. In response to satiation, ASI releases DAF-7 that inhibits dwelling and initiates satiety quiescence, a state of reduced locomotion and pharyngeal pumping (Davis *et al.* 2018; Gallagher *et al.* 2013; You *et al.* 2008).

Alongside ASI, integration of internal and external stimuli could also take place in other *npr-6* expressing neurons, including NSM, which directly senses food, AIM, which expresses *mod-5* and actively decreases 5-HT concentrations, and ASK, since ASK ablated animals display similar food-patch leaving behaviours as ASI ablated animals, and (Harris *et al.* 2019; Jafari *et al.* 2011; Oranth *et al.* 2018; Rhoades *et al.* 2019).

To conclude, these combined results suggest a mechanism by which nutritional status is integrated with food availability to fine-tune locomotive behaviour. Moreover, satiety signalling seems to involve multiple ligands and receptors (Harris *et al.* 2019; McCloskey *et al.* 2017; You *et al.* 2008). Therefore, we hypothesise that NPR-6 signalling might contribute to relay an anorexigenic signal alongside other signals, including ILPs and other neuropeptides.

4. NPR-6 as a global anorexigenic signal?

4.1 Predicted ligands of NPR-6 affect various food-dependent behaviours

Oranth *et al.* (2018) reported FLP-1 as a low affinity ligand of NPR-6, suggesting that high-affinity ligands possibly remain unidentified. By the use of a calcium mobilisation assay, we identified novel neuropeptides that were able to activate NPR-6 *ex vivo*.

Confirming host lab unpublished data, we identified *flp-26* derived peptides a and b as potential ligands (FLP-26a and FLP-26b). Since FLP-26 was already known as a high-potential ligand for NPR-6, we included *flp-26* deletion mutants in the DA assay to evaluate whether they would show a similar phenotype as *npr-6* mutants. When compared to all other strains, *flp-26* mutants showed decreased chemotaxis in both naive state and after conditioning. Hence, we concluded that the phenotype displayed by *flp-26* mutants is not directly or exclusively mediated by NPR-6. However, we cannot exclude confounding factors, such as a deviating locomotion phenotype which might have affected this behaviour. Therefore we do not reject FLP-26 as a potential ligand for NPR-6 in other functions than chemotaxis behaviour and FLP-26 should still be taken into account in future searches for functional ligands for NPR-6. No biological functions for FLP-26 have been reported.

Reported functions for the other identified potential ligands comprise of various behaviours. However, all of these peptides appear to modulate behaviours that are directly dependent on food-availability or nutritional status.

Next to FLP-26, we identified *nlp-2* derived peptide a (NLP-2a) and nlp-24 derived peptide d2 (NLP-24d2) as potent *ex vivo* ligands of NPR-6. *nlp-2* is only expressed in the diacetyl sensing AWA neuron pair and four uterine cells (Frooninckx 2015). NLP-2 binding to the human gonadotropin-releasing hormone receptor 3 has been reported to cause cessation of locomotion during lethargus (Frooninckx 2015; Nathoo *et al.* 2001). Lethargus is a sleep-like state between larval stages during which locomotion, as well as pharyngeal pumping is reduced to a minimum (Choi *et al.* 2013).

Cheong *et al.* (2015) showed that NLP-24, expressed in ASI, regulates basal pharyngeal pumping rates that are independent of the main pharyngeal pumping regulating MC neuron pair (Avery and Horvitz 1989; Raizen *et al.* 1995). This effect is at least in part achieved by autocrine signalling from ASI, a neuron pair that also expresses *npr-17*, a gene encoding an identified receptor for NLP-24 (Cheong *et al.* 2015). Since *nlp-24* expression increased upon prolonged starvation and *nlp-24* mutant animals spontaneously leave food lawns, NLP-24 seems to transmit an orexigenic signal in the absence of food (Cheong *et al.* 2015; Harris *et al.* 2019).

Other candidate ligands include the sNPF homologues *flp-15* derived peptide a (FLP-15a), *flp-18* derived peptides b2, c, d1, e2, h and j2 and peptide FLP-21, of which especially FLP-18j2 is of high potential. As described in the introduction (§3.3.2), FLP-15, FLP-18 and FLP-21 have been structurally identified as sNPF homologues (Cardoso *et al.* 2012; Fadda *et al.* 2019; Nässel and Wegener 2011).Therefore, these are promising ligands too, given the increased percentage of identical recurring residues in NPR-6 at positions predicted to be important for ligand binding to the insect sNPFR. Apart from FLP-15, for which no biological role has been described yet, FLP-18 and FLP-21 also display striking functional similarities to sNPF signalling in insects and seem to integrate nutritional status or food-availability into a range of food-related behaviours. FLP-18 and FLP-21 are produced by a limited subset of head neurons and bind several neuropeptide receptors (Rogers *et al.* 2003).

FLP-18 binding to NPR-1 and NPR-4 decreases both number and duration of turns and reversals, thus initiating a switch from dwelling to exploration behaviour upon prolonged starvation (Bhardwaj *et al.* 2018; Cohen *et al.* 2009b). *npr-4* and *npr-5* (another identified FLP-18 receptor gene) are expressed in a variety of neurons, allowing for diverse additional downstream signalling (Cohen *et al.* 2009b). For instance, FLP-18 binding to NPR-5 enhances dauer formation in *daf-7* mutants, a trait that is typically associated with stress, including starvation (Cohen *et al.* 2009).

Whereas starvation increases *C. elegans*' responsiveness towards attractive stimuli, it enhances adaptation towards repellents by decreasing sensory acuity for noxious stimuli such as cupper (Colbert and Bargmann 1997; Ezcurra *et al.* 2011). *npr-1* mutants displayed a retarded adaptation towards cupper (Ezcurra *et al.* 2011, 2016). In this way, *npr-1* mutant phenotypes resemble the deviating *npr-6* mutant phenotypes we observed in the DA learning assay. *flp-18* and *flp-21* mutants could not copy *npr-1* mutant phenotypes, indicating that there might be unidentified ligands for NPR-1 and NPR-2, or a more complex signalling network, in which NPR-6 may perform a role as well (Ezcurra *et al.* 2016).

Although these examples indicate that sNPF-like peptides in *C. elegans* signal the absence of food, other examples show that FLP-18 and FLP-21 are also capable of signalling food availability: NPR-1 activation by FLP-18 and FLP-21 inhibits social feeding, a behaviour that is known to be enhanced by several stresses, including starvation (Rogers *et al.* 2003). Moreover *npr-1* mutants also showed higher speed in the presence of food, like we observed for *npr-6* mutants (de Bono *et al.* 2002). Finally, FLP-18 and FLP-21 binding to NPR-1 on the pharyngeal neuron M4 induced lethargus, a sleep-like state between larval stages in which general locomotion, as well as pharyngeal pumping is reduced to a minimum (Choi *et al.* 2013). Unlike NLP-2, FLP-18 and FLP-21 probably also decrease sensitivity to arousal (Frooninckx 2015; Nagy *et al.* 2014)

Surprisingly, the assay we performed failed to identify FLP-1 as a ligand to NPR-6, possibly due to its low-affinity binding properties. Because of time restraints, we were not able to produce a dose-response curve. Importantly, we thereby also did not check for activation of an endogenous receptor of the CHO K1 cells. Therefore, our results may contain false positives. However, all identified peptides that have a reported function appear to be actively modulating behaviours in response to changes in food availability.

4.2 *npr-6* is expressed in neural circuits that modulate food-related behaviours

Next to the locomotion-associated neurons ASI and ASK, *npr-6* is also expressed in several pharyngeal neurons, including the locomotion modulating NSM neurons, as well as MI, MC, I4 and I6. Next to these five neurons, the pharyngeal nervous system contains only fifteen other neurons and is known to maintain normal pharyngeal pumping (Albertson and Thomson 1975). Moreover, NLP-24, an *ex vivo* predicted ligand of NPR-6, was shown to modulate pharyngeal pumping rates.

Just like food-dependent locomotion, pharyngeal pumping is affected by food availability (Avery and Horvitz 1990; Croll and Smith 1978; Niacaris and Avery 2003). Parallel to initiation of dwelling behaviour on food, 5-HT released by NSM binds several 5-HT receptors on MC – which we found to express *npr-6* as well – and other pharyngeal neurons to increase pharyngeal pumping rates in the presence of food (Hobson *et al.* 2006; Lee *et al.* 2017; McKay *et al.* 2004; Niacaris and Avery 2003). Alongside increased locomotory responses to starvation, inhibiting 5-HT reabsorption in the *npr-6* expressing AIM neurons increases 5-HT concentrations, which in turn increases pumping rates (Cunningham *et al.* 2012; Jafari *et al.* 2011).

We also observed expression of *npr-6* in ALA, a high pressure mechanosensory neuron that has been implicated in initiation of lethargus (Van Buskirk and Sternberg 2007; Katz *et al.* 2018; Raizen *et al.* 2008). As mentioned before, predicted ligands of NPR-6, NLP-2, FLP-18 and FLP-21, have been shown to be responsible for the decrease locomotion during lethargus (Frooninckx 2015; Nagy *et al.* 2014).

Therefore, we suspect that NPR-6 signalling is not only restricted to modulation of food-related locomotion, but rather tunes several behaviours to meet metabolic needs. We base this hypothesis on two observations: *npr-6* is expressed in neurons that adjust other behaviours than locomotion in response to food availability and several predicted NPR-6 ligands were already reported to be involved in such behaviours.

4.3 NPR-6 and sensory modulation

The amphid sheath glial cell is the last nerve cell in which we confidently found expression of *npr-6* (AMsh). This glial cell executes a wide range of functions (Bacaj *et al.* 2008; Han *et al.* 2013; as reviewed by Shaham 2015). In perspective of the behavioural deficiencies we observed for *npr-6* mutants, AMsh ablation has been reported to reduce chemotaxis towards odours sensed by the AWA sensory neuron, including diacetyl (Bacaj *et al.* 2008). Even though this effect on responsiveness towards such odours can be mainly contributed to AWA developmental deficiencies upon AMsh ablation, AMsh and other glia have been reported to modulate postsynaptic excitability in response to olfactory, gustatory and stimuli (Bacaj *et al.* 2008; Han *et al.* 2013; Wang *et al.* 2008, 2011). In addition, AMsh morphology alters when *C. elegans* enters the dauer stage upon prolonged starvation and other stresses, after which AMsh guides remodelling of other sensory neurons (Procko *et al.* 2011, 2012). AMsh ablation thereby inhibits dauer formation. These results show that AMsh seems to be responsive to starvation and is able to modulate sensory acuity. Therefore, NPR-6 mediated signalling in response to food might act on AMsh to decrease olfactory responsiveness towards attractive odours, such as DA.

Expression of the DA receptor gene *odr-10* in hermaphrodites is equal in well-fed and starved conditions and stimulus adaptation is does not depend on the ability to sense odours (Nuttley *et al.* 2002; Ryan *et al.* 2014). Therefore, alteration of olfactory acuity upon starvation is caused by an alteration in the electrophysiological signalling properties of downstream neural circuits. Glial modulation of synaptic transmission could explain how olfactory acuity towards DA is altered upon prolonged starvation and could contribute to the deviating phenotypes of *npr-6* mutants and the rescue strain in the DA learning assay. However, we'd like to stress that more knowledge on the active modulatory role of glia on neural circuits is needed and this hypothesis is therefore purely speculative.

5. NPR-6, a functional sNPFR homologue

We and others showed that NPR-6 is a *C. elegans* sNPFR homologue (Cardoso *et al.* 2012; Jekely 2013; Mi *et al.* 2019a, 2019b; Mirabeau and Joly 2013). Especially regions of the NPR-6 sequence that are predicted to be important for sNPFR function appear better conserved in (Figure 8; supplementary figure C; Christ *et al.* 2017; Käll *et al.* 2004). We already mentioned several examples to illustrate how sNPF signalling might help us understand *npr-6* mutant phenotypes. In the next paragraph, we further summarise functional analogy between the insect sNPF-signalling system and *C. elegans* sNPF-like signalling in regard of our results.

As we stated earlier, sNPF-like signalling in *C. elegans* is ambiguous and dependent on the particular behaviour under investigation (§4.1). Similarly, sNPF signalling in insects is not uniformly orexigenic or anorexigenic either – even across related species. Nevertheless, many similarities can be found regarding the general role of sNPF and sNPF-like signalling in insect and *C. elegans* feeding behaviour (Fadda *et al.* 2019; Nässel and Wegener 2011).

Similar to starvation-dependent upregulation of *npr-1, D. melanogaster sNPFR* expression is upregulated in response to starvation (Bhardwaj *et al.* 2018; Ko *et al.* 2015). Our hypothesis on *npr-6* mutant chemotaxis behaviour towards DA resembles sNPF-mediated increases in attraction towards appetitive odours in *D. melanogaster, A. aegypti* and *B. dorsalis* (Christ *et al.* 2017; Jiang *et al.* 2015; Ko *et al.* 2015; Lee *et al.* 2008; Lushchak *et al.* 2015; Root *et al.* 2011; Tsao *et al.* 2018). Similarly, *C. elegans* NPR-1 has been shown to increase olfactory preference towards attractive odours too (Macosko *et al.* 2009).

Analogous to described functions for sNPF-like signals in *C. elegans* and the described roles for predicted *ex vivo* ligands of NPR-6, insect sNPF is also involved in odour-independent exploration behaviour, modulation of gustatory preference, sleep, larval development, and resistance to stress, including starvation, desiccation and immune responses (cf. supra; Farhan *et al.* 2013; Inagaki *et al.* 2014; Jayakumar *et al.* 2016; Kahsai 2010a, 2010b; Kaneko and Hiruma 2014; Shen *et al.* 2016). Likewise, *C. elegans* NPR-1 is also required for immune responses and resistance to hypoxia (Pocock and Hobert 2010; Styer *et al.* 2008). Finally, sNPF is usually secreted together with other peptides that are often required alongside sNPF for sNPF-mediated behaviours (Christ *et al.* 2017; Kahsai *et al.* 2010b; Liesch *et al.* 2013)

In line with our hypothesis, these examples illustrate how sNPF signalling is not only informative of food availability, but rather reflects general metabolic status. sNPF signalling appears to function in concert with other signals and is thereby able to modulate a wide variety of behaviours.

6. Why we care

Even though the vertebrate NPY receptors Y1 and Y2 are more closely related to the insect NPFR, both vertebrate receptors were previously mentioned as the closest vertebrate homologue to the insect sNPFR (Cardoso *et al.* 2012; Mi *et al.* 2019; Mirabeau and Joly 2013). Alternatively, the prolactin releasing peptide (PrRP) receptor (PrRP-R) has been proposed as a vertebrate homologue of the insect sNPFR too (Fadda *et al.* 2019; Jekely 2013). Although the detailed phylogeny of these receptors relative to one another remains partially indecisive, all receptors are thought to share a distant common ancestor and show functional similarities (Fadda *et al.* 2019; Mirabeau and Joly 2013).

NPY and PrRP are mainly known to affect food intake. In parallel to ambiguity in the reported effects of sNPF signalling in arthropods and sNPF-like signalling in *C. elegans*, the effect of these vertebrate peptides depends on receptor to which they bind. Binding of NPY to NPY receptors Y1 and Y5, as well as PrRP to the PrRP receptor subtype 2 promote orexigenic behaviours (Naveilhan *et al.* 1998; Tachibana and Sakomoto 2014 and references therein). In contrast, binding of NPY and peptide YY (PYY) on NPY2R or binding of PrRP to PrRP-R transmit an anorexigenic signal (Batterham *et al.* 2002; Bjursell *et al.* 2007; Broberger *et al.* 1997; Naveilhan *et al.*, 2001). Moreover, single nucleotide polymorphisms (SNPs) in NPY2R and PrRP-R malfunction have repeatedly been linked to obesity and diabetes (Bjursell *et al.* 2007; Friedlander *et al.* 2010; Lavebratt *et al.* 2006; Siddiq *et al.* 2007; Yamashita *et al.* 2013). Analogously, SNPs in *npr-1* have been shown to affect *C. elegans* metabolism and feeding behaviour (Choi *et al.* 2013; Cohen *et al.* 2009). Likewise, SNPs in *D. melanogaster sNPFR* has been related to differences in metabolic profile too (Jehrke *et al.* 2018).

Other functions of these vertebrate receptors resemble aforementioned effects of sNPF signalling in invertebrates as well (§5): NPY1R, NPY2R and PrRP-R also affect starvation resistance, sleep, nociception, and immunity (reviewed by Ayachi and Simonin 2014 and Tachibana and Sakamoto 2014; Malis *et al.* 1999; Naveilhan *et al.* 2001; Sapunar *et al.* 2011; Singh *et al.* 2017). Notably, NPY1R and NPY2R are also required for proper learning in various paradigms (reviewed by Gøtzsche and Woldbye 2016). Furthermore, NPY1R, NPY2R and PrRP-R are expressed in brain regions involved in processing of olfactory cues and have been suggested to modulate olfactory acuity (Blakemore *et al.* 2006; Kaniganti *et al.* 2019; Loch *et al.* 2015; Stanić *et al.* 2006). These results are reminiscent to our interpretation of the olfactory learning phentoypes for *npr-6* mutants and to functions in alteration of olfactory acuity have been shown for the sNPFR (Ko *et al.* 2015; Root *et al.* 2011).

Together, these examples illustrate the importance of the distantly related NPY and PrRP receptors on animal well-being, including that of humans. These reported functions largely overlap with functions of ecdysozoan (s)NPF and sNPF-like signalling, suggesting that insights in protostomian sNPF signalling systems might improve our understanding of analogous signalling systems in vertebrates (Jekely 2013; Mirabeau and Joly 2013).

Despite the pathophysiological relevance of understanding the (s)NPF/Y signalling system, hunger is the second main driver of nearly all animal behaviours, with the first being reproduction. Therefore, understanding satiety signalling and how satiety signalling steers behaviour is of high economic and societal importance too. In search of food, important vector species transmit diseases that form a major threat to millions of people around the globe and the sNPF system has been identified in many of these, including vectors for malaria, yellow fever, dengue fever and sleeping sickness (Caers *et al.* 2016; Christ *et al.* 2017; Garczynski

et al. 2005). Not only insects, but also nematodes endanger our health (Bryant and Hallem 2018). Similarly, plant-parasitic nematodes give rise to huge agricultural losses and bring about uncertainty regarding food security in the near future (Bernard *et al.* 2016; Dong *et al.* 2014). Moreover, parasitic nematodes and disease vectors rely on a multitude of cues to guide their decisions. These include odours and nutritional signals to find or start searching hosts, be it plants or animals (Bryant and Hallem 2018, and references therein). In this context, the sNPF homologue FLP-18 has, for instance, already been shown to be involved in plant-host searching of a plant-parasitic nematode (Dong *et al.* 2014). Since sNPF signalling is restricted to the protostomian lineage, sNPF signalling effectors might even provide a useful target to combat these pathogenic and pest species.

7. Conclusion and perspectives

We set out to characterise the role of a *C. elegans* short neuropeptide F receptor (sNPFR) homologue neuropeptide receptor 6 (NPR-6) in learning and memory. We were initially guided by preliminary data that suggested a learning deficiency in *npr-6* mutants. However, our results of the *npr-6* mutant phenotype and a presumed overexpression phenotype in the diacetyl olfactory learning assays remain partially unresolved. Instead, this work provides multiple lines of evidence that point towards a potential role of NPR-6 signalling in satiety signalling. In this regard, *npr-6* mutants showed a tendency towards roaming-like locomotion on food, a behaviour that is usually elicited upon prolonged starvation. In line with this hypothesis, we interpreted deviations of *npr-6* mutants in the olfactory learning assay as a deficiency to alter sensory acuity in response to starvation, a trait that has been reported before.

In addition to altered locomotive patterns in the presence of food, neural circuits in which we found *npr-6* expression and newly identified promising *ex vivo* ligands to the NPR-6 receptor were previously reported to modulate behaviours that optimise *C. elegans*' behaviour to environmental food availability, including the transition from dwelling to roaming that appeared defective in *npr-6* mutants, as well as pharyngeal pumping rates, initiation of lethargus and possibly modulation of sensory acuity in response to starvation. Unlike an earlier study, we failed to identify FLP-1 as a potent ligand for NPR-6. In contrast, we confirmed earlier findings of the host lab that FLP-26 has *ex vivo* affinity for NPR-6. However, naive *flp-26* mutants showed aberrant chemotaxis towards diacetyl in our learning assay, indicating that FLP-26 does not signal exclusively through NPR-6. Based on this sole observation, we cannot exclude *in vivo* NPR-6 activatino by FLP-26.

This work is only a starting point to further explore the role of NPR-6 in anorexigenic signalling. In order to elucidate the exact mode of action, a functional *in vivo* ligand remains to be identified. A first step would be to evaluate dose-dependent activation of NPR-6 by each of the identified ligands. Secondly, of those ligands that were shown to have affinity within

physiological concentrations, mutants should be submitted to functional assays. Such deletion mutants exist for each of the ligands for which we showed binding affinity to NPR-6. Since the locomotion assay is less sensitive to environmental fluctuations, we propose to use this assay to initially characterise possible *in vivo* receptor-ligand couples, instead of the olfactory learning assay.

After identification of a ligand, a second major goal is to characterise the behavioural profile of *npr-6* mutants in those behaviours that were already reported in literature, such as pharyngeal pumping and lethargus. Conveniently, locomotion, pharyngeal pumping and lethargus are all traits that have been previously assessed in the host lab and consequently, required materials and protocols to evaluate these behaviours are available. Since we propose NPR-6 signalling as a general anorexigenic signal, it is valuable to assess multiple satiety-related traits, instead of focussing on only one of them. Finally, although our results for the diacetyl learning assay were partially inconclusive, *npr-6* mutants did show significant deviations from wild-type behaviour. Therefore, it is relevant to couple findings on the other behaviours back to the presumed deficient alteration in sensory acuity by performing chemotaxis assays under varying food regimes.

When a functional ligand is characterised and *npr-6* mutant phenotypes have been identified, the neural network in which NPR-6 is active should be identified. In this regard, cell-specific or overlapping promotors have already been reported to allow rescuing protein expression in most of the nerve cells which we identified.

We deem the identification of a functional sNPFR homologue particularly valuable, since the effects of sNPF signalling share many functional aspects with arthropod NPF, as well as with vertebrate NPY and PrRP mediated signalling. Moreover, satiety signals are a prime driver of metazoan behaviour, including that of both animal and plant parasites that pose major threats to society and economy. A deeper understanding of satiety signalling in Protostomia, such as *C. elegans*, can thereby not only help to better understand satiety-related pathophysiology, but could also prove useful to improve health and agricultural challenges ■

V. REFERENCES

1. List of cited webpages

WormBase: www.wormbase.org
FlyBase: www.flybase.org
NCBI: www.ncbi.nlm.nih.gov

2. Bibliography

Albertson, D.G. and Thomson J.N. 1975. "The Pharynx of *Caenorhabditis elegans*." Proceedings. Biological sciences / The Royal Society 308: 299–325.

Alcock, J. 2012. Animal Behaviour: An Evolutionary Approach. 10th ed. Sunderlands: Sinauer Associates.

Altschul, S.F. *et al.* 1990. "Basic Local Alignment Search Tool." Journal of Molecular Biology 215(3): 403–10.

Altschul, S.F. *et al.* 1997. "Gapped BLAST and PSI-BLAST: A New Generation of Protein Database Search Programs." Nucleic Acids Research 25(17): 3389–3402.

Altun, Z.F. and Hall D.H. . 2005. "Cell Identification in *C. elegans*." In WormAtlas, http://www.wormatlas.org/cellID.html.

Ament, S A *et al.* 2011. "Neuropeptide Y-like Signalling and Nutritionally Mediated Gene Expression and Behaviour in the Honey Bee." Insect Molecular Biology 20(3): 335–45.

Ardiel, E.L. *et al.* 2016. "Dopamine Receptor DOP-4 Modulates Habituation to Repetitive Photoactivation of a *C. elegans* Polymodal Nociceptor." Learning & memory 23: 495–503.

Ardiel, E.L. and Rankin, C.H. 2010. "An Elegant Mind: Learning and Memory in *Caenorhabditis elegans*." Learning & memory 17(4): 191–201.

Avery, L. and Horvitz, H.R. 1990. "Effects of Starvation and Neuroactive Drugs on Feeding in *Caenorhabditis elegans*." Journal of Experimental Zoology 253: 263–70.

Avery, L. and Horvitz, H.R. 1989. "Pharyngeal Pumping Continues after Laser Killing of the Pharyngeal Nervous System of *C. elegans*." Neuron 3(1981): 473–85.

Ayachi, S. and Simonin, F. 2014. "Involvement of Mammalian RF-Amide Peptides and Their Receptors in the Modulation of Nociception in Rodents." Frontiers in Endocrinology 5(October): 1–13.

Bacaj, T., Maya T., Yun L., and Shaham, S. 2008. "Glia Are Essential for Sensory Organ Function in *C. elegans*." Science 322(October): 744–48.

Van Bael, S. *et al.* 2018. "Mass Spectrometric Evidence for Neuropeptide-Amidating Enzymes in *Caenorhabditis elegans*." Journal of Biological Chemistry 293(16).

Bao, C., Yanan Y., Huiyang H., and Ye, H. 2018. "Inhibitory Role of the Mud Crab Short Neuropeptide F in Vitellogenesis and Oocyte Maturation via Autocrine/Paracrine Signaling." Frontiers in Endocrinology 9(July): 1–11.

Bargmann, C.I. 2012. "Beyond the Connectome: How Neuromodulators Shape Neural Circuits." Bioessays 34(1): 458–65.

Bargmann, C.I., Hartwieg, E., and Horvitz, R.H. 1993. "Odorant-Selective Genes and Neurons Mediate Olfaction in *C. elegans*." Cell 74(August): 515–27.

Bargmann, C.I., and Horvitz, R.H. 1991. "Chemosensory Neurons with Overlapping Direct Chemotaxis to Multiple Chemicals in *C. elegans*" Neuron 7(November): 729–42.

Barnstedt, O. *et al.* 2016. "Memory-Relevant Mushroom Body Output Synapses Are Cholinergic." Neuron 89(6): 1237–47. http://dx.doi.org/10.1016/j.neuron.2016.02.015.

Batterham, R.L. *et al.* 2002. "Gut Hormone PYY_{3-36} Physiologically Inhibits Food Intake." Nature 418(August): 728–30.

Bear, M.F., Connors, B.W., and Paradiso, M.A. 2016. Neuroscience: Exploring the Brain. 4th ed. Philadelphia: Wolters Kluwers.

Beets, I. *et al.* 2012. "Associative Learning in *C. elegans*." Science 338(October): 543–46.

Beets, I., Lindemans, M., Janssen, T. and Verleyen, P.. 2011. "Deorphanizing G Protein-Coupled Receptors by a Calcium Mobilization Assay." In Neuropeptides, ed. Merighi, A. New York: Springer Science+Business Media, 416.

Bendesky, A. *et al.* 2011. "Catecholamine Receptor Polymorphisms Affect Decision-Making in *C. elegans*." Nature 472(7343): 313–doi:10.1038/nature09821.

Bentley, B. *et al.* 2016. "The Multilayer Connectome of *Caenorhabditis elegans*." PLoS computational biology 12(12): e1005283. doi:10.1371/journal.pcbi.1005283

Bernard, G.C., Egnin, M. and Bonsi, B. 2016. "The Impact of Plant-Parasitic Nematodes on Agriculture and Methods of Control." In Nematology - Concepts, Diagnosis and

Control, ed. Shah, M.M. and Mahamood, doi: 10.5772/intechopen.68958123
Bhardwaj, A., Thapliyal, S., Dahiya, Y. and Babu, K. 2018. "FLP-18 Functions through the G-Protein-Coupled Receptors NPR-1 and NPR-4 to Modulate Reversal Length in *Caenorhabditis elegans*." The Journal of Neuroscience 38(20): 4641–54. http://www.jneurosci.org/lookup/doi/10.1523/JNEUROSCI.1955-17.2018.
Bjursell, M. *et al.* 2007. "GPR10 Deficiency in Mice Results in Altered Energy Expenditure and Obesity." Biochemical and Biophysical Research Communications 363(3): 633–38.
Blakemore, L.J., Levenson, C.W. and Trombley, P.Q. 2006. "Neuropeptide Y Modulates Excitatory Synaptic Transmission in the Olfactory Bulb." Neuroscience 138(2): 663–74.
de Bono, M. *et al.* 2002. "Social Feeding in *Caenorhabditis elegans* Is Induced by Neurons That Detect Aversive Stimuli." Nature 419(6910): 899–903.
de Bono, M., and Maricq, A.V. 2005. "Neuronal Substrates of Complex Behaviours in *C. elegans.*" Annual Review of Neuroscience 28(1): 451–501.
Brenner, S. 1974. "The DNA of *Caenorhabditis elegans*." Genetics 77(1): 95–104.
Broberger, C. *et al.* 1997. "Subtypes Y1 and Y2 of the Neuropeptide Y Receptor Are Respectively Expressed in Pro-Opiomelanocortin- and Neuropeptide-Y-Containing Neurons of the Rat Hypothalamic Arcuate Nucleus." Neuroendocrinology 66: 393–408.
Bryant, A.S., and Hallem, E.A. 2018. "Terror in the Dirt: Sensory Determinants of Host Seeking in Soil-Transmitted Mammalian-Parasitic Nematodes." International Journal for Parasitology: Drugs and Drug Resistance 8(3): 496–510. doi: 10.1016/j.ijpddr.2018.10.008.
Van Buskirk, C., and Sternberg, P.W. 2007. "Epidermal Growth Factor Signaling Induces Behavioral Quiescence in *Caenorhabditis elegans*." Nature neuroscience 10(10): 1300–1307.
Caers, J. *et al.* 2016. "Molecular Characterization of a Short Neuropeptide F Signaling System in the Tsetse Fly, *Glossina morsitans morsitans*." General and Comparative Endocrinology 235: 142–49. doi: 10.1016/j.ygcen.2016.06.005.
Calhoun, A.J., Chalasani, S.H. and Sharpee, T.O. 2014. "Maximally Informative Foraging by *Caenorhabditis elegans*." eLife 3: 1–13.
Cardoso, J., Rute, C.R., Félix, C., Fonseca, V.G. and Power, D.M. 2012. "Feeding and the Rhodopsin Family G-Protein Coupled Receptors in Nematodes and Arthropods." Frontiers in Endocrinology 3(December): 1–22.
Carulli, D., Foscarin, S. and Rossi, F. 2011. "Activity-Dependent Plasticity and Gene Expression Modifications in the Adult CNS." Frontiers in Molecular Neuroscience 4(November): 1–12.
Chao, M.Y. *et al.* 2004. "Feeding Status and Serotonin Rapidly and Reversibly Modulate a *Caenorhabditis elegans* Chemosensory Circuit." PNAS 101(43): 15512–17.
Chen, M., and Patricia, V. 2006. "The Short Neuropeptide F-Like Receptor From the Red Imported Fire Ant, *Solenopsis invicta* Buren (Hymenoptera : Formicidae)." Archives of Insect Biochemistry and Physiology 208(August): 195–208.
Chen, Z. *et al.* 2013. "Two Insulin-like Peptides Antagonistically Regulate Aversive Olfactory Learning in *C. elegans*." Neuron 77(3): 572–85. doi:10.1016/j.neuron.2012.11.025.
Cheong, M.C., Artyukhin, A.B., You, Y-J. and Avery, L. 2015. "An Opioid-like System Regulating Feeding Behavior in *C. elegans*." eLife 4: e06683.
Chevenet, F. *et al.* 2006. "TreeDyn: Towards Dynamic Graphics and Annotations for Analyses of Trees." BMC Bioinformatics 7: 1–9.
Choi, S. *et al.* 2013. "Analysis of NPR-1 Reveals a Circuit Mechanism for Behavioral Quiescence in *C. elegans*." Neuron 78(5): 869–80. doi:10.1016/j.neuron.2013.04.002.
Christ, P. *et al.* 2017. "Feeding-Induced Changes in Allatostatin-A and Short Neuropeptide F in the Antennal Lobes Affect Odor-Mediated Host Seeking in the Yellow Fever Mosquito, *Aedes aegypti*." PLoS ONE 12(11): 1–15.
———. 2018. "Functional Characterization of Mosquito Short Neuropeptide F Receptors." Peptides 103(March): 31–39. doi:10.1016/j.peptides.2018.03.009.
Cohen, M. *et al.* 2009a. "Coordinated Regulation of Foraging and Metabolism in *C. elegans* by RFamide Neuropeptide Signaling." Cell Metabolism 9(4): 375–85. doi:10.1016/j.cmet.2009.02.003.
Colbert, H.A., and Bargmann, C.I. 1997. "Environmental Signals Modulate Olfactory Acuity, Discrimination, and Memory in *Caenorhabditis elegans*." Learning and Memory 4(2): 179–91.
Colbert, H.A., and Bargmann, C.I.. 1995. "Odorant-Specific Adaptation Pathways Generate Olfactory Plasticity in *C. elegans*." Neuron 14(4): 803–12.
Crocker, A., Guan, X-J., Murphy, C.T. and Murthy, M. 2016. "Cell-Type-Specific Transcriptome Analysis in the *Drosophila* Mushroom Body Reveals Memory-Related Changes in Gene Expression." Cell Reports 15(7): 1580–96. doi:10.1016/j.celrep.2016.04.046.
Croll, N.A., and Smith, J.M.. 1978. "Integrated Behaviour in the Feeding Phase of *Caenorhabditis elegans* (Nematoda)." Journal of Zoology 184(4): 507–17. doi:10.1111/j.1469

Cunningham, K.A. *et al.* 2012. “AMP-Activated Kinase Links Serotonergic Signaling to Glutamate Release for Regulation of Feeding Behavior in *C. elegans*.” Cell Metabolism 16(1): 113–21. doi:10.1016/j.cmet.2012.05.014.

Davis, K.C., Choi, Y.I., Kim, J. and You, Y.J. 2018. “Satiety Behavior Is Regulated by ASI/ASH Reciprocal Antagonism.” Scientific Reports 8(1): 3–9. doi:10.1038/s41598-018-24943-6.

Dereeper, A. *et al.* 2008. “Phylogeny.Fr: Robust Phylogenetic Analysis for the Non-Specialist.” Nucleic acids research 36(July). www.phylogeny.fr.

Dillen, S. *et al.* 2014. “Identification of the Short Neuropeptide F Precursor in the Desert Locust: Evidence for an Inhibitory Role of sNPF in the Control of Feeding.” Peptides 53: 134–39. doi:10.1016/j.peptides.2013.09.018.

Dong, L. *et al.* 2014. “Lauric Acid in Crown Daisy Root Exudate Potently Regulates Root-Knot Nematode Chemotaxis and Disrupts *Mi-flp-18* Expression to Block Infection.” Journal of Experimental Botany 65(1): 131–41.

Ezcurra, M. *et al.* 2016. “Neuropeptidergic Signaling and Active Feeding State Inhibit Nociception in *Caenorhabditis elegans*.” Journal of Neuroscience 36(11): 3157–69. doi:10.1523/JNEUROSCI.1128-15.2016.

Ezcurra, M., Tanizawa, Y., Swoboda, P. and Schafer, W.R.. 2011. “Food Sensitizes *C. elegans* Avoidance Behaviours through Acute Dopamine Signalling.” The EMBO Journal 30(6): 1110–22. doi:10.1038/emboj.2011.22.

Fadda, M. and Hasakiogullari, I. *et al.* 2019. “Regulation of Feeding and Metabolism by F in Invertebrates.” Frontiers in Endocrinology 10(February): 1–17.

Farhan, A. *et al.* 2013. “The CCHamide 1 Receptor Modulates Sensory Perception and Olfactory Behavior in Starved *Drosophila*.” Scientific Reports 3: 1–6.

Flavell, S.W. *et al.* 2013. “Serotonin and the Neuropeptide PDF Initiate and Extend Opposing Behavioral States in *C. elegans*.” Cell 154(5): 1023–35.

Friedlander, Y. *et al.* 2010. “Candidate Molecular Pathway Genes Related to Appetite Regulatory Neural Network, Adipocyte Homeostasis and Obesity: Results from the CARDIA Study.” Annals of Human Genetics 74(5): 387–98.

Frooninckx, L. *et al.* 2012. “Neuropeptide GPCRs in *C. elegans*.” Frontiers in Endocrinology 3(December): 167.

———. 2015. “Novel Gonadotropin-Releasing Hormone, Tachykinin and Neuromedin U Neuropeptide Signaling Systems in *Caenorhabditis elegans*.” KU Leuven.

Fujiwara, M., Sengupta, P., and McIntire, S.P. 2002. “Regulation of Body Size and Behavioral State of *C. elegans* by Sensory Perception and the EGL-4 CGMP-Dependent Protein Kinase.” Neuron 36(6): 1091–1102.

Gallagher, T. *et al.* 2013. “ASI Regulates Satiety Quiescence in *C. elegans*.” Journal of Neuroscience 33(23): 9716–24.

Garczynski, S.F., Crim, J.W., and Brown, M.R. 2005. “Characterization of Neuropeptide F and Its Receptor from the African Malaria Mosquito, *Anopheles gambiae*.” Peptides 26(1): 99–107.

Gilbert, S.F., and Barresi, M.J. 2018. “Rapid Specification in Snails and Nematodes.” In Developmental Biology, Oxford: Oxford University Press, 810.

Glauser, D.A. *et al.* 2011. “Heat Avoidance Is Regulated by Transient Receptor Potential (TRP) Channels and a Neuropeptide Signaling Pathway in *Caenorhabditis elegans*.” Genetics 188(1): 91–103.

Gøtzsche, C. R., and Woldbye, D.P.D.. 2016. “The Role of NPY in Learning and Memory.” Neuropeptides 55: 79–89. doi:10.1016/j.npep.2015.09.010.

Gray, J. M., Hill, J.J. and Bargmann, C.I. 2005. “A Circuit for Navigation in *Caenorhabditis elegans*.” Proceedings of the National Academy of Sciences 102(9): 3184–91.

Guindon, S., Dufayard, J-F. and Lefort, V. 2010. “New Algorithms and Methods to Estimate Maximim-Likelihood Phylogenies Assessing the Performance of PhyML 3.0.” Systematic Biology 59(3): 301–21.

Ha, H-I. *et al.* 2010. “Functional Organization of a Neural Network for Aversive Olfactory Learning in *Caenorhabditis elegans*.” Neuron 68(6): 1173–86.

De Haes, W. *et al.* 2015. “Functional Neuropeptidomics in Invertebrates.” Biochimica et Biophysica Acta - Proteins and Proteomics 1854(7): 812–26. doi:10.1016/j.bbapap.2014.12.011.

Han, L. *et al.* 2013. “Two Novel DEG/ENaC Channel Subunits Expressed in Glia Are Needed for Nose-Touch Sensitivity in *Caenorhabditis elegans*.” Journal of Neuroscience 33(3): 936–49.

Harris, G. *et al.* 2019. “Molecular and Cellular Modulators for Multisensory Integration in *C. elegans*.” PLoS genetics 15(3): e1007706.

Hilliard, M.A.., Bargmann, C.I. and Bazzicalupo, P.. 2002. “*C. elegans* Responds to Chemical Repellents by Integrating Sensory Inputs from the Head and the Tail.” Current Biology 12(9): 730–34.

Hobson, R.J. *et al.* 2006. “SER-7, a *Caenorhabditis elegans* 5-HT$_7$-like Receptor, Is Essential for the 5-HT Stimulation of Pharyngeal Pumping and Egg Laying.” Genetics 172(1): 159–69.

Hu, Y. *et al.* 2011. “An Integrative Approach to Ortholog Prediction for Disease-Focused

and Other Functional Studies." BMC Bioinformatics 12.
Husson, S.J. *et al.* 2005. "Discovering Neuropeptides in *Caenorhabditis elegans* by Two Dimensional Liquid Chromatography and Mass Spectrometry." Biochemical and Biophysical Research Communications 335(1): 76–86.
———. 2007. "Neuropeptidergic Signaling in the Nematode *Caenorhabditis elegans*." Progress in Neurobiology 82(1): 33–55.
———. 2014. "Worm Peptidomics." EuPA Open Proteomics 3: 280–90. doi:10.1016/j.euprot.2014.04.005.
Huybrechts, J., De Loof, A. and Schoofs, L. 2004. "Diapausing Colorado Potato Beetles Are Devoid of Short Neuropeptide F I and II." Biochemical and Biophysical Research Communications 317: 909–16.
Iino, Y., and Yoshida, K. 2009. "Parallel Use of Two Behavioral Mechanisms for Chemotaxis in *Caenorhabditis elegans*." Journal of Neuroscience 29(17): 5370–80.
Ikeda, D.D. *et al.* 2008. "CASY-1, an Ortholog of Calsyntenins/Alcadeins, is Essential for Learning in *Caenorhabditis elegans*." PNAS 105(13): 5260–65.
Inagaki, H.K., Panse, K.M., and Anderson, D.J.. 2014. "Independent, Reciprocal Neuromodulatory Control of Sweet and Bitter Taste Sensitivity during Starvation in *Drosophila*." Neuron 84(4): 806–20. doi:10.1016/j.neuron.2014.09.032.
Ishihara, T. *et al.* 2002. "HEN-1, a Secretory Protein with an LDL Receptor Motif, Regulates Sensory Integration and Learning in *Caenorhabditis elegans*." Cell 109(5): 639–49.
Jafari, G. *et al.* 2011. "Regulation of Extrasynaptic 5-HT by Serotonin Reuptake Transporter Function in 5-HT-Absorbing Neurons Underscores Adaptation Behavior in *Caenorhabditis elegans*." Journal of Neuroscience 31(24): 8948–57.
Jayakumar, S. *et al.* 2016. "*Drosophila* Larval to Pupal Switch under Nutrient Stress Requires IP_3R/Ca^{2+} signalling in Glutamatergic Interneurons." eLife 5(August): 1–27.
Jehrke, L., Stewart, F.A., Droste, A. and Beller, M.. 2018. "The Impact of Genome Variation and Diet on the Metabolic Phenotype and Microbiome Composition of *Drosophila melanogaster*." Scientific Reports 8: 1–15. doi:10.1038/s41598-018-24542-5.
Jekely, G. 2013. "Global View of the Evolution and Diversity of Metazoan Neuropeptide Signaling." Proceedings of the National Academy of Sciences 110(21): 8702–7. doi:10.1073/pnas.1221833110
Jiang, H.B. *et al.* 2017. "The Short Neuropeptide F Modulates Olfactory Sensitivity of *Bactrocera dorsalis* upon Starvation." Journal of Insect Physiology 99(March): 78–85.
Jin, X., Pokala, N. and Bargmann, C.I. 2016. "Distinct Circuits for the Formation and Retrieval of an Imprinted Olfactory Memory." Cell 164: 632–43. doi:10.1016/j.cell.2016.01.007.
Johard, H.A.D., Enell, L.E. and Gustafsson, E. 2008. "Intrinsic Neurons of Drosophila Mushroom Bodies Express Short Neuropeptide F : Relations to Extrinsic Neurons Expressing Different Neurotransmitters." The Journal of Comparative Neurology 507(October): 1479–96.
Johns, S.J. 1996. "TOPO2, Transmembrane Protein Display Software." http://www.sacs.ucsf.edu/TOPO2/
Jones, S.G., Nixon, K.C.J., Chubak, M.C. and Kramer, J.M. 2018. "Mushroom Body Specific Transcriptome Analysis Reveals Dynamic Regulation of Learning and Memory Genes After Acquisition of Long-Term Courtship Memory in *Drosophila*." G3: Genes|Genomes|Genetics 8(November): 3433–46.
Kage, E. *et al.* 2005. "MBR-1, a Novel Helix-Turn-Helix Transcription Factor, Is Required for Pruning Excessive Neurites in *Caenorhabditis elegans*." Current Biology 15(17): 1554–59.
Kahsai, L., Kapan, N. *et al.* 2010a. "Metabolic Stress Responses in *Drosophila* Are Modulated by Brain Neurosecretory Cells That Produce Multiple Neuropeptides." PLoS ONE 5(7).
Kahsai, L., Martin, J.R. and Winther, Å.M.E. 2010b. "Neuropeptides in the *Drosophila* Central Complex in Modulation of Locomotor Behavior." Journal of Experimental biology 213: 2256–65.
Käll, L., Krogh, A. and Sonnhammer E.L.L. 2004. "A Combined Transmembrane Topology and Signal Peptide Prediction Method." Journal of Molecular Biology 338(5): 1027–36.
Kandel, E.R. 2012. "The Molecular Biology of Memory: CAMP, PKA, CRE, CREB-1, CREB-2, and CPEB." Molecular Brain 5(14)
Kandel, E.R. 2001. "The Molecular Biology of Memory Storage : A Dialogue Between Genes and Synapses." Science 294(November): 1030–39.
Kaneko, Y., and Hiruma, K. 2014. "Short Neuropeptide F (sNPF) Is a Stage-Specific Suppressor for Juvenile Hormone Biosynthesis by Corpora Allata, and a Critical Factor for the Initiation of Insect Metamorphosis." Developmental Biology 393(2): 312–19. doi:org/10.1016/j.ydbio.2014.07.014.
Kaniganti, T. *et al.* 2019. "Sensitivity of Olfactory Sensory Neurons to Food Cues Is Tuned to Nutritional States by Neuropeptide Y Signalling." bioRxiv. doi:10.1101/573170
Kapustin, Y., Souvorov, A., Tatusova, T. and Lipman, D. 2008. "Splign: Algorithms for Computing Spliced Alignments with

Identification of Paralogs.” Biology Direct 3: 1–13.
Katz, M. *et al.* 2018. “Glia Modulate a Neuronal Circuit for Locomotion Suppression during Sleep in *C. elegans*.” CellReports 22(10): 2575–83. doi:10.1016/j.celrep.2018.02.036.
Kauffman, A.L. *et al.* 2010. “Insulin Signaling and Dietary Restriction Differentially Influence the Decline of Learning and Memory with Age.” PLoS biology 8(5).
Klein, M. *et al.* 2017. “Exploratory Search during Directed Navigation in *C. elegans* and *Drosophila* Larva.” eLife 6: 1–14.
Knapek, S. *et al.* 2013. “Short Neuropeptide F Acts as a Functional Neuromodulator for Olfactory Memory in Kenyon Cells of *Drosophila* Mushroom Bodies.” Annals of Internal Medicine 158(6): 5340–45.
Ko, K.I. *et al.* 2015. “Starvation Promotes Concerted Modulation of Appetitive Olfactory Behavior via Parallel Neuromodulatory Circuits.” eLife 4: 1–17.
Kobayashi, K. *et al.* 2016. “Single-Cell Memory Regulates a Neural Circuit for Sensory Behavior.” Cell Reports 14(1): 11–21. doi:10.1016/j.celrep.2015.11.064.
Kõressaar, T. *et al.* 2018. “Primer3-Masker: Integrating Masking of Template Sequence with Primer Design Software.” Bioinformatics 34(11): 1937–38.
Koressaar, T., and Remm, M. 2007. “Enhancements and Modifications of Primer Design Program Primer3.” Bioinformatics 23(10): 1289–91.
Kubiak, T.M. *et al.* 2003. “Functional Annotation of the Putative Orphan *Caenorhabditis elegans* G-Protein-Coupled Receptor C10C6.2 as a FLP-15 Peptide Receptor.” Journal of Biological Chemistry 278(43): 42115–20.
Kuneš, J. *et al.* 2016. “Prolactin-Releasing Peptide: A New Tool for Obesity Treatment.” Journal of Endocrinology 230(2): R51–58.
Larsch, J. *et al.* 2015. “A Circuit for Gradient Climbing in *C. elegans* Chemotaxis.” Cell Reports 12(11): 1748–60. doi:10.1016/j.celrep.2015.08.032.
Lavebratt, C. *et al.* 2006. “Common Neuropeptide Y2 Receptor Gene Variant Is Protective against Obesity among Swedish Men.” International Journal of Obesity 30(3): 453–59.
Lee, K.S. *et al.* 2004. “*Drosophila* Short Neuropeptide F Regulates Food Intake and Body Size.” Journal of Biological Chemistry 279(49): 50781–89.
———. 2008. “*Drosophila* Short Neuropeptide F Signalling Regulates Growth by ERK-Mediated Insulin Signalling.” Nature Cell Biology 10(4): 468–75.
Lee, K.S. *et al.* 2017. “Serotonin-Dependent Kinetics of Feeding Bursts Underlie a Graded Response to Food Availability in *C. elegans*.” Nature Communications 8: 1–11. doi:10.1038/ncomms14221.
Lee, R.Y.N. *et al.* 1999. “EAT-4, a Homolog of a Mammalian Sodium-Dependent Inorganic Phosphate Cotransporter, Is Necessary for Glutamatergic Neurotransmission in *Caenorhabditis elegans*.” Journal of Neuroscience 19(1): 159–67.
Li, C., and Kim, K.. 2008. “Neuropeptides.” WormBook: 1–36.
———. 2014. “Family of FLP Peptides in *Caenorhabditis elegans* and Related Nematodes.” Frontiers in Endocrinology 5(OCT): 1–16.
Li, Q., and Liberles, S.D. 2015. “Aversion and Attraction through Olfaction.” Current Biology 25(3): 120–29. doi:10.1016/j.cub.2014.11.044.
Li, Z. *et al.* 2012. “Dissecting a Central Flip-Flop Circuit That Integrates Contradictory Sensory Cues in *C. elegans* Feeding Regulation.” Nature Communications 3: 776–78. doi:10.1038/ncomms1780.
Liesch, J., Bellani, L.L. and Vosshall, L.B. 2013. “Functional and Genetic Characterization of Neuropeptide Y-Like Receptors in *Aedes aegypti.*” PLoS ONE 7(10).
Loch, D., Breer, H. and Strotmann, J.. 2015. “Endocrine Modulation of Olfactory Responsiveness: Effects of the Orexigenic Hormone Ghrelin.” Chemical Senses 40(7): 469–79.
Lowe, T.M., and Eddy, S.R. 1997. “tRNAscan-SE: A Program for Improved Detection of Transfer RNA Genes in Genomic Sequence.” Nucleic Acids Research 25(5): 955–64. doi:10.1093/nar/25.5.955.
Lushchak, O.V., Carlsson, M.A., and Nässel D.R.. 2015. “Food Odors Trigger an Endocrine Response That Affects Food Ingestion and Metabolism.” Cellular and Molecular Life Sciences 72(16): 3143–55.
Macosko, E.Z. *et al.* 2009. “A Hub-and-Spoke Circuit Drives Pheromone Attraction and Social Behaviour in *C. elegans*.” Nature 458(7242): 1171–75. doi:10.1038/nature07886.
Madeira, F. *et al.* 2019. “The EMBL-EBI Search and Sequence Analysis Tools APIs in 2019.” Nucleic acids research. doi:10.1093/nar/gkz268.
Malis, D.D. *et al.* 1999. “Influence of TASP-V, a Novel Neuropeptide Y (NPY) Y2 Agonist, on Nasal and Bronchial Responses Evoked by Histamine in Anaesthetized Pigs and in Humans.” British Journal of Pharmacology 126(4): 989–96.
Marder, E. 2012. “Neuromodulation of Neuronal Circuits: Back to the Future.” Neuron 76(1): 1–11. doi:10.1016/j.neuron.2012.09.010.
Marvin, J.S. *et al.* 2013. “An Optimized Fluorescent Probe for Visualizing Glutamate Neurotransmission.” 10(2).

McCloskey, R.J., Fouad, A.D., Churgin, M.A. and Fang-Yen, C.. 2017. " Food Responsiveness Regulates Episodic Behavioral States in *Caenorhabditis elegans* ." Journal of Neurophysiology 117(5): 1911–34.
McDiarmid, T.A., Yu, A.J. and Rankin, C.H. 2018. "Beyond the Response—High Throughput Behavioral Analyses to Link Genome to Phenome in *Caenorhabditis elegans*." Genes, Brain and Behavior 17(3): 1–14.
McDiarmid, T.A., Ardiel, E.L. and Rankin C.H. 2015. "The Role of Neuropeptides in Learning and Memory in *Caenorhabditis elegans*." Current Opinion in Behavioral Sciences 2: 15–20. doi:10.1016/j.cobeha.2014.07.002.
McKay, J.P. *et al.* 2004. "*eat-2* and *eat-18* Are Required for Nicotinic Neurotransmission in the *Caenorhabditis elegans* Pharynx." Genetics 166(1): 161–69.
Meisel, J.D., and Kim, D.H. 2014. "Behavioral Avoidance of Pathogenic Bacteria by *Caenorhabditis elegans*." Trends in Immunology 35(10): 465–70. doi:10.1016/j.it.2014.08.008.
Mi, H., Muruganujan, A., Ebert, D. *et al.* 2019a. "PANTHER Version 14: More Genomes, a New PANTHER GO-Slim and Improvements in Enrichment Analysis Tools." Nucleic Acids Research 47(D1): D419–26.
Mi, H., Muruganujan, A., Huang, X. *et al.* 2019b. "Protocol Update for Large-Scale Genome and Gene Function Analysis with the PANTHER Classification System (v.14.0)." Nature Protocols 14(3): 703–21. doi:10.1038/s41596-019-0128-8.
Mikani, A., Wang, Q-S. and Takeda, M.. 2012. "Peptides Brain-Midgut Short Neuropeptide F Mechanism That Inhibits Digestive Activity of the American Cockroach, *Periplaneta americana* upon Starvation." Peptides 34(1): 135–44. doi:10.1016/j.peptides.2011.10.028
Mirabeau, O., and Joly, J-S. 2013. "Molecular Evolution of Peptidergic Signaling Systems in Bilaterians." Proceedings of the National Academy of Sciences 110(22): E2028–37. doi:10.1073/pnas.1219956110.
Mitchell, A.L. *et al.* 2019. "InterPro in 2019: Improving Coverage, Classification and Access to Protein Sequence Annotations." Nucleic Acids Research 47(D1): D351–60.
Mori, I., and Ohshima, Y. 1995. "Neural Regulation of Thermotaxis in *Caenorhabditis elegans*." Nature 376(July): 344–48.
Morrison, G.E., Wen, J.Y.M., Runciman, S. and Van Der Kooy D. 1999. "Olfactory Associative Learning in *Caenorhabditis elegans* Is Impaired in *lrn-1* and *lrn-2* Mutants." Behavioral Neuroscience 113(2): 358–67.
Morrison, G.E., and Van Der Kooy, D. 2001. "A Mutation in the AMPA-Type Glutamate Receptor, g*lr-1*, Blocks Olfactory Associative and Nonassociative Learning in *Caenorhabditis elegans*." Behavioral Neuroscience 115(3): 640–49.
Nagata, S. *et al.* 2011. "General and Comparative Endocrinology Effects of Neuropeptides on Feeding Initiation in Larvae of the Silkworm, *Bombyx mori*." General and Comparative Endocrinology 172(1): 90–95. doi:10.1016/j.ygcen.2011.03.004.
Nagy, S., Raizen, D.M. and Biron, D.. 2014. "Measurements of Behavioral Quiescence in *Caenorhabditis elegans*." Methods 68(3): 500–507.
Nässel, D.R., and Wegener C. 2011. "A Comparative Review of Short and Long Neuropeptide F Signaling in Invertebrates: Any Similarities to Vertebrate Neuropeptide Y Signaling?" Peptides 32(6): 1335–55.
Nässel, D.R. *et al.* 2008. "A Large Population of Diverse Neurons in the *Drosophila* Central Nervous System Expresses Short Neuropeptide F, Suggesting Multiple Distributed Peptide Functions." BMC Neuroscience 35: 1–35.
Nathoo, A.N., Moeller, R.A., Westlund, B.A. and Hart, A.C. 2001. "Identification of Neuropeptide-like Protein Gene Families in *Caenorhabditis elegans* and Other Species." Proceedings of the National Academy of Sciences 98(24): 14000–5. doi:10.1073/pnas.241231298
Naveilhan, P., Neveu, I., Arenas, E. and Ernfors, P. 1998. "Complementary and Overlapping Expression of Y1, Y2 and Y5 Receptors in the Developing and Adult Mouse Nervous System." Neuroscience 87(1): 289–302.
Naveilhan, P., Canals, J.M., Arenas, E. and Ernfors, P. 2001. "Distinct Roles of the Y1 and Y2 Receptors on Neuropeptide Y-Induced Sensitization to Sedation." Journal of Neurochemistry 78(6): 1201–7.
Nawrocki, E.P. *et al.* 2015. "Rfam 12.0: Updates to the RNA Families Database." Nucleic Acids Research 43(D1): D130–37.
Niacaris, T. and Avery, L. 2003. "Serotonin Regulates Repolarization of the *C. elegans* Pharyngeal Muscle." Journal of Experimental Biology 206(2): 223–31. doi:doi/10.1242/jeb.00101 (July 9, 2018).
Ohno, H. *et al.* 2014. "Role of Synaptic Phosphatidylinositol 3-Kinase in a Behavioral Learning Response in *C. elegans*." Science 345(6194): 313–17.
Onken, H., Moffett, S.B. and Moffett, D.F. 2004. "The Anterior Stomach of Larval Mosquitoes (*Aedes aegypti*): Effects of Neuropeptides on Transepithelial Ion Transport and Muscular Motility." Journal of Experimental biology 207: 3731–39.
Oranth, A. *et al.* 2018. "Food Sensation Modulates Locomotion by Dopamine and

Neuropeptide Signaling in a Distributed Neuronal Network Food Sensation Modulates Locomotion by Dopamine and Neuropeptide Signaling in a Distributed Neuronal Network." Neuron 100(6): 1414-1428. doi:10.1016/j.neuron.2018.10.024.
Peymen, K. *et al.* 2014. "The FMRFamide-like Peptide Family in Nematodes." Frontiers in Endocrinology 5(JUN).
———. 2019a. "Myoinhibitory Peptide Signaling as a Modulator of Aversive Gustatory Learning in *C. elegans*." KU Leuven.
———. 2019b. "Myoinhibitory Peptide Signaling Modulates Aversive Gustatory Learning in *Caenorhabditis elegans*" ed. Gregory S. Barsh. PLOS Genetics 15(2): e1007945.
Pierce-Shimomura, J.T., Morse, T.M. and Lockery, S.R. 1999. "The Fundamental Role of Pirouettes in *Caenorhabditis elegans*." Journal of Neuroscience 19(21): 9557–69.
Piggott, B.J. *et al.* 2011. "The Neural Circuits and Synaptic Mechanisms Underlying Motor Initiation in *C. elegans*." Cell 147(4): 922–33.
Pocock, R., and Hobert, O. 2010. "Hypoxia Activates a Latent Circuit for Processing Gustatory Information in *C. elegans*." Nature Neuroscience 13(5): 610–14.
Procko, C., Lu, Y., and Shaham, S.. 2011. "Glia Delimit Shape Changes of Sensory Neuron Receptive Endings in *C . elegans*." 1381: 1371–81.
———. 2012. "Sensory Organ Remodeling in *Caenorhabditis*." Genetics 190(April): 1405–15.
Pruitt, K.D. *et al.* 2014. "RefSeq: An Update on Mammalian Reference Sequences." Nucleic Acids Research 42(D1): 756–63.
Raizen, D.M., Lee, R.Y.N. and Avery, L. 1995. "Interacting Genes Required for Pharyngeal Excitation by Motor Neuron MC in *Caenorhabditis elegans*." Genetics 141(4): 1365–82.
Raizen, D.M. *et al.* 2008. "Lethargus Is a *Caenorhabditis elegans* Sleep-like State." Nature 451(7178): 569–72.
Rankin, C.H., Beck, C.D.O. and Chiba C.M. 1990. "*Caenorhabditis elegans*: A New Model System for the Study of Learning and Memory." Behavioural Brain Research 37: 89–92.
Rhoades, J.L. *et al.* 2019. "ASICs Mediate Food Responses in an Enteric Serotonergic Neuron That Controls Foraging Behaviors." Cell 176(January): 85-97.e14.
Roayaie, K., Crump, J.G., Sagasti, A. and Bargmann, C.I. 1998. "The Gα Protein ODR-3 Mediates Olfactory and Nociceptive Function and Controls Cilium Morphogenesis in *C. elegans* Olfactory Neurons." Neuron 20(January): 55–67.
Roberts, W.M. *et al.* 2016. "A Stochastic Neuronal Model Predicts Random Search Behaviors at Multiple Spatial Scales in *C. elegans*." eLife 5: 1–41.
Rogers, C. *et al.* 2003. "Inhibition of *Caenorhabditis elegans* Social Feeding by FMRFamide-Related Peptide Activation of NPR-1." Nature Neuroscience 6(11): 1178–85.
Root, C.M., Ko, K.I., Jafari, A. and Wang, J.W. 2011. "Presynaptic Facilitation by Neuropeptide Signaling Mediates Odor-Driven Food Search." Cell 145(1): 133–44. doi:10.1016/j.cell.2011.02.008.
Rose, J.K, Kaun, K.R., Chen, S.H. and Rankin, C.H. 2003. "GLR-1, a Non-NMDA Glutamate Receptor Homolog, Is Critical for Long-Term Memory in *Caenorhabditis elegans*." Journal of Neuroscience 23(29): 9595–99.
Ryan, D.A. *et al.* 2014. "Sex, Age, and Hunger Regulate Behavioral Prioritization through Dynamic Modulation of Chemoreceptor Expression." Current Biology 24(21): 2509–17. doi:10.1016/j.cub.2014.09.032.
Santos-Carvalho, A. *et al.* 2013. "Neuropeptide Y Receptors Y1 and Y2 Are Present in Neurons and Glial Cells in Rat Retinal Cells in Culture." Investigative Ophthalmology and Visual Science 54(1): 429–43.
Sapunar, D., Vukojević, K., Kostić, S. and Puljak L. 2011. "Attenuation of Pain-Related Behavior Evoked by Injury through Blockade of Neuropeptide y Y2 Receptor." Pain 152(5): 1173–81.
Sasakura, H., and Mori I. 2013. "Behavioral Plasticity, Learning, and Memory in *C. elegans*." Current Opinion in Neurobiology 23(1): 92–99. doi:10.1016/j.conb.2012.09.005.
Schoofs, L., De Loof, A. and Van Hiel, M.B. 2017. "Neuropeptides as Regulators of Behavior in Insects." Annual Review of Entomology 62(1): 35–52. doi:10.1146/annurev-ento-031616-035500.
Sengupta, P., Chou, J.H. and Bargmann, C.I. 1996. "*odr-10* Encodes a Seven Transmembrane Domain Olfactory Receptor Required for Responses to the Odorant Diacetyl." Cell 84(6): 899–909.
Shaham, S. 2015. "Glial Development and Function in the Nervous System of *Caenorhabditis elegans*." Cold Sprint Harbor Perspectives in Biology 7: 1–14.
Shen, R. *et al.* 2016. "Neuronal Energy-Sensing Pathway Promotes Energy Balance by Modulating Disease Tolerance." Proceedings of the National Academy of Sciences 113(23): E3307–14.
Shen, Y., Zhang, J., Calarco, J.A. and Zhang Y. 2014. "EOL-1, the Homolog of the Mammalian Dom3Z, Regulates Olfactory Learning in *C. elegans*." Journal of Neuroscience 34(40): 13364–70. doi:10.1523/JNEUROSCI.0230-14.2014.
Siddiq, A. *et al.* 2007. "Single Nucleotide Polymorphisms in the Neuropeptide Y2

Receptor (NPY2R) Gene and Association with Severe Obesity in French White Subjects." Diabetologia 50(3): 574–84.
Van Sinay, E. *et al.* 2017. "Evolutionarily Conserved TRH Neuropeptide Pathway Regulates Growth in *Caenorhabditis elegans*." PNAS 114(20): 4065–74.
Singh, C., Rihel, J. and Prober, D.A. 2017. "Neuropeptide Y Regulates Sleep by Modulating Noradrenergic Signaling." Current Biology 27(24): 3796-3811.e5. doi:10.1016/j.cub.2017.11.018.
Stanić, D. *et al.* 2006. "Characterization of Neuropeptide Y2 Receptor Protein Expression in the Mouse Brain. I. Distribution in Cell Bodies and Nerve Terminals." The Journal of Comparative Neurology 499: 357–90.
States, D.J., and Gish, W. 1991. "Combined Use of Sequence Similarity and Codon Bias for Coding Region Identification." Journal of Computational Biology 1(1): 39–50.
Stein, G.M., and Murphy C.T. 2014. "*C. elegans* Positive Olfactory Associative Memory Is a Molecularly Conserved Behavioral Paradigm." Neurobiology of Learning and Memory 115: 86–94. doi:10.1016/j.nlm.2014.07.011.
Stetak, A. *et al.* 2009. "Neuron-Specific Regulation of Associative Learning and Memory by MAGI-1 in *C. elegans*." PLoS ONE 4(6).
Styer, K.L. *et al.* 2008. "Innate Immunity in *Caenorhabditis elegans* Is Regulated by Neurons Expressing." Science 322(October): 460–65.
Tachibana, T., and Sakamoto T. 2014. "Functions of Two Distinct 'Prolactin-Releasing Peptides' Evolved from a Common Ancestral Gene." Frontiers in Endocrinology 5(November): 1–12.
Taghert, P.H., and Nitabach, M.N. 2012. "Peptide Neuromodulation in Invertebrate Model Systems." Neuron 76(1): 82–97. doi:10.1016/j.neuron.2012.08.035.
Talavera, G., and Castresana, J. 2007. "Improvement of Phylogenies after Removing Divergent and Ambiguously Aligned Blocks from Protein Sequence Alignments." Systematic Biology 56(4): 564–77.
Thibaud-nissen, F., Souvorov, A., Murphy T. *et al.* 2013. "Eukaryotic Genome Annotation Pipeline." In: The NCBI Handbook [Internet]. 2nd edition. Bethesda (MD): National Center for Biotechnology Information (US); 2013-.
Tobin, D.M. *et al.* 2002. "Combinatorial Expression of TRPV Channel Proteins Defines Their Sensory Functions and Subcellular Localization in *C. elegans* Neurons." Neuron 35: 307–18.
Tsao, C-H. *et al.* 2018. "*Drosophila* Mushroom Bodies Integrate Hunger and Satiety Signals to Control Innate Food-Seeking Behavior." eLife 7: 1–35.
Untergasser, A. *et al.* 2012. "Primer3-New Capabilities and Interfaces." Nucleic Acids Research 40(15): 1–12.
Vukojevic, V. *et al.* 2012. "A Role for α-Adducin (ADD-1) in Nematode and Human Memory." EMBO Journal 31(6): 1453–66.
Wakabayashi, T., Kitagawa, I. and Shingai R. 2004. "Neurons Regulating the Duration of Forward Locomotion in *Caenorhabditis elegans*." Neuroscience Research 50(1): 103–11.
Wang, Y. *et al.* 2008. "A Glial DEG/ENaC Channel Functions with Neuronal Channel DEG-1 to Mediate Specific Sensory Functions in *C. elegans*." The EMBO Journal 27(18): 2388–99.
Wang, Y., D'Urso, G. and Bianchi, L. 2011. "Knockout of Glial Channel ACD-1 Exacerbates Sensory Deficits in a *C. elegans* Mutant by Regulating Calcium Levels of Sensory Neurons." Journal of Neurophysiology 107(1): 148–58.
Waterhouse, A.M. *et al.* 2009. "Jalview Version 2-A Multiple Sequence Alignment Editor and Analysis Workbench." Bioinformatics 25(9): 1189–91.
Wen, J.Y.M. *et al.* 1997. "Mutations That Prevent Associative Learning in *C . elegans*." Behavioral Neuroscience 111(2): 354–68.
White, J.G., Southgate, E., Thomson, J.N. and Brenner, S. 1986. "The Structure of the Nervous System of the Nematode *Caenorhabditis elegans*." Philosophical Transactions of the Royal Society B: Biological Sciences 314(1165): 1–340. doi:10.1098/rstb.1986.0056.
Yamashita, M. *et al.* 2013. "Involvement of Prolactin-Releasing Peptide in the Activation of Oxytocin Neurones in Response to Food Intake." Journal of Neuroendocrinology 25(5): 455–65.
Yan, G. *et al.* 2017. "Network Control Principles Predict Neuron Function in the *Caenorhabditis elegans* Connectome." Nature 550(7677): 519–23. doi:10.1038/nature24056.
You, Y.J., Kim, J., Raizen, D.M. and Avery, L. 2008. "Insulin, cGMP, and TGF-β Signals Regulate Food Intake and Quiescence in *C. elegans*: A Model for Satiety." Cell Metabolism 7(3): 249–57.
Zhang, Y., Lu, H. and Bargmann, C.I. 2005. "Pathogenic Bacteria Induce Aversive Olfactory Learning in *Caenorhabditis elegans*." Nature 438(7065): 179–84

VI. SUPPLEMENTARY MATERIALS AND METHODS

a. Safety, Health and Environment

Neither *C. elegans*, nor any of the bacterial strains used for culture or transgenesis are pathogenic. Accordingly, except for the eukaryotic cell line culture which necessitates L2 laboratory requirements, all practices for this master's dissertation comply with institutional health and safety rules for L1 laboratories. When starting experiments in the lab, all students read and signed the Laboratory Good Practices manual, provided by the host lab. Thereby the host lab ensures good knowledge on safety practices to reduce risks for oneself and others in all laboratory environments. This includes wearing lab coats, nitrile gloves, UV-protective goggle/screens when appropriate and informing others when needed. Lab coats are kept at the entrance of laboratory spaces and are forbidden in recreational/public spaces. Personal hygiene is highly valued and hands were thoroughly washed when leaving lab spaces. The use of any laboratory devices following manufacturers guidelines, such as autoclaves, electrophoresis apparatuses, -80°C freezers, thermocycler blocks or centrifuges, was only allowed under supervision or after a special training by qualified staff. Since laboratory spaces are shared with many others, surfaces and laminar flows were cleaned with 70% ethanol before and after use and materials were autoclaved. Moreover, special attention and measures were taken into account to avoid physical dangers. These include Bunsen burner flames, that can never be left unguarded, sharp objects, i.e. glass needles, capillaries, microscope slides and cover slips, or scalpels which were collected in the appropriate containers, as well as UV-radiation protective measures, and care when carrying or using hot liquids and extremely cold substances, such as dry ice and liquid nitrogen.

All liquid chemical wastes were collected in categorically labelled jerry cans, according to KU Leuven's approved institutional waste categories. Biological waste was gathered in plastic containers for hazardous medical/biological waste when liquid, or in a cardboard box with yellow liner destined for the same purpose when solid. Several chemicals (e.g. NaN3, GelRed®, diacetyl, ampicillin, etc.) are toxic to the environment or hazardous when in inhaled, ingested or contacted with skin or mucosal surfaces and these were handled with additional care following the VGM prescriptions and manufacturer kits were used according to the co-provided guidelines. GelRed®, used to visualise nucleic acids when performing agarose gel electrophoresis, is suspected to cause genetic defects. The use of all reagents and materials during this protocol was therefore restricted to a strictly assigned working space. This includes a microwave, assigned lab coats, gloves, UV-protective gear, liquid waste containers, pens and markers, DNA ladders, gel electrophoresis apparatuses and bottles.

b. Buffers and Solutions

Table A: Buffers and solutions used in the experiments performed for this master's thesis.

Name	Content
M9 buffer	1M H_2PO_4/Na_2HPO_4 pH 7.5, 85 mM NaCl, 1 mM $MgSO_4$ in mQ
NGM	1.7% agar, 0.75% bactopeptone, 25 mM KH_2PO_4/K_2HPO_4 pH 6.6, 50 mM NaCl, 13 mM cholesterol, 1 mM $CaCl_2$, 1mM $MgSO_4$ in AD
bleaching solution	40% 1M NaOH, 60% 1M NaClO
chemotaxis plates	2% agar, 5 mM KH_2PO_4/K_2HPO_4 pH 6.6, 1 mM $CaCl_2$, 1mM $MgSO_4$ in AD
CTX buffer	5 mM KH_2PO_4/K_2HPO_4 pH 6.6, 1 mM $CaCl_2$, 1mM $MgSO_4$
CHO K1 cell culture medium	Dulbecco's Modified Eagles Medium nutrient mixture F12-Ham (Sigma-Aldrich), 10% fetal bovine serum (Invitrogen), 100 units/ml penicillin/streptomycin (Invitrogen), 250 µg/ml zeocin (Invitrogen) and 2.5µg/ml fungizone (Amphotericin B; Invitrogen)
trypsin-EDTA solution	0.25%, 2.5 g/l porcine trypsin, 0.2 g/l EDTA·4 Na in Hanks' Balanced Salt solution with phenol red; Sigma-Aldrich
BSA medium	DMEM/F12 without phenol red, L-glutamine, 15 mM 4-(2-hydroxyethyl)-1-piperazineethanesulfonic acid (HEPES; Gibco) and 0.1% BSA (Sigma-Aldrich)
lysis buffer	5 µl proteinase K (10 mg/ml; Sigma-Aldrich), 100 µl 1X Advantage® 2 SA PCR buffer (Clontech)
TAE buffer	20 mM acetic acid [Sigma-Aldrich], 1mM EDTA·2Na [Sigma-Aldrich], 40 mM Trizma base [Sigma-Aldrich], 50 X GelRed® in dimethyl sulfoxide [Biotium])
Agarose gel	1% agarose [Sigma-Aldrich] in TAE buffer,], 50 X GelRed® in dimethyl sulfoxide [Biotium]
LB (broth)	25 g/l lysogeny broth (Sigma-Aldrich) in AD
LB (agar)	35 g/l LB agar (Sigma-Aldrich) in AD, optionally: 100 mg/l Ampicillin

c. Supplementary Molecular Work

1. Genomic DNA preparation

GENOMIC DNA EXTRACTION – To extract *C. elegans* gDNA, hermaphrodite worms are lysed by heating in proteinase K-containing lysis buffer: 5 µl proteinase K (10 mg/ml; Sigma-Aldrich) is added to 100 µl 1X Advantage® 2 SA PCR buffer (Clontech). The desired amount of lysis buffer is added to a a MicroAMP™ Reaction Tube (ThermoFisher Scientific) and 1 worm/µl is transferred to the tube. Next, the reaction mixture is incubated at -80°C for 30 minutes, after which it is heated in a thermocycler (TProfessional Thermocycler; Biometra) to 60°C for 60 minutes. Proteinase K is heat inactivated at 95°C for 15 minutes and the lysate is stored at 4°C for immediate usage or at -20°C for later use.

COMPLEMENTARY DNA SYNTHESIS – cDNA was reverse-transcribed using the First-strand Synthesis System for RT-PCR (Invitrogen) from mRNA which was extracted using the QuickPrep Micro mRNA Purification Kit (Amersham Biosciences).

2. PCR amplification

PRIMER DESIGN – Primers were adapted from automatically designed primers by the Primer3 webtool (Kõressaar *et al.* 2018; Koressaar and Remm 2007; Untergasser *et al.* 2012). Adaptor sequences were designed using the NEBuilder v2.2.3 (NEB). The vector map published in this dissertation as well as all primers and envisioned constructs were visualised and evaluated using SnapGene Viewer v2.4.6.

Q5® HIGH-FIDELITY DNA POLYMERASE – Q5® High-Fidelity DNA polymerase (NEB) was used to amplify DNA fragments for injection, i.e. for plasmid vector construction and for linearly amplified constructs. Guided by the manufacturer's instructions, 2 µl template DNA was added to a master mix containing 10 µl 5X Q5 Reaction Buffer (NEB), 1 µl 10 mM balanced deoxynucleoside triphosphate solution, 2.5 µl 10µM forward primer, 2.5 µl 10µM reverse primer, and 31.5 µl nuclease-free water. This reaction mixture was kept on ice throughout the preparation steps. Finally, 0.5 µl 0.2 units/µl Q5® High-Fidelity DNA Polymerase (NEB) was added to the reaction mixture on ice. Amplification happens in a thermocycler (TProfessional Thermocycler; Biometra) according to annealing temperatures customised for individual primer pairs (Supplementary table B). The general cycler program for Q5® High-Fidelity DNA polymerase (NEB) consists of 30 s preheating at 98°C, followed by 35 rounds of cycling between 10 s of denaturation at 98°C, 30 s at the primer-specific annealing temperature, and 1 minute per thousand base pairs to allow for elongation. After two more minutes at 72°C, the product is stored at 4°C for immediate use or stored at -20°C for later uses.

REDTAQ® DNA POLYMERASE – REDTaq® DNA polymerase (Sigma-Aldrich) was used for genotyping *C. elegans* strains and to assess success of transformation in DH5α *E. coli* strains (supplementary figure A). Generally, a reaction mixture was set up on ice in MicroAMP™ reaction tubes (ThermoFisher Scientific) by adding 5 µl template DNA, 5.5 µl nuclease-free water, 1 µl 10 mM forward primer, 1 µl 10 mM reverse primer, 12.5 µl REDTaq ReadyMix (Sigma-Aldrich) already containing 1 unit/µl REDTaq DNA polymerase (Sigma-Aldrich). Again, the general thermocycler program (TProfessional Thermocycler; Biometra) consisted of two minutes preheating at 95°C, 35 cycles of 30 s denaturation at 95°C, 60 s of annealing at primer-specific annealing temperature and 1 minute per thousand base pairs annealing at 72°C (Supplementary table D). Next, after eight more minutes at 72°C, products are stored at 4°C or -20°C for direct or later use respectively.

AGAROSE GEL ELECTROPHORESIS – We assessed whether amplicon size was as expected to check the quality of the amplified fragments. To prepare PCR Q5® DNA polymerase amplified samples, loading dye is added in a 2:5 dye:product ratio (ThermoFisher Scientific). Samples were loaded on an in situ prepared agarose gel (1% agarose [Sigma-Aldrich], 50 X GelRed®

in dimethyl sulfoxide [Biotium] in Tris-Acetate-EDTA buffer [TAE]: 20 mM acetic acid [Sigma-Aldrich], 1mM EDTA·2Na [Sigma-Aldrich], 40 mM Trizma base [Sigma-Aldrich] in mQ) in an electrophoresis chamber filled with TAE buffer. Alongside an appropriate DNA ladder (usually: 1 kb plus; Invitrogen), samples were let to migrate through the gel at 130V and 180 mA until all bands are clearly resolved. Visualisation upon UV-irradiation was done using the ProXima 2500-T gel imaging system and software.

3. Restriction-Digestion

For restriction-digestion, the vector was first purified from transformed *E. coli* strains, using the GenElute™ HP Plasmid Miniprep Kit (Sigma-Aldrich). After photometric quantification of the vector using a NanoPhotometer® (IMPLEN), 1 µl of FastDigest® BamHI (ThermoFisher Scientific) was added to a solution of 2 µl 10X FastDigest Buffer and up to 10 µg purified vector. After adding nuclease-free water to a final volume of 20 µl, the sample is placed in a thermal block at 37°C. After two hours, the digestion enzyme is inactivated by heating to 80°C for five minutes. Products are stored at 4°C or -20°C for either direct or later use, respectively.

4. Ligation

Depending on the trial, fragments and linearized vectors were optionally purified using the Wizard® SV PCR Clean-Up System (Promega). Each time, purity and concentration (ng/µl) of the product are assessed using a NanoPhotometer® (IMPLEN).

GIBSON HI-FI ASSEMBLY MIX – For ligation of fragments with overlapping ends we used the Gibson Assembly® kit (NEB): maximally 10 picomol of DNA fragments was added to 10 µl of Gibson Assembly Master Mix (2X). Nuclease-free water was added to a final volume of 20 µl. The reaction mix was subsequently incubated for two hours at 50°C in a thermocycler block (TProfessional Thermocycler; Biometra).

5. Transformation of DH5α E.coli

HEAT TRANSFORMATION – To transform of DH5α *E. coli* that were made competent in the host lab (Elke Vandewyer), 5 µl of circularised vector was added to a NalgeneTM General Long-Term Storage Cryogenic Tube (ThermoFisher Scientific) in which competent cells are stored. After letting the mixture to thaw slowly on ice for 30 minutes, cells are heat shocked at 42°C for 40 s in a water bath. Subsequently, the transformed cells are left on ice for two minutes after which 250 µl lysogeny broth was added (25 g/l lysogeny broth in mQ [Sigma-Aldrich]). The bacteria are left to acclimate and proliferate in a shaking incubator at 37°C and after one hour, 5 and 200 µl of DH5α-containing lysogeny broth is spread on preheated lysogeny broth agar plates containing the selection marker ampicillin (35 g/l lysogeny broth agar [Sigma-

Aldrich]; 100 mg/l ampicillin [Sigma-Aldrich]). Colonies were left to proliferate overnight in an incubator set at 37°C and genotyped the next morning, to assess for correct insertion of the fragment of interest in the vector. Inoculated plates are stored at 4°C.

COLONY PCR – To prepare approximately 48 colonies for genotyping PCR, the colony surface was scratched with a micropipette tip and samples with which 30 µl mQ was inoculated. Amplification of the region of interest was done according to the general protocol for the use of REDTaq® DNA Polymerase, except for an extension of the initial preheating step to ten instead of 2 minutes in order to lyse the bacterial cells prior to amplification. If the fragment of interest is present in the vector, plasmids are purified and sequenced by LGC genomics.

PLASMID PURIFICATION – 5 µl of water-dissolved DH5α *E. coli* colonies containing the desired construct are transferred to 10 ml lysogeny broth (25 g lysogeny broth [Sigma-Aldrich], 100 mg/ml ampicillin [Sigma-Aldrich]) in a 15 ml Falcon® tube. Part of the desired colonies is stored at -20°C. Plasmids for injection and sequencing are purified with the GenEluteTM HP Plasmid Miniprep Kit (Sigma-Aldrich) and concentration is calculated with a NanoPhotometer® (IMPLEN).

6. Primers

Table B: Primers used for PCR amplification of fragments for transgenesis. *Method (if applicable) denotes the method in which we attempted to create the plasmid:* ***R/D,*** *restriction/digestion with BamHI followed by ligation;* ***PCR-ligation,*** *PCR amplification with adaptors on the primers followed by ligation;* ***Linear rescue,*** *linear amplified fragment; Forward* ***(FW: 5'-3')*** *and reverse* ***(REV: 3'-5')*** *primers are as indicated. Lower case characters indicate adaptor regions, upper case characters indicate hybridisation sites to the targeted fragment.* ***T°,*** *annealing temperature is optimised for the use of the appropriate polymerase, i.e. Q5® High-Fidelity DNA polymerase (NEB). Fragment size is given in number of base pairs (****bp****).*

Amplicon	Method	Name	Primers	T°	Size
npr-6 gDNA	R/D	pSM npr-6 gDNA F pSM npr-6 gDNA R	FW: 5′-ggcgcgcctctagagCTCTTCGTTTATCCCAATTTC REV:5′-ttggccaatcccgggTTAAAGCAGAAGCGTCTG	55°C	2584 bp
npr-6 gDNA	PCR - Ligation	gDNA npr-6 PCR F gDNA npr-6 PCR R gDNA npr-6 PCR new	FW: 5′-cctctagaggatccccgggaCTCTTCGTTTATCCCAATTTC REV:5′-tccgacgctagccaagggtcTTAAAGCAGAAGCGTCTG REV:5′-gtcgacgctagcCAGGGTCTTAAAGCAGAAGCGTCTG	59°C	2624 bp 2584 bp
Linear pSM (*npr-6p::sl2::gfp)*	PCR - Ligation	pSM npr-6 PCR F pSM npr-6 PCR R	FW: 5′-GACCCTTGGCTAGCGTCG REV:5′-TCCCGGGGATCCTCTAGAG	69°C	7590 bp
npr-6p::npr-6 gDNA	Linear Rescue	Linear rescue npr6 F new Linear rescue npr6 R new	FW: 5′-GCTGATGAAGCTGTACAGTGC REV:5′-TATCAACCACACCAGTTGAACC	66°C	4909 bp
Linear pSM(*npr-6p::gfp)*	Reporter plasmid	SL-2 splicing primer F1 SL-2 splicing primer R	FW: 5′-ATGAGTAAAGGAGAAGAACTTTTCAC REV:3′- CCGGGGATCCTCTAGAG	63°C	7311 bp

Table C: Primers used for C. elegans and bacterial strain genotyping*. Forward (FW: 5'-3'), reverse (REV: 3'-5') or nested forward (Pfw) or reverse (Prev) primers are as indicated. T°, annealing temperature is optimised for the use of the appropriate polymerase, i.e. REDTaq® DNA polymerase (Sigma-Aldrich). Expected fragment size is given for each strain, or for the construct with insert (+) and without insert (-) in number of base pairs (**bp**). Forward **(FW: 5'-3')** and reverse **(REV: 3'-5')** primers are as indicated**. Prv** indicates a poison reverse primer, i.e. a reverse primer located in a region that is absent in one or multiple strains. **NaN:** not a number, e.g. when no bands are expected. Strains: **N2,** wild-type Bristol strain C. elegans; **npr-6,** LSC1493, i.e. npr-6 deletion mutants; **DH5α**, competent E. coli strain for heat induced transformation.*

Strain(s)	Name	Primers	T°	Size (bp)
N2, *npr-6*	npr6 F (new) npr6 P (new) npr6 R (new)	FW: 5′-GCGGTAGCTGTCATACTCAT Prv:5′- CGAGACACATCGCAACCAAA REV:3′-CGCGTCTAGAATTGCAAGTC	53°C	N2: 2186, *npr-6:* 1253 N2: 1674, *npr-6:* NaN
DH5α *[*pSM-*npr-6p::npr-6::sl2::gfp]*	pSM cDNA npr-6 F pSM R	FW: 5′-GAGACACATCGCAACCAAAC REV:5′-ACAACCTTTATTGAGAAGAGACC	50°C	(+) *npr-6:* 2924 bp (-) *npr-6:* 339 bp
DH5α [pSM (*npr-6::sl2::gfp))]*	pSM F pSM R	FW: 5′-TGACCATGATTACGCCAAGC REV:5′-ACAACCTTTATTGAGAAGAGACC	55°C	(+) *npr-6*: 2818 bp
DH5α [pSM-*npr-6p::gfp]*	Colony PCR pSM SL2(-) F Colony PCR pSM SL2(-) R	FW: 5′- AGACACATCGCAACCAAACA REV:5′- TTGCATCACCTTCACCCTCT	52°C	(+) SL2: 520 bp (-) SL2: 241 bp

d. Strains

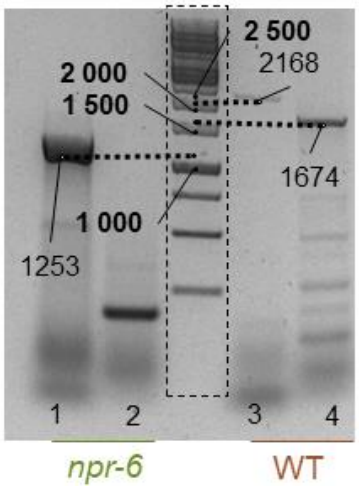

Figure A: Genotyping of LSC1493 to confirm a 99 bp deletion spanning exons 9 and 10. *Lane 1: npr-6 gDNA + forward and reverse primers: as expected, there is a band at 1253 bp; lane 2 : npr-6 gDNA + poison and reverse primers: no band at significant Mw; lane 3: wild-type gDNA + forward and reverse primers: expected band at 2168 bp; lane 4: wild-type gDNA + poison and reverse primers: expected band at 1674 bp The observed pattern is according to a deletion in the npr-6 gene in npr-6 mutants.*

Table D: Table of strains used in the experiments leading to this master's dissertation.

Strain	Genotype
N2	Wild-type Bristol variety
LSC1493	*npr-6(tm1497)* (5x outcrossed)
ZX2038	*npr-6*; *zxEx906*[pAO07-*npr-6p::npr-6::sl2::gfp*, 50 ng/µl + pCFJ90-*pmyo-2::mCherry,* 1.5-2.5 ng/µl]
LSC1585	*flp-26(gk3015)* (4x outcrossed)
LSC1821	*npr-6; lstEx1017*[pSM-*npr-6p::npr-6::sl2::gfp,* 25 ng/µl + pCIM02-*unc-22p::dsRED*, 50 ng/µl]
LSC1823	*npr-6;lstEx1019*[pSM-*npr-6p::npr-6::sl2::gfp,* 25 ng/µl + pCIM02-*unc-22p::dsRED*, 50 ng/µl]

e. Phylogenetic Analysis

(See next page)

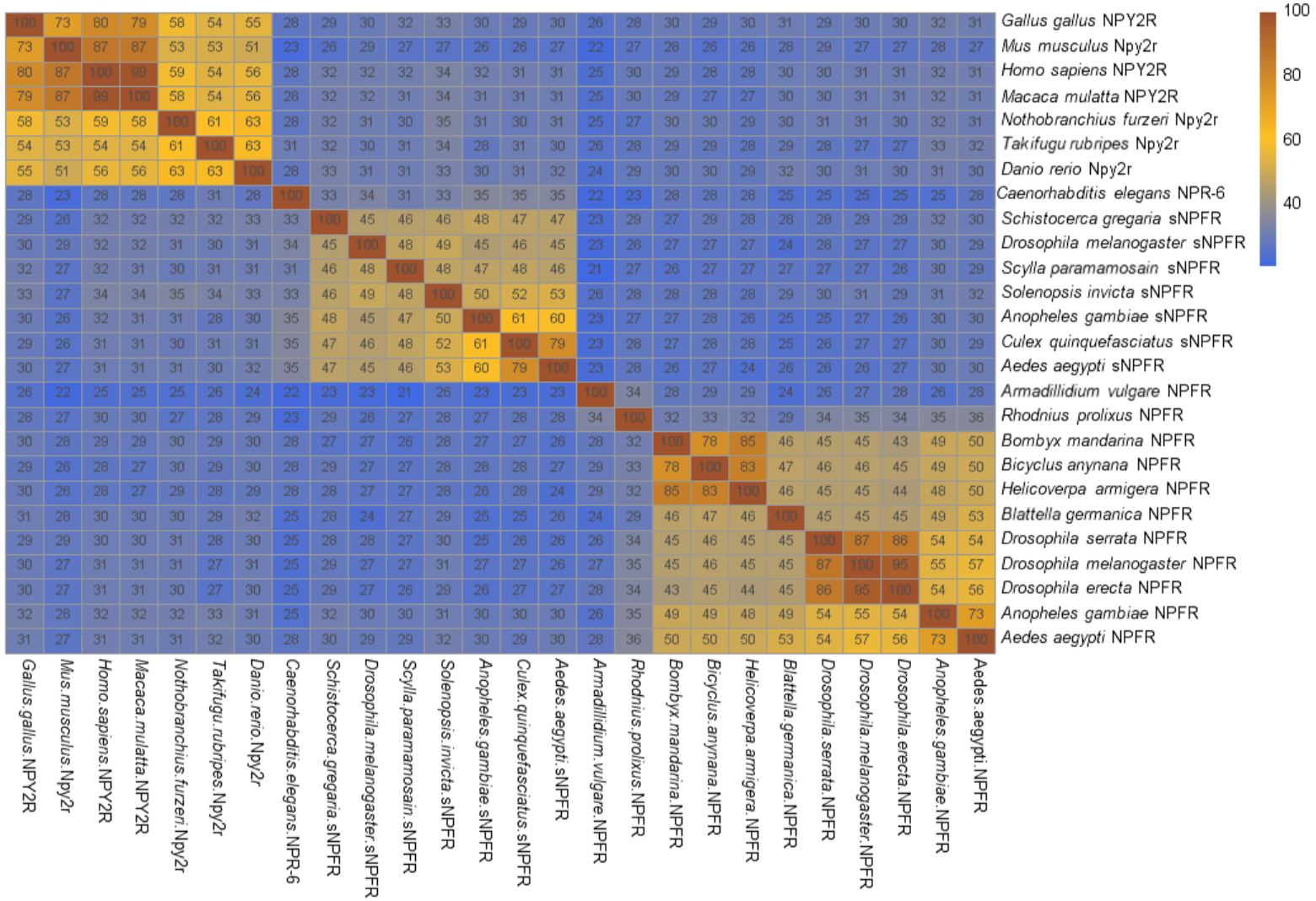

Figure B: Percentage identity matrix for multiple sequence alignment of protein sequences. *High percentages identity suggest close phylogenetic relation for the arthropod NPFR, vertebrate NPY2R and arthropod sNPFR proteins. The predicted translated* C. elegans *NPR-6 shows highest overall identity percentages with arthropod sNPFR;* ***sNPFR****, short neuropeptide F receptor;* ***NPFR****, neuropeptide F receptor;* ***NPR-6,*** *neuropeptide receptor family protein 6,* ***NPY2R,*** *neuropeptide Y receptor Y2.*

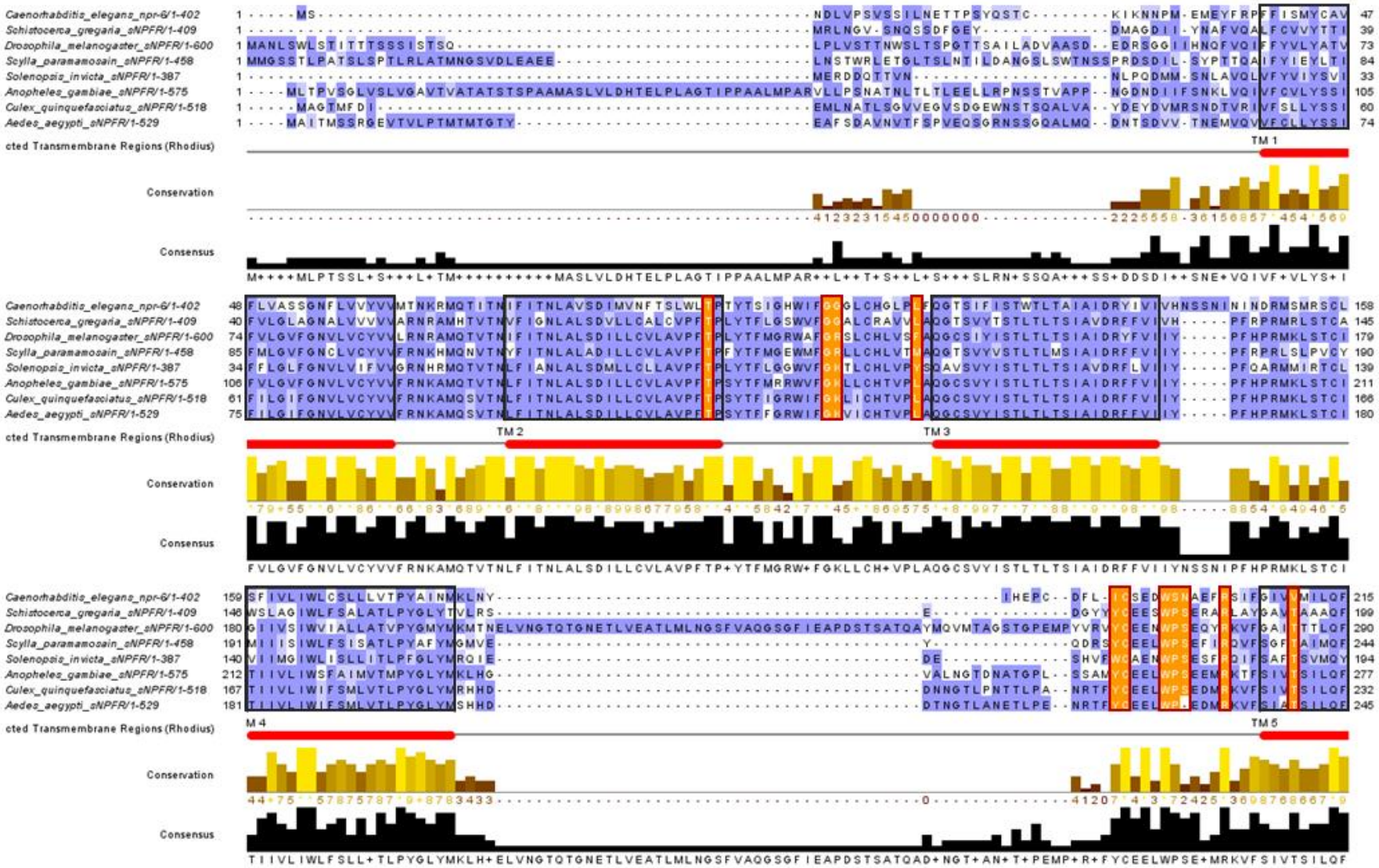
Caenorhabditis_elegans_npr-6/1-402
Schistocerca_gregaria_sNPFR/1-409
Drosophila_melanogaster_sNPFR/1-600
Scylla_paramamosain_sNPFR/1-458
Solenopsis_invicta_sNPFR/1-387
Anopheles_gambiae_sNPFR/1-575
Culex_quinquefasciatus_sNPFR/1-518
Aedes_aegypti_sNPFR/1-529
cted Transmembrane Regions (Rhodius)
TM 1
Conservation
Consensus
TM 2
TM 3
TM 4
TM 5

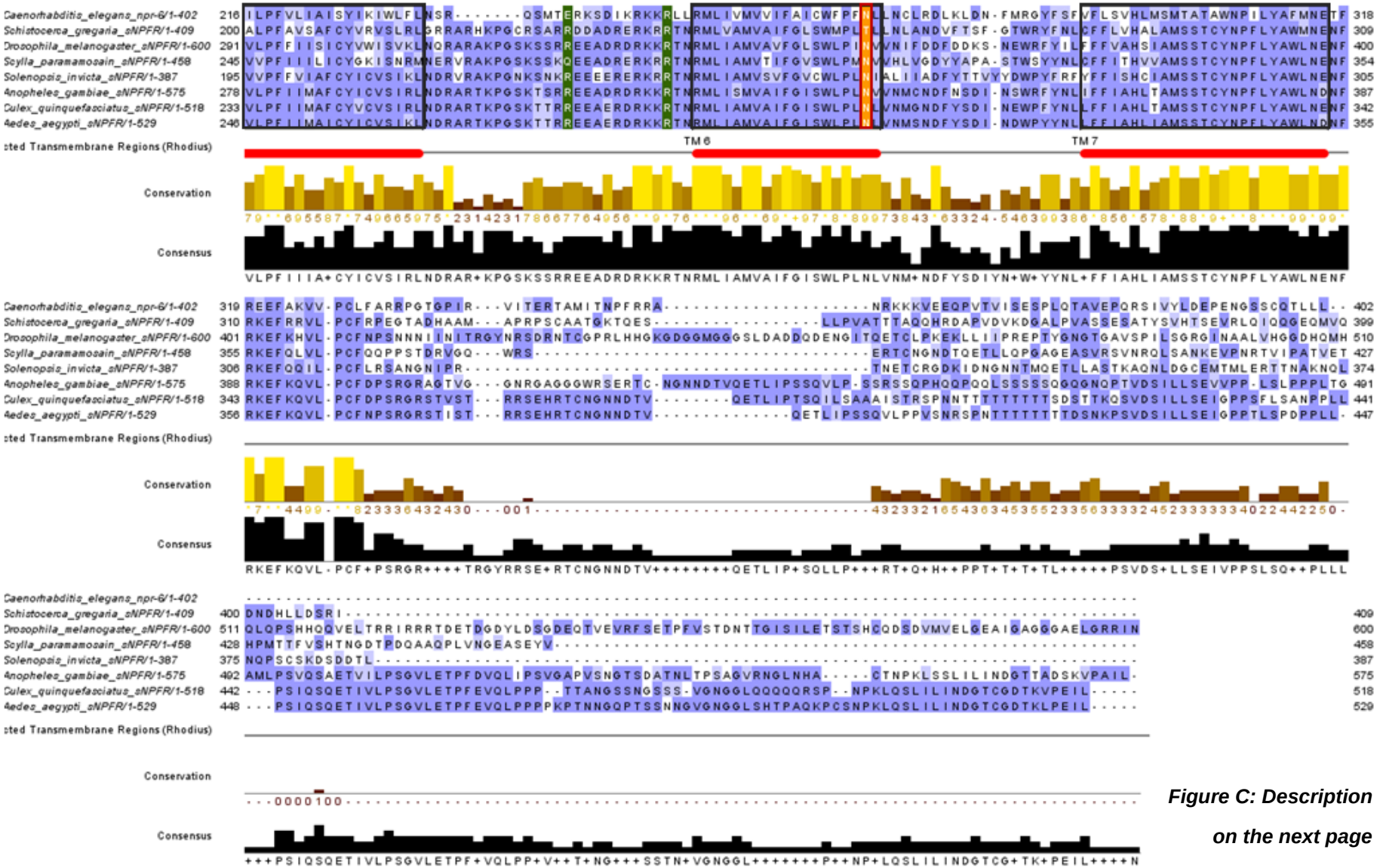

Figure C: Description on the next page

Figure C: MUSCLE alignment of the predicted C. elegans NPR-6 with the homologous arthropod sNPFR protein sequences. *Transmembrane regions predicted for C. elegans NPR-6 by Rhodius are underlined in red and framed by a black box. Residues which were predicted to be important for ligand binding are highlighted in green and framed by a red box. Predicted protein kinase C phosphorylation residues are highlighted in darker green without a frame. All residues are coloured according to the BLOSUM62 matrix.*

f. Localisation

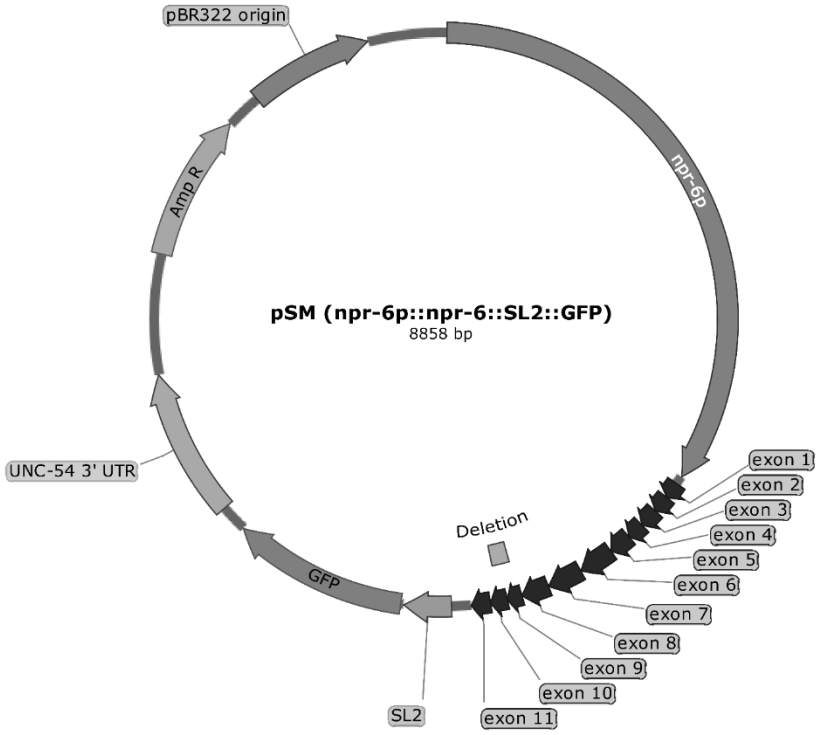

Figure D: Schematic representation of the vector *pSM-npr-6p::npr-6::sl2::gfp, including a 99 bp deletion in exons 9 and 10.* ***Amp-R,*** *ampicillin resistance gene.*

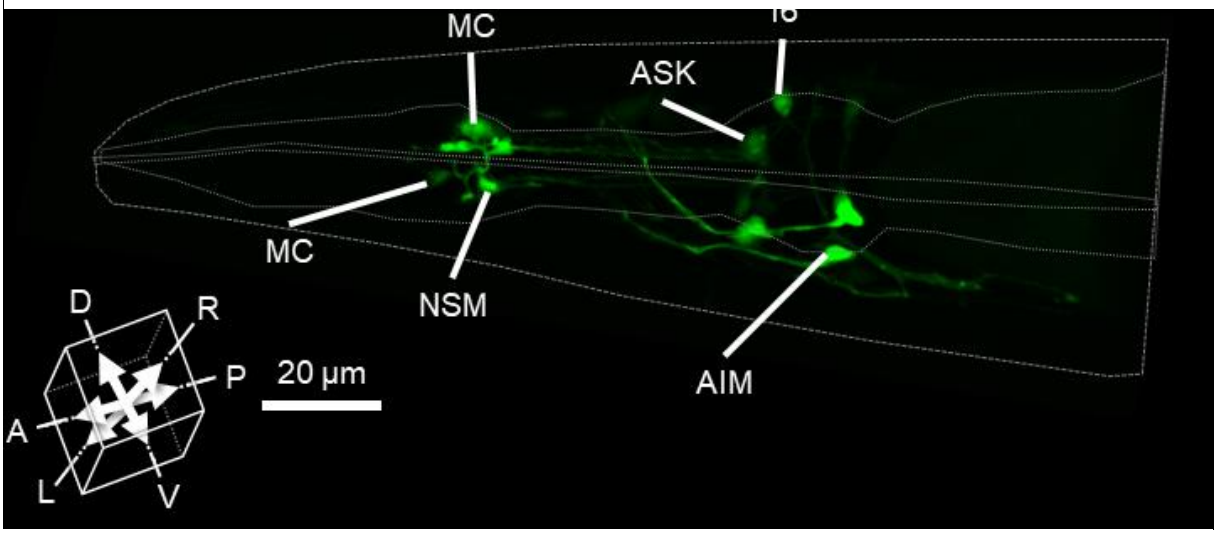

Figure E: Clear expression in presumed AIM neurons. *AIM always showed expression, although not always equally bright;* ***D****, dorsal;* ***V****, ventral, R; right;* ***L****, left;* ***P****, posterior;* ***A****, anterior*

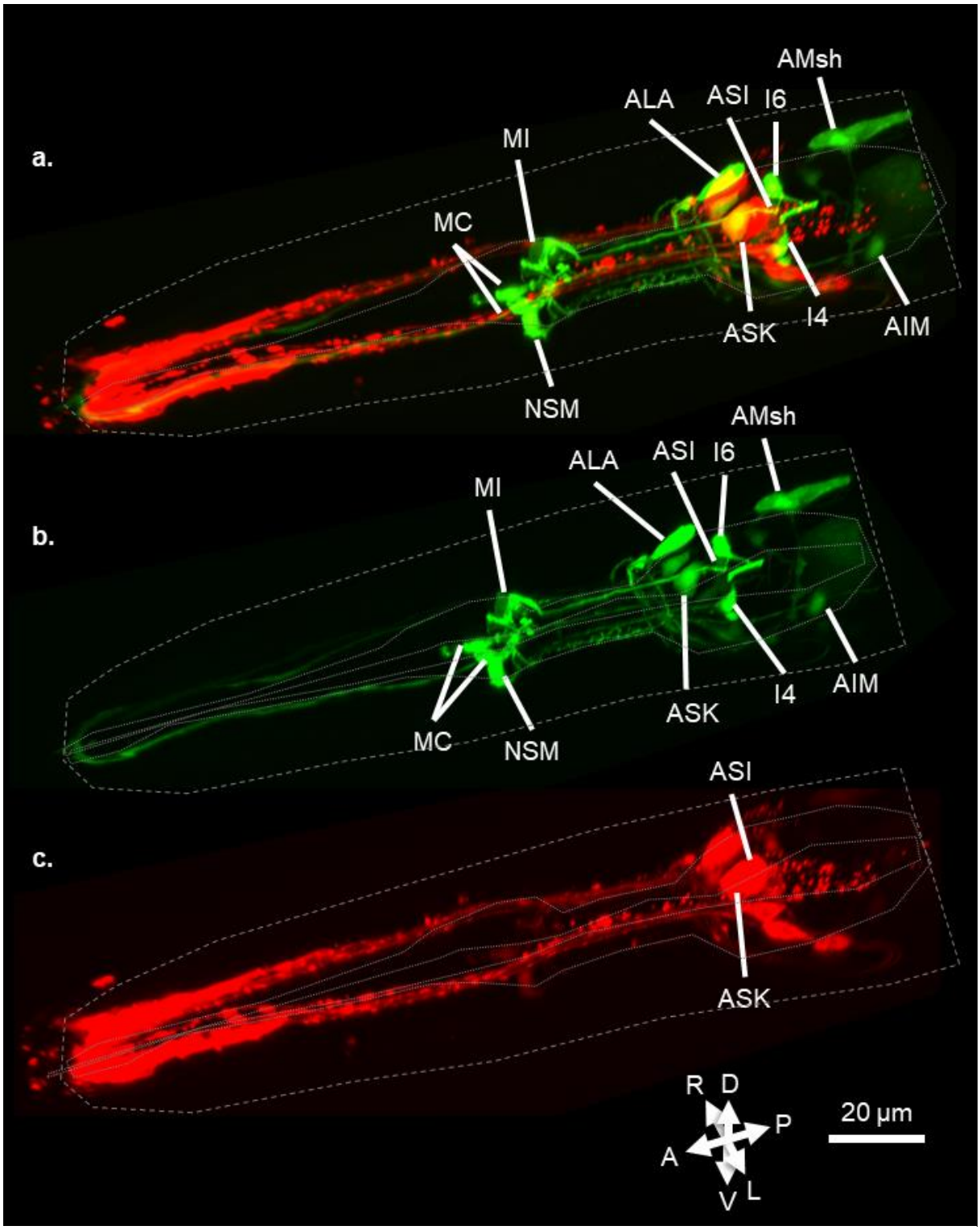

Figure F: Representative example of gfp reporter gene expression *in MC, NSM, MI, ALA, ASI, ASK, I6, I4, AMsh and AIM****. a)*** *overlay of gfp channel with DiI staining;* ***b)*** *gfp channel only;* ***c)*** *DiI channel only*

g. Calcium Mobilisation Assays

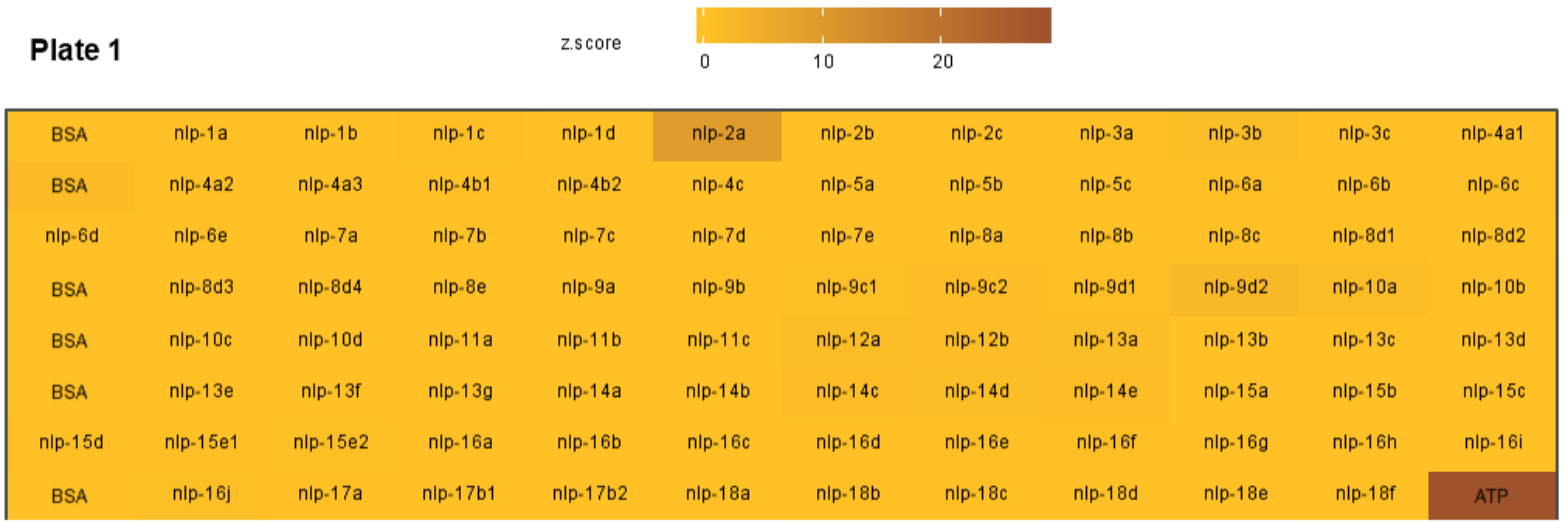

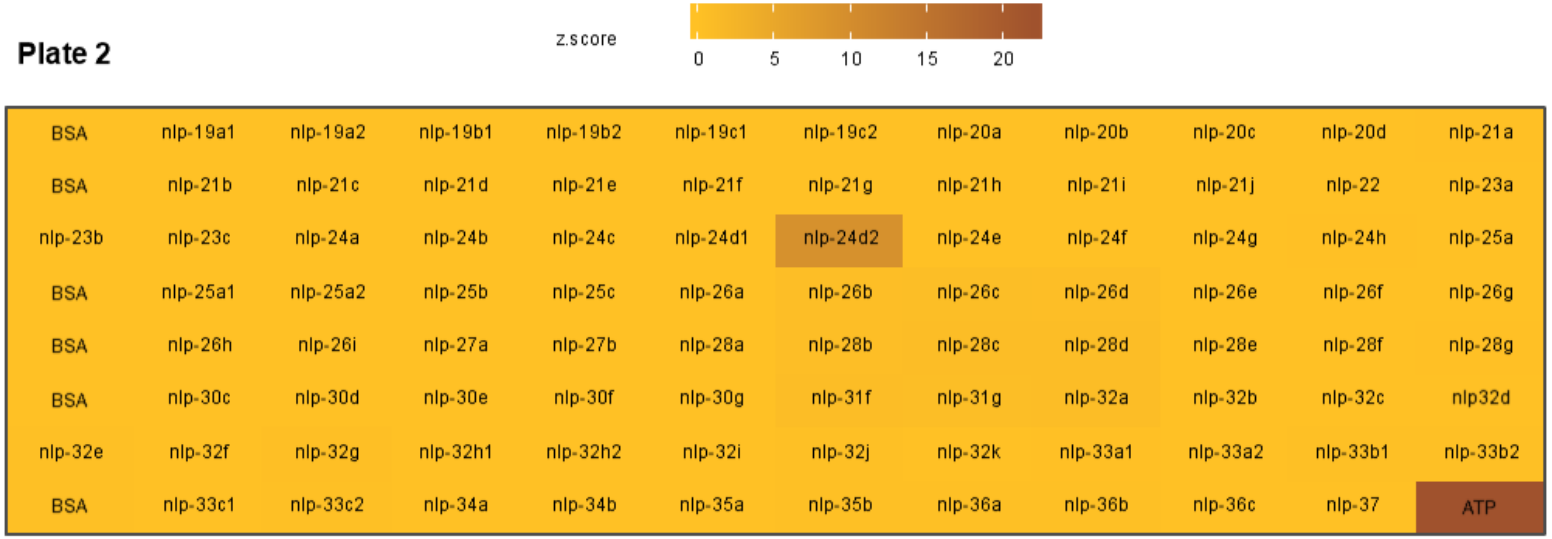

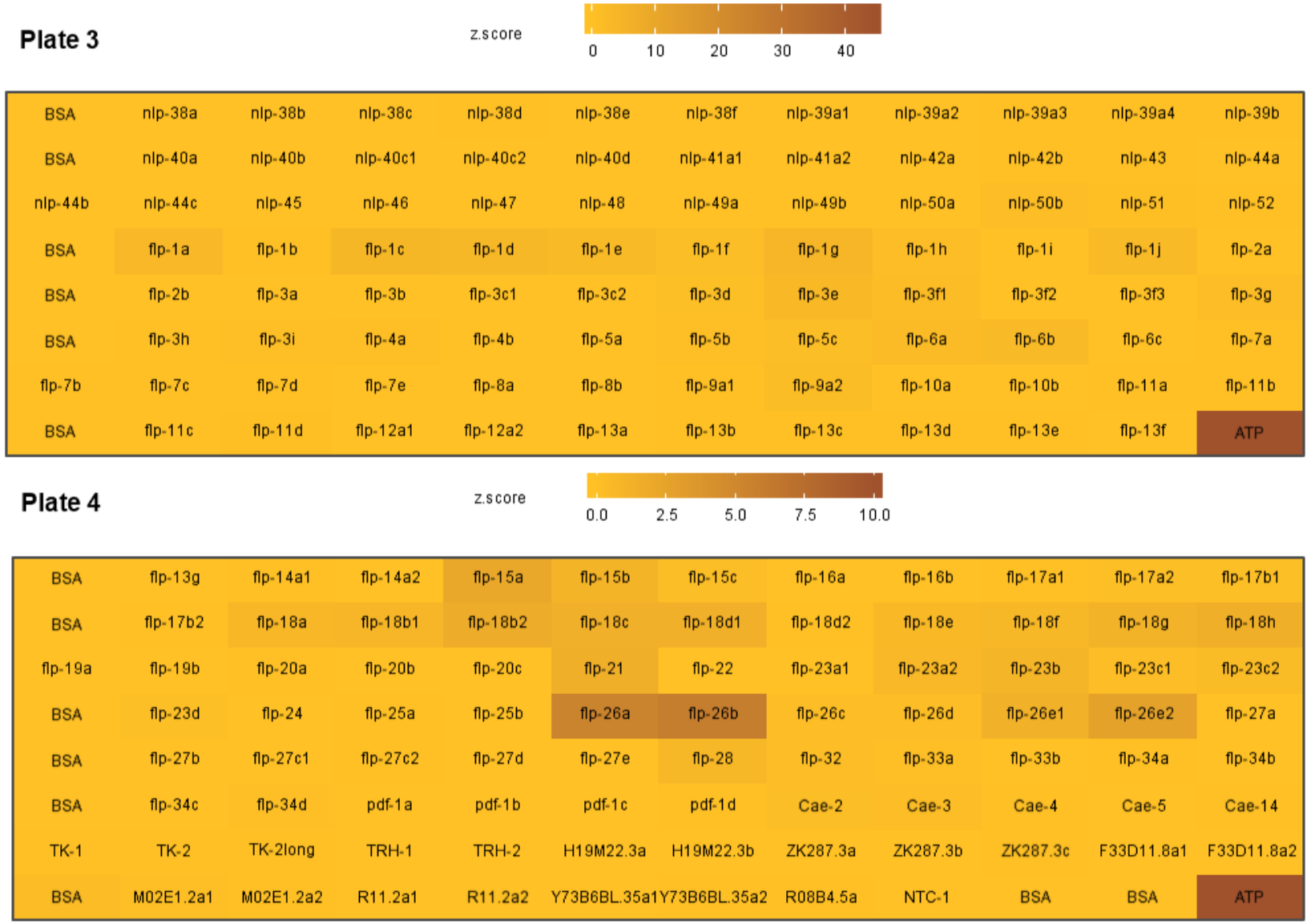
Plate 3
z.score
0
10
20
30
40
BSA nlp-38a nlp-38b nlp-38c nlp-38d nlp-38e nlp-38f nlp-39a1 nlp-39a2 nlp-39a3 nlp-39a4 nlp-39b
BSA nlp-40a nlp-40b nlp-40c1 nlp-40c2 nlp-40d nlp-41a1 nlp-41a2 nlp-42a nlp-42b nlp-43 nlp-44a
nlp-44b nlp-44c nlp-45 nlp-46 nlp-47 nlp-48 nlp-49a nlp-49b nlp-50a nlp-50b nlp-51 nlp-52
BSA flp-1a flp-1b flp-1c flp-1d flp-1e flp-1f flp-1g flp-1h flp-1i flp-1j flp-2a
BSA flp-2b flp-3a flp-3b flp-3c1 flp-3c2 flp-3d flp-3e flp-3f1 flp-3f2 flp-3f3 flp-3g
BSA flp-3h flp-3i flp-4a flp-4b flp-5a flp-5b flp-5c flp-6a flp-6b flp-6c flp-7a
flp-7b flp-7c flp-7d flp-7e flp-8a flp-8b flp-9a1 flp-9a2 flp-10a flp-10b flp-11a flp-11b
BSA flp-11c flp-11d flp-12a1 flp-12a2 flp-13a flp-13b flp-13c flp-13d flp-13e flp-13f ATP
Plate 4
z.score
0.0
2.5
5.0
7.5
10.0
BSA flp-13g flp-14a1 flp-14a2 flp-15a flp-15b flp-15c flp-16a flp-16b flp-17a1 flp-17a2 flp-17b1
BSA flp-17b2 flp-18a flp-18b1 flp-18b2 flp-18c flp-18d1 flp-18d2 flp-18e flp-18f flp-18g flp-18h
flp-19a flp-19b flp-20a flp-20b flp-20c flp-21 flp-22 flp-23a1 flp-23a2 flp-23b flp-23c1 flp-23c2
BSA flp-23d flp-24 flp-25a flp-25b flp-26a flp-26b flp-26c flp-26d flp-26e1 flp-26e2 flp-27a
BSA flp-27b flp-27c1 flp-27c2 flp-27d flp-27e flp-28 flp-32 flp-33a flp-33b flp-34a flp-34b
BSA flp-34c flp-34d pdf-1a pdf-1b pdf-1c pdf-1d Cae-2 Cae-3 Cae-4 Cae-5 Cae-14
TK-1 TK-2 TK-2long TRH-1 TRH-2 H19M22.3a H19M22.3b ZK287.3a ZK287.3b ZK287.3c F33D11.8a1 F33D11.8a2
BSA M02E1.2a1 M02E1.2a2 R11.2a1 R11.2a2 Y73B6BL.35a1 Y73B6BL.35a2 R08B4.5a NTC-1 BSA BSA ATP

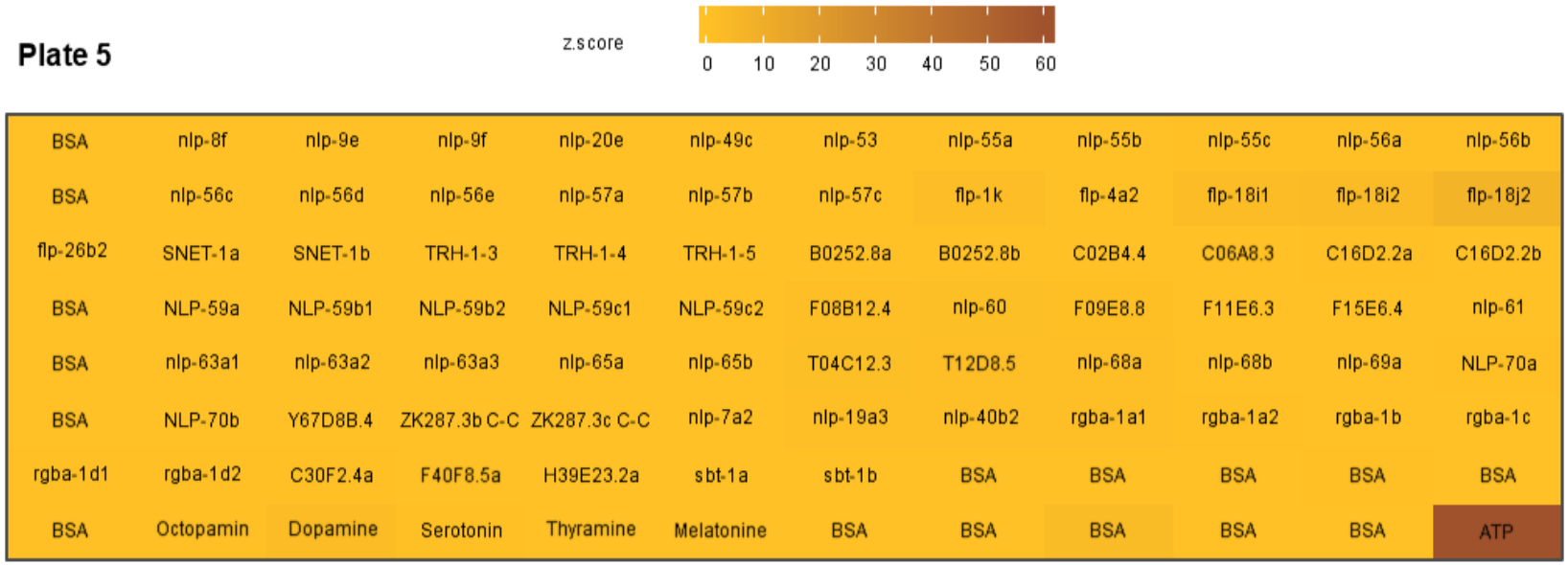

Figure G: levelplot of the z-scores *for each of the wells per plate in the Ca^{2+}-mobilisation assay. ATP is a positive control, whereas BSA is the solvent in which all peptides were diluted, accounting for baseline levels.*

DEPARTMENT OF BIOLOGY
Kasteelpark Arenberg 31- bus 2436
3001 LEUVEN, BELGIË
tel. + 32 16 32 45 81
fax + 32 16 32 07 71
bio.kuleuven.be